

A humanized zebrafish screening platform to identify GPR17 inhibitors for the treatment of multiple sclerosis

Dissertation

zur

Erlangung des Doktorgrades (Dr. rer. nat)

der Mathematisch-Naturwissenschaftlichen Fakultät
der Rheinischen Friedrich-Wilhelms-Universität Bonn

vorgelegt von

Felix Häberlein

aus Marburg

Bonn 2019

Angefertigt mit Genehmigung der Mathematisch-Naturwissenschaftlichen Fakultät der Rheinischen Friedrich-Wilhelms-Universität Bonn.

1. Gutachter: Prof. Dr. Evi Kostenis

2. Gutachter: Prof. Dr. Benjamin Odermatt

Tag der Promotion: 17.02.2020

Erscheinungsjahr: 2020

Die vorliegende Arbeit wurde in der Zeit von November 2016 bis Oktober 2019 am Institut für Pharmazeutische Biologie und am Anatomischen Institut der Rheinischen Friedrich-Wilhelms-Universität Bonn unter der Leitung von Frau Prof. Dr. Evi Kostenis angefertigt.

Abstract

Multiple sclerosis (MS), a demyelinating disease of the central nervous system (CNS) with devastating symptoms, is characterized by the progressive destruction of myelin and myelinating oligodendrocytes (Ol). Currently, there is still an unmet therapeutic need to promote remyelination to treat MS.

The restoration of myelin sheaths requires the invasion of oligodendrocyte precursor cells (OPC) into demyelinated lesions and their differentiation into mature myelinating Ols. However, despite the large numbers of OPC in demyelinated lesions of MS patients, remyelination fails. This indicates insufficient Ol differentiation due to either the absence of pro-myelinating signals or the presence of myelination inhibitors in the MS lesion. One such myelination inhibitor is the *GPR17 gene*, which codes for an orphan G protein-coupled receptor (GPCR) that has attracted particular attention as oligodendroglial maturation inhibitor in mice. In humans, GPR17 is also disease-relevant: it is highly abundant within active white matter plaques of MS patients. Moreover, absence of GPR17 promotes remyelination in a murine autoimmune model of MS, proposing inhibitors of GPR17 as a promising therapy to promote remyelination in patients with MS.

To develop novel therapeutic approaches, animal experiments are still considered the gold standard, because *in vivo* experiments allow examination of both therapeutic and potential adverse effects of drugs on the whole organism. Experimental drugs that function across animal species might be expected to show superior efficacy in humans, and, therefore, eventually promote remyelination in MS. Unfortunately, drugs emerging from preclinical studies in animal MS models have a poor record of success in human clinical trials, highlighting the need of “humanized” *in vivo* models.

In search for improved animal models, zebrafish (*Danio rerio*) has emerged as a popular vertebrate model. It is a widely-used organism for studying developmental processes and for drug testing. Especially, zebrafish larvae have become a powerful tool for the *in vivo* study of Ol biology and (re-)myelination, because of its high genetical and experimental versatility and its transparency for *in vivo* imaging.

Therefore, this study focusses on investigating the functional role of Gpr17 in zebrafish in order to establish a “humanized” zebrafish screening platform for the identification of GPR17 inhibitors as a potential therapy for MS. We found that *gpr17* mRNA is expressed in OPCs, pre-Ols but not in mature Ols in zebrafish. Consistent with data obtained in mice, we deciphered the functional role of Gpr17 to be an Ol differentiation inhibitor in zebrafish. Furthermore, “humanized” zebrafish lines expressing the human GPR17 or a chimeric GPR17, containing the ligand binding

Abstract

domain of human GPR17 and the intracellular loops of zebrafish Gpr17, were generated. We demonstrated that both the human and the chimeric GPR17 receptors are functional in zebrafish and therefore provide a tool to perform drug screenings for antagonists of human GPR17 in a humanized zebrafish model. To facilitate the search of inhibitors of human GPR17 we also developed an automated screening system using the EnSight™ multimode plate reader.

Zusammenfassung

Multiple Sklerose (MS), eine demyelinisierende Krankheit mit verheerenden Symptomen, ist gekennzeichnet durch die fortschreitende Zerstörung von Myelin und myelinisierenden Oligodendrozyten (Ol) im Zentralnervensystem. Für demyelinisierende Erkrankungen wie der MS verspricht die Aktivierung und Förderung der Remyelinisierung großes therapeutisches Potenzial, das durch gegenwärtig verfügbare pharmazeutische Therapien nur unzureichend genutzt werden kann.

Die Wiederherstellung der Myelinscheiden erfordert die Migration von Ol-Vorläuferzellen in demyelinisierte Läsionen und deren Differenzierung in reife myelinisierende Ols. Trotz der großen Anzahl von Ol-Vorläuferzellen in demyelinisierten Läsionen von MS-Patienten, die in der Lage sein sollten, die beschädigten Myelinscheiden wiederherzustellen, scheitert die Remyelinisierung. Dies deutet auf eine unzureichende Ol-Differenzierung hin, die entweder auf das Fehlen von pro-myelinisierenden Signalen oder auf das Vorhandensein von Myelinierungshemmern in der MS-Läsion zurückzuführen ist. Ein solches Kandidatengen ist *GPR17*, das für einen orphanen G-Protein-gekoppelten Rezeptor (GPCR) kodiert, der als Differenzierungshemmer von Ols in Mäusen besondere Aufmerksamkeit erregt hat. Während *GPR17* in aktiven Plaques von MS-Patienten hochreguliert ist, fördert die Abwesenheit des Rezeptors die Remyelinisierung in einem murinen MS-Autoimmunmodell. Deshalb stellt die Inhibition von *GPR17* einen vielversprechenden Therapieansatz zur Förderung der Remyelinisierung bei Patienten mit MS dar.

Um neuartige Therapieansätze zu entwickeln, gelten Tierversuche nach wie vor als Goldstandard, da *in vivo*-Experimente die Untersuchung therapeutischer- als auch potenzieller Nebenwirkungen von Medikamenten auf den gesamten Organismus ermöglichen. Leider haben Medikamente, die in präklinischen Studien mit tierischen MS-Modellen eingesetzt werden bisher eine schlechte Erfolgsbilanz in menschlichen klinischen Studien, was die Notwendigkeit von "humanisierten" *in vivo*-Modellen verdeutlicht.

Auf der Suche nach optimierten Tiermodellen hat sich der Zebrafisch (*Danio rerio*) zu einem beliebten Wirbeltiermodell entwickelt. Besonders für die Erforschung von Entwicklungsprozessen und die Testung von Arzneimittelkandidaten stellt die Larve des Zebrafisches ein etabliertes Tiermodell dar. Wegen seiner hohen genetischen und experimentellen Vielseitigkeit sowie seiner optischen Transparenz wird der Zebrafisch als ein leistungsstarkes Werkzeug für die *in vivo*-Studie der Oligodendrozytenbiologie und (Re-)Myelinisierung verwendet.

Zusammenfassung

Daher konzentriert sich diese Arbeit unter anderem auf die Untersuchung der funktionellen Rolle von Gpr17 im Zebrafisch, um eine „humanisierte“ Zebrafisch-Screening Plattform zur Identifizierung von GPR17 Inhibitoren als mögliche Therapie für MS zu etablieren. Wir konnten zeigen, dass *gpr17* mRNA in OPCs, pre-Ols, aber nicht in reifen Ols im Zebrafisch exprimiert wird. In Übereinstimmung mit den Daten, die bei Mäusen gewonnen wurden, haben wir die funktionelle Rolle von Gpr17 als Ol-Differenzierungshemmer bei Zebrafischen entschlüsselt. Folgedessen, wurden "humanisierte" Zebrafischlinien entwickelt, die den humanen oder ein chimären GPR17, der aus der Ligandenbindungsdomäne des menschlichen GPR17 und den intrazellulären Schleifen des Zebrafisches-Gpr17 besteht, exprimieren. Wir konnten zeigen, dass der humane GPR17-Rezeptor, aber auch der chimäre GPR17-Rezeptor bei Zebrafischen funktionsfähig ist und daher ein Werkzeug bietet, um Wirkstofffindung im Hochdurchsatzmaßstab für Antagonisten des humanen GPR17 in einem humanisierten Zebrafisch-Modell durchzuführen. Um die Suche nach Inhibitoren des menschlichen GPR17 zu erleichtern, haben wir zudem ein automatisiertes Screening-System mit dem EnSight™ Multimode Plattenleser entwickelt.

Table of contents

Abstract.....	V
Zusammenfassung.....	VII
Table of contents.....	IX
List of figures and tables	XII
Abbreviation	XIV
1. Introduction.....	1
1.1 Multiple sclerosis.....	2
1.1.1 Treatment of multiple sclerosis	2
1.1.2 Remyelination	3
1.2 Neurulation, neurogenesis and gliogenesis.....	4
1.3 Oligodendrogenesis.....	9
1.3.1 Regulators of oligodendrogenesis.....	10
1.3.2 The orphan G protein-coupled receptor 17 and its role during oligodendrocyte development.....	12
1.4 The zebrafish.....	14
1.4.1 Oligodendrocyte development, myelination and remyelination in zebrafish	15
1.4.2 Zebrafish as a powerful model organism to study CNS myelination and remyelination.....	17
1.4.3 Zebrafish: a tool for <i>in vivo</i> drug discovery	18
1.5 Aim of this study	19
2 Materials	21
2.1 Chemicals	21
2.2 Enzymes.....	23
2.3 Buffer and solution-Recipes	23
2.4 Antibodies.....	25
2.4.1 Primary antibodies.....	25
2.4.2 Secondary antibodies	25
2.5 Oligonucleotides.....	26
2.5.1 Oligonucleotides for RNAscope.....	26
2.5.2 Oligonucleotides for sequencing and genotyping <i>gpr17</i> knockout lines	26
2.5.3 Morpholino oligonucleotides	26
2.6 Plasmids.....	27
2.7 Zebrafish lines.....	27

Table of contents

2.8	Commercial Assays	28
2.9	Consumables and other used materials	28
2.10	Software and algorithm.....	29
2.11	Equipment	30
3	Methods.....	32
3.1	Zebrafish maintenance	32
3.2	DNA extraction.....	32
3.3	Genotyping and sequencing of adult and larval zebrafish.....	32
3.3.1	Polymerase chain reaction	32
3.3.2	Sequencing of <i>gpr17</i> knockout fish.....	33
3.3.3	Genotyping of <i>gpr17</i> knockout fish.....	33
3.4	TA- Cloning.....	34
3.5	Microinjections of zebrafish embryos.....	34
3.5.1	Morpholino injections	34
3.5.2	RNA injections	35
3.6	Whole-mount fluorescent labeling techniques	36
3.6.1	Fixation and dehydration of zebrafish larvae	36
3.6.2	Whole-mount in situ hybridization using RNAscope.....	36
3.6.3	Whole-mount immunohistochemistry.....	37
3.6.4	Immunohistochemistry of larvae sections	38
3.7	Compound treatment.....	39
3.7.1	GANT 61 treatment	39
3.7.2	SKP-C25 treatment.....	39
3.7.3	Trichostatin A treatment	39
3.8	Two-photon imaging of zebrafish.....	39
3.8.1	Mounting of zebrafish	39
3.8.2	Two-photon imaging	40
3.9	Automated Enight™ imaging protocol	40
3.9.1	Imaging settings for proper detection of <i>Tg(olig2:EGFP)</i>	40
3.9.2	Larvae positioning protocol.....	41
3.9.3	Automated image analysis algorithm	41
3.10	Quantification and analysis	42
3.10.1	Cell counting.....	42
3.10.2	Measurement of the mean fluorescence intensity of the ventral spinal cord.....	43
3.10.3	Statistical analysis.....	43
4	Results.....	44

4.1	The G protein-coupled receptor Gpr17 in zebrafish.....	44
4.1.1	<i>Gpr17</i> mRNA expression in zebrafish.....	44
4.1.2	The functional role of Gpr17 in zebrafish.....	49
4.2	A humanized zebrafish as a model organism for human disease research.....	64
4.2.1	Transient overexpression of <i>hGPR17</i> and <i>h+zfGpr17</i> do not affect oligo-dendrocyte development in zebrafish.....	65
4.2.2	<i>hGPR17</i> and <i>h+zfGpr17</i> are functional in zebrafish.....	66
4.3	A novel plate reader-based automated high throughput <i>in vivo</i> imaging and analysis platform to investigate oligodendrocyte development in living zebrafish larvae.....	68
4.3.1	EnSight™ multimode plater reader's image resolution is sufficient to detect fluorescent spinal cord and dorsal olig2 ⁺ cells.....	68
4.3.2	Kaleido's™ novel image analysis algorithm automatically detects zebrafish larva, its fluorescent spinal cord and dorsal olig2 ⁺ cells.....	71
4.3.3	Data verification with the image algorithm's heatmap function.....	72
4.3.4	A novel positioning protocol forces zebrafish larvae into their lateral position....	74
4.3.5	Efficient detection of zebrafish morphometry, fluorescent spinal cord and dorsal olig2 ⁺ cell number by the image analysis algorithm.....	76
4.3.6	Automated image acquisition and analysis algorithm detects drug induced changes in the number of dorsal olig2 ⁺ cells and morphometry.....	76
4.3.7	Novel image analysis algorithm enables automatic time-lapse imaging and analysis of 96 zebrafish.....	80
5	Discussion.....	82
5.1	Expression and function of Gpr17 in zebrafish is similar to mice.....	82
5.1.1	<i>Gpr17</i> is expressed in OPCs, pre-Ols but not in mature Ols in zebrafish.....	82
5.1.2	Absence of Gpr17 decreases OPC migration and therefore the number of dorsal OPCs and mature Ols.....	83
5.1.3	Gpr17 is a negative regulator of Ol differentiation in zebrafish.....	85
5.2	Human and chimeric receptors can be used as tools to humanize zebrafish.....	87
5.3	A rapid automated screening system.....	89
5.4	Gliotherapeutics as a promising strategy to promote remyelination in MS patients.....	92
5.5	Summary.....	94
6	Conclusion and outlook.....	96
7	References.....	97
	Publications.....	110
	Acknowledgements.....	111

List of figures and tables

Figure 1: Vertebrate Neurulation.....	5
Figure 2: Dorso- ventral patterning of the developing spinal cord.....	6
Figure 3: Hypothetical vertebrate regulation of neurogenesis and gliogenesis.....	8
Figure 4: Vertebrate oligodendrogenesis.	10
Figure 5: Expression pattern of G-protein coupled receptors during mouse oligodendrogenesis.	12
Figure 6: Orthology relationships between vertebrate genomes.....	15
Figure 7: Oligodendrocyte development during zebrafish embryogenesis.	16
Figure 8: Calculation of the injected amount of agent.	34
Figure 9. Gpr17 mRNA is localized within olig2+ oligodendrocyte lineage cells in zebrafish spinal cord between 56 hpf and 4 dpf.....	45
Figure 10: <i>Gpr17</i> mRNA is expressed in pre-oligodendrocytes in zebrafish.	46
Figure 11: <i>Gpr17</i> mRNA is not expressed in mature oligodendrocytes in zebrafish.....	47
Figure 12: <i>Gpr17</i> mRNA is not expressed in neurons in zebrafish.....	48
Figure 13: <i>Gpr17</i> knockdown decreases the number of claudinK+ mature oligodendrocytes in the zebrafish dorsal spinal cord.	50
Figure 14: <i>Gpr17</i> knockdown decreases the number of mbp+ mature oligodendrocytes in the zebrafish dorsal spinal cord.	51
Figure 15: <i>Gpr17</i> knockdown decreases the number of olig2+ oligodendrocyte precu-rsor cells and Ol lineage cells in the dorsal spinal cord.	52
Figure 16: <i>Gpr17</i> knockdown does not affect apoptosis or proliferation.....	53
Figure 17: <i>Gpr17</i> knockdown does not impair general or neuronal development of ze-brafish...	54
Figure 18: Truncated Gpr17 upon CRISPR/Cas-9 genome editing.	55
Figure 19: Number of mature oligodendrocytes is decreased in the dorsal spinal cord of <i>gpr17</i> deficient <i>Tg(claudinK:EGFP)</i> zebrafish embryos.	57
Figure 20: Number of mature oligodendrocytes is decreased in the dorsal spinal cord of <i>gpr17</i> deficient <i>Tg(mbp:EGFP)</i> larvae.....	58
Figure 21: Number of myelinated axons in the dorsal spinal cord of <i>gpr17</i> deficient <i>Tg(mbp:CAAX- EGFP)</i> is reduced.....	59

Figure 22: Migration of olig2 ⁺ oligodendrocyte precursor cells is impaired in <i>gpr17</i> knockout fish.	60
Figure 23: <i>Gpr17</i> knockout does not affect apoptosis or proliferation.....	61
Figure 24: <i>Gpr17</i> knockout does not impair neuronal development and is specific.....	62
Figure 25: <i>Gpr17</i> is a differentiation inhibitor of oligodendrocyte lineage cells in ze-brafish.....	64
Figure 26: Transient overexpression of hGPR17 and h+zfGpr17 does not affect oligo-dendrocyte development in zebrafish.	65
Figure 27: hGPR17 and h+zfGpr17 are functional in zebrafish.	67
Figure 28. Sharp image acquisition with maximum projection of six focal planes.	69
Figure 29: EnSight™ multimode plater reader's image resolution is sufficient to detect fluorescent spinal cord and dorsal olig2 ⁺ cells.	70
Figure 30: Kaleido's™ novel image analysis algorithm automatically detects zebrafish, its fluorescent spinal cord and dorsal olig2 ⁺ cells.	72
Figure 31: Image analysis output parameters and data verification with the image algorithm's heatmap function.	74
Figure 32: A novel positioning protocol forces zebrafish larvae into their lateral position.....	75
Figure 33: Efficient detection of zebrafish morphometry and dorsal olig2 ⁺ cell number by the image analysis algorithm.	76
Figure 34: Automated image acquisition and analysis algorithm detects drug induced changes in the number of dorsal olig2 ⁺ cells and morphometric changes.....	77
Figure 35: The automated image analysis algorithm accurately detects a subtle reduction of dorsal olig2 ⁺ cell number in GANT61-treated zebrafish.....	78
Figure 36: The automated image analysis algorithm detects a subtle increase of dorsal olig2 ⁺ in SKP-C25-treated zebrafish.....	80
Figure 37: Novel image analysis algorithm enables automatic time-lapse imaging and analysis of 96 zebrafish.....	81
Table 1. Imaging settings for proper detection of Tg(olig2:eGFP) in the Kaleido™ software.....	41
Table 2. Input parameters of the image analysis algorithm in the Kaleido™ software.....	42

Abbreviations

Abbreviation

Action potential (AP)

Arbitrary units (au)

Basic-helix-loop helix (bHLH)

Bone morphogenetic protein (Bmp)

Central canal (CC)

Central nervous system (CNS)

Chimeric Gpr17 (h+zfGpr17)

Ciliary neurotrophic factor (CNTF)

Control Morpholino (CoMO)

Days post fertilization (dpf)

Dorsal root ganglion (drg)

Erythropoietin (Epo)

Exaggerated green fluorescent protein (EGFP)

Fibroblast growth factor (FGF)

Gpr17 Morpholino (MO)

G-protein coupled receptor (GPCR)

Hairy and enhancer of split (Hes)

Hepatocyte growth factor (HGF)

Hours post fertilization (hpf)

Human GPR17 (hGPR17)

Immunohistochemistry (ICH)

Inhibitor of differentiation (Id)

Insuline-like growth factor 1 (IGF1)

Mantle zone (MZ)

Messenger ribonucleic acid (mRNA)

Motor neuron (MN)
Multiple sclerosis (MS)
Muscarinic acetylcholine (MA)
Myelin associated glycoprotein (MAG)
Myelin basic protein (mbp)
Myelin oligodendrocyte glycoprotein (Mog)
Myelin protein zero (Mpz/P0)
Neural folds (NF)
Neural plate (NP)
Neural tube (NT)
Notochord (N)
Oligodendrocytes (Ols)
Oligodendrocyte precursor cells (OPCs)
Peripheral nervous system (PNS)
Phenylthiourea (PTU)
Platelet derived growth factor (PDGF)
Polymerase chain reaction (PCR)
Pre-mature oligodendrocytes (pre-Ols)
Primary motor neuron (pMN)
Proteolipid protein (plp)
Retinoic acid (RA)
Rohon-Beard sensory neurons (rb)
Roof plate (RF)
Seven transmembrane (7TM)
Sonic hedgehog (Shh)
Sphingosin-1 phosphate receptor (S1P1)

Abbreviations

Thyroid hormones (TH)

TrichostatinA (TSA)

Vascular endothelial growth factor (VEGF)

Ventricular zone (VZ)

Wingless/Integrated(Wnts)

Gene/Protein nomenclature

Species	Gene symbol	Protein symbol
<i>Homo sapiens</i>	<i>GPR17</i>	GPR17
<i>Mus musculus, Rattus norvegicus</i>	<i>Gpr17</i>	GPR17
<i>Danio rerio</i>	<i>gpr17</i>	Gpr17

1. Introduction

The nervous system requires a proper myelination of axons for an efficient transduction of action potentials. Myelin is a multi-layered lipidous sheath covering neuronal axons. The sheath is segmentally organized along the length of the axon, defining ensheathed internodes which are separated by nodes of Ranvier where the axonal plasma membrane is in direct contact with the extracellular fluid. The action potential (AP) traveling along the axon is carried by ion flow, traversing the axonal membrane which can only occur at the unmyelinated nodes of Ranvier, while the internodes are electrically insulated by the myelin sheath. This process is called saltatory conduction and allows to achieve a small axon diameter while maintaining a high AP conduction speed. From an evolutionary point of view, the increase in organism size was only possible through the process of myelination, mainly due to its improvements for space and energy consumption within the nervous system (Zalc, 2016).

In the central nervous system (CNS), myelin is generated by oligodendrocytes (Ols). During vertebrate CNS development, Ol precursor cells (OPCs) start to proliferate and migrate dorsally from the neural tube to subsequently differentiate into myelinating Ols. Once OPCs start to differentiate, migration stops and a subset of OPCs turn into pre-myelinating Ols (pre-Ols). Pre-Ols next differentiate into immature Ols, which ensheath multiple axon segments. Eventually, differentiation from immature Ols to mature myelinating Ols occurs, wrapping and insulating their associated axon segments by producing myelin sheaths. The importance of myelination is evidenced by the fact that loss of myelin, a hallmark of demyelinating diseases like multiple sclerosis (MS), leads to devastating neurological symptoms such as paralysis. The progressive loss of Ols and destruction of CNS myelin of patients suffering from MS exacerbate the severe neurological deficits. However, despite the large numbers of OPCs, potentially capable of restoring the damaged myelin sheath in demyelinated lesions, remyelination fails in MS, indicating insufficient Ol differentiation due to either the absence of pro-myelinating signals or the presence of myelination inhibitors in the MS lesion (Fancy et al., 2011).

Recently, G protein-coupled receptors (GPCRs) have emerged as key regulators of Ol development (Mogha et al., 2016). One such GPCR is the orphan receptor *Gpr17*, which has been revealed as a differentiation inhibitor of the Ol lineage in mice. GPR17 knockout mice show an early onset of differentiation of OPCs, whereas transgenic overexpression impairs Ol development and myelination (Chen et al., 2009). Notably, GPR17 is highly abundant within active white matter plaques of MS patients as well as in drug-induced mouse models of demyelinating diseases (Chen et al., 2009). Moreover, genetic absence of *Gpr17* prevents demyelination

and fosters remyelination in a murine autoimmune model of MS, proposing inhibitors of GPR17 as a promising therapeutic strategy to induce remyelination (Ou et al., 2016).

Because GPCRs are excellent therapeutic targets, a screening platform searching for pharmacological blockade of GPR17 may address the unmet therapeutic need to promote remyelination in patients with MS. Unfortunately, complex biological processes like (re-)myelination are difficult to recapitulate *in vitro* and drugs emerging from preclinical studies in rodent MS models have a poor record of success in human clinical trials, thus highlighting the need of novel and/or “humanized” *in vivo* models (Baker and Amor, 2015). In this regard, zebrafish has recently emerged as a new and powerful *in vivo* tool to study particular biological processes, including (re-)myelination (Almeida et al., 2011; Buckley et al., 2010; Czopka, 2016; Early et al., 2018; Nawaz et al., 2015).

1.1 Multiple sclerosis

MS is the most common non-traumatic, neurodegenerative, demyelinating, chronic inflammatory disease of the CNS affecting young adults between 20 and 40 years of age with a higher prevalence in women (Greer and McCombe, 2011; Kobelt et al., 2017). The pathological hallmark of MS is inflammatory lesions leading to demyelinating plaques in the brain and the spinal cord. These lesions are caused by inflammatory infiltrates such as T-cells, B-cells and plasma cells that destroy the myelin sheaths, their associated axons and Ols (Lassmann, 2013). As a consequence, the communication between the brain and the peripheral parts of the body is disrupted. The clinical features and etiopathology of MS are very heterogenous giving MS the prominent name “the disease with thousand faces”. MS is a progressive disease with muscular, balance, visual and sensory symptoms such as stiffness, paralysis, numbness, blurred vision or lightheadedness. Typically, the initial phase of MS is characterized by periods of relapsing neurological deficits that often completely recover in the beginning of the disease. However, as the disease progresses remyelination of the inflammatory lesions becomes insufficient and irreversible damage develops (Franklin and Ffrench-Constant, 2008a; Prineas and Connell, 1979).

1.1.1 Treatment of multiple sclerosis

Since there is no curative therapy for MS, current therapeutic strategies apply disease-modifying drugs to shorten the duration and to decrease the frequency of acute autoimmune outbreaks (Tintore et al., 2019). These therapies include immunosuppressant drugs such as fingolimod, natalizumab or ocrelizumab and immunomodulatory drugs, such as interferon beta,

glatiramer acetate or teriflunomide. Acute MS attacks are treated with short-term therapies consisting of corticosteroids such as methylprednisolone, prednisolone or dexamethasone.

However, there still remains an urgent unmet need for drugs that foster remyelination of demyelinated lesions to preserve the health-related quality of life of patients suffering from demyelinating diseases such as MS. Therefore, to develop new drugs it is important to understand the process of remyelination and why it possibly fails in patients with MS.

1.1.2 Remyelination

Remyelination is the process in which disrupted myelin sheaths of demyelinated axons are replaced or repaired to maintain the saltatory conduction. However, remyelination mostly results in a thinner and shorter myelin sheath compared to the original correlation between axon diameter and myelin sheath thickness (Ludwin and Maitland, 1984). The restoration of myelin sheaths needs the generation of new mature myelinating Ols (Bill et al., 2009)(Prayoonwiwat and Rodriguez, 1993; Sim et al., 2002). Therefore, there is strong evidence that the process of remyelination is triggered by the formation of new OPCs, infiltrating and repopulating the demyelinated lesion (Fancy et al., 2004; Gensert and Goldman, 1997; Groves et al., 1993; Watanabe et al., 2002). Eventually, these newly formed OPCs need to get in contact with those axons to be remyelinated, and differentiate into mature myelinating Ols that replace the destroyed myelin sheaths. Microglia and astrocytes, which are activated by injury, are known to release factors, such as PDGF and FGF that induce the proliferation of OPCs (Murtie et al., 2005; Rhodes et al., 2006; Wilson et al., 2006).

Interestingly, CNS lesions from patients suffering from MS are infiltrated by many OPCs that fail to differentiate into mature myelinating Ols suggesting enhancement of Ol differentiation as potentially promising therapeutic strategy to foster remyelination (Franklin and Ffrench-Constant, 2008b; Huang et al., 2011a).

The process of remyelination is very similar to developmental myelination, thus highlighting the importance to fully recapitulate the process of myelination and oligodendrogenesis during early development. Therefore, a wide range of research focuses on the analysis of promoting remyelination in developing embryos of animal models such as mice or zebrafish (Buckley et al., 2008; Hooijmans et al., 2019).

1.2 Neurulation, neurogenesis and gliogenesis

Prior to oligodendrogenesis and myelination one of the earliest and most complex processes during vertebrate embryogenesis is the neural development (Hill, 2012). Neurulation is initiated when the notochord induces the overlying embryonic ectoderm to become neuroectoderm, which then thickens to form the neural plate (NP). The lateral edges of the NP elevate into neural folds (NFs). As the NFs continue to rise, they start to converge and eventually fuse to form the neural tube (NT). The tissue at the interface between NT and remaining embryonic ectoderm is called neural crest, whose cells delaminate and migrate through the embryo to form, among other structures, the peripheral nervous system (PNS) (Hall, 2008; Ladher and Schoenwolf, 2005). The fusion of the NP to form the NT begins in the middle of the embryo, from where it continues cranially and caudally, with the cranial section becoming the brain and the caudal section becoming the spinal cord (Schoenwolf and Smith, 1990). Neural development is not only one of the most complex, but also the longest lasting embryonic process as the nervous system undergoes continuous remodeling, partially reflected by life-long myelin sheath adaptation, long after developmental completion (Bercury and Macklin, 2015). Vertebrate neurulation is illustrated in **Figure 1**.

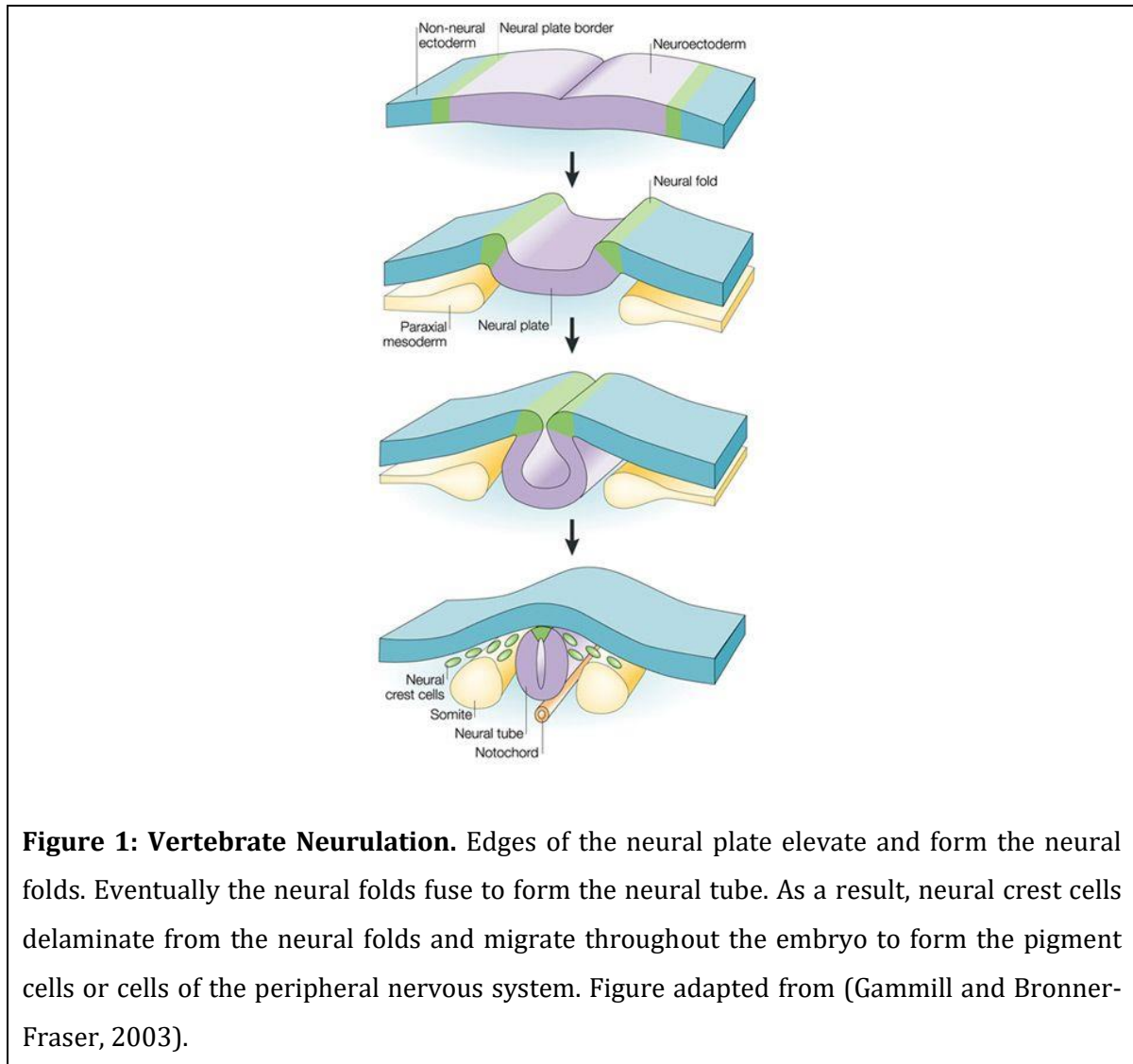
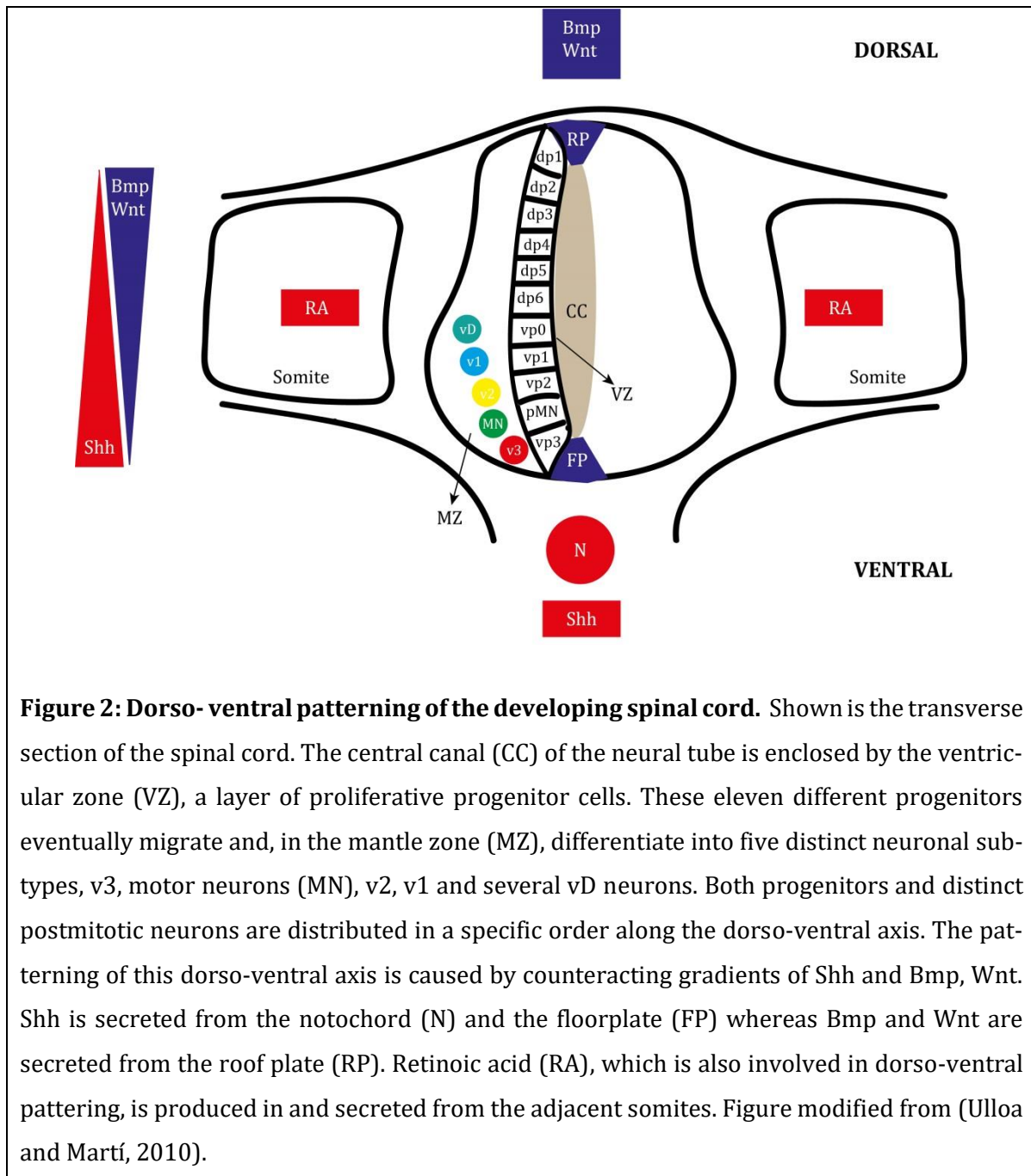


Figure 1: Vertebrate Neurulation. Edges of the neural plate elevate and form the neural folds. Eventually the neural folds fuse to form the neural tube. As a result, neural crest cells delaminate from the neural folds and migrate throughout the embryo to form the pigment cells or cells of the peripheral nervous system. Figure adapted from (Gammill and Bronner-Fraser, 2003).

The NT accommodates distinct classes of stem cells that eventually give rise to two major classes of neural progenitor cells: neuronal progenitors and glial progenitors (Murphy et al., 1997; Hill, 2002). Neuronal progenitor and glial progenitor cells undergo complex stages of maturation (James Briscoe, 2008; Ulloa and Martí, 2010) to differentiate into neurons and glia cells respectively, that are the most abundant cells in the CNS (Morest and Silver, 2003).

The ventral spinal cord occupies five distinct neuronal subtypes arising from eleven different neuronal progenitor cells in a precise spatial order (Wilson and Maden, 2005; James Briscoe, 2008). Interestingly, neuronal progenitor cells that differentiate in the ventral part of the spinal cord are responsible for the efferent motor control while in the dorsal region they differentiate into neurons that process and organize afferent sensory information. This dorso-ventral (DV) patterning of the spinal cord is controlled by different secreted signaling molecules during development, including Sonic hedgehog (Shh), Wingless/Integrated (Wnts), Bone morphogenetic proteins (Bmp), Fibroblast Growth Factors (FGF) and Retinoic Acid (RA) (Wilson

and Maden, 2005). Counteracting gradients of Shh, which is secreted from the notochord and the floor plate, and Bmps and Wnts, produced from the dorsal roof plate of the ventral spinal cord, are believed to be the main players of DV pattern formation (Bertrand et al., 2002; Ulloa and Martí, 2010). Vertebrate DV patterning of the developing spinal cord is displayed in **Figure 2**.



After initial formation of the spinal cord, neural progenitor cells arranged around the ventral midline of the neural tube, namely primary motor neuron (pMN) region, start to express the basic-helix-loop helix (bHLH) transcription factors Olig1 and Olig2. These progenitor cells are

called pMN progenitors and give rise to motor neurons and subsequently to Ols (Lu *et al.*, 2002). The transition of stem cells to become neurons or glia cells is a complex interaction between regulatory proneural and proglial signals during vertebrate neural development. It starts with a change in stem-cell properties that is controlled by intrinsic and extrinsic cues (Qian *et al.*, 2000; Temple, 2001). The first period of differentiation is mainly determined by neurogenic signals leading to expression of proneural genes. Among others, bone morphogenic protein 2 (BMP2) and erythropoietin (Epo) have been shown to induce expression of proneural proteins like ASCL1 (Bertrand *et al.*, 2002; Shingo *et al.*, 2001), resulting in the induction of the neuronal signaling pathway, the inhibition of glial differentiation and cell cycle arrest. At the same time these proneural signals induce the Notch signaling pathway in adjacent cells, which inhibit proneural genes and thereby preventing them from entering the neuronal pathway (Casarosa *et al.*, 1999; Chitnis and Kintner, 1996; Ma *et al.*, 1998). Keeping the balance between cells that enter the neuronal pathway and cells that remain undifferentiated is essential to maintain a pool of cells that later become glial cells (Perron and Harris, 2000). Subsequently, gliogenesis is initiated by several gliogenic signals like fibroblast growth factor 2 (FGF2), ciliary neurotrophic factor (CNTF) and BMPs, resulting in glial differentiation and inhibition of neurogenesis (Johe *et al.*, 1996). Differentiation towards glial cells and inhibition of neurogenesis is mediated by downstream signaling molecules of these gliogenic signals, such as proneural inhibitors of the inhibitor of differentiation (Id)- and hairy and enhancer of split (Hes) family (Nakashima *et al.*, 2001). Furthermore, gliogenic pathways lead to degradation of proneural proteins and to repression of proneural gene transcription (Shou *et al.*, 1999). Supposedly, proneural proteins, inducing both neurogenic and gliogenic signals, are essential intrinsic factors that alter the fate of neural stem cells in response to their changing environment (Anderson, 2001). A schematic model of neurogenic and gliogenic molecular pathways is illustrated in **Figure 3**.

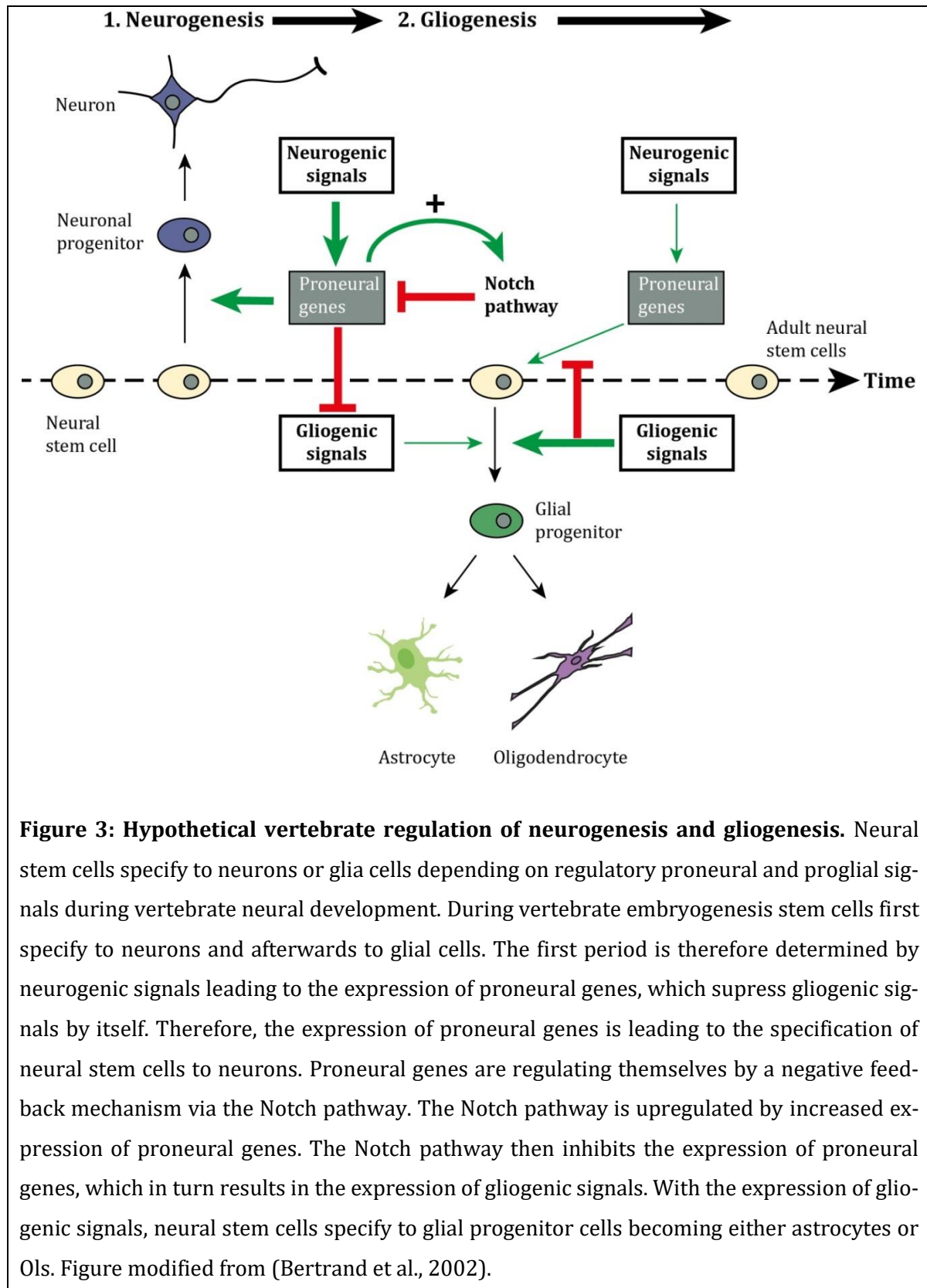
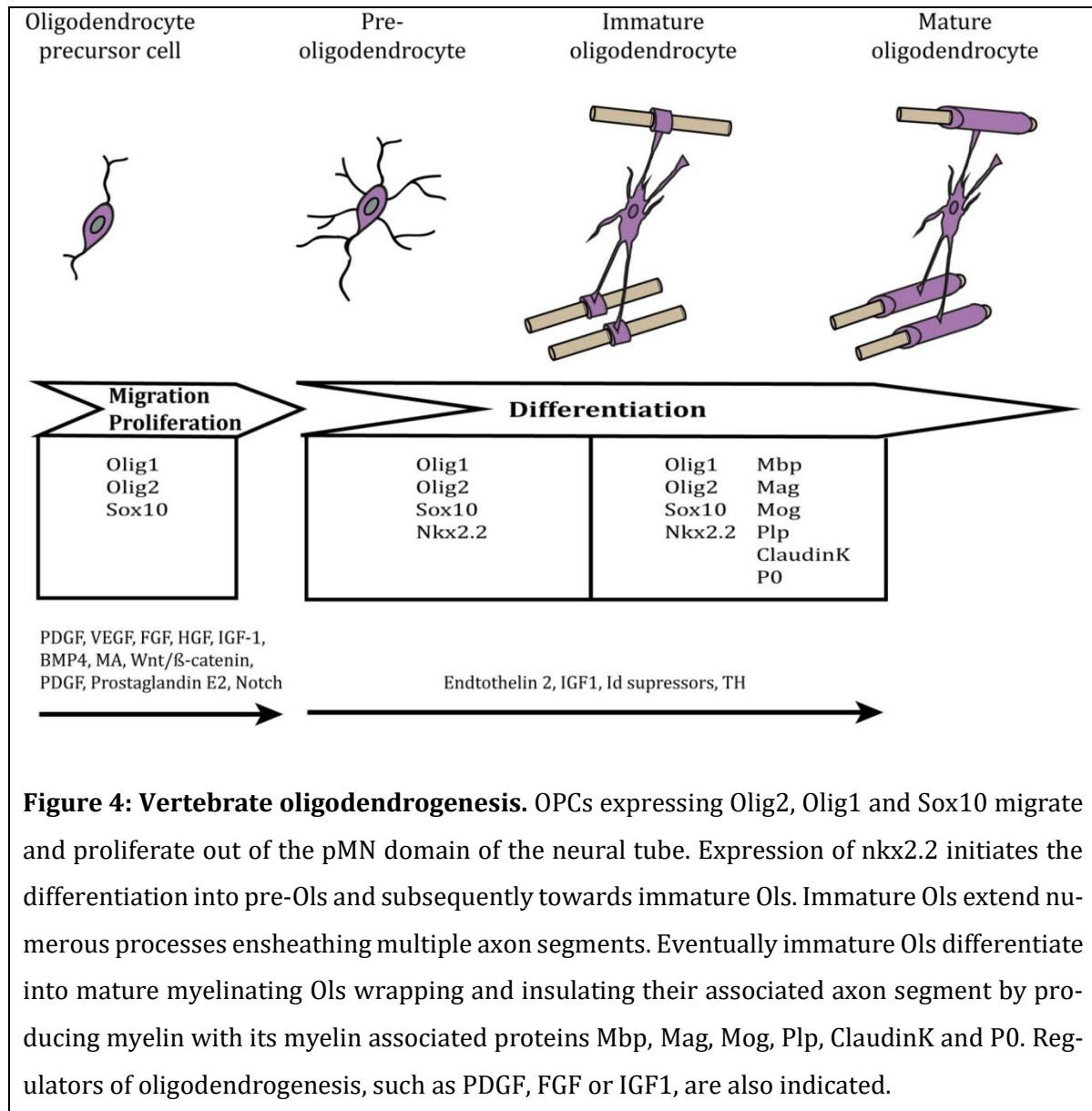


Figure 3: Hypothetical vertebrate regulation of neurogenesis and gliogenesis. Neural stem cells specify to neurons or glia cells depending on regulatory proneural and progial signals during vertebrate neural development. During vertebrate embryogenesis stem cells first specify to neurons and afterwards to glial cells. The first period is therefore determined by neurogenic signals leading to the expression of proneural genes, which suppress gliogenic signals by itself. Therefore, the expression of proneural genes is leading to the specification of neural stem cells to neurons. Proneural genes are regulating themselves by a negative feedback mechanism via the Notch pathway. The Notch pathway is upregulated by increased expression of proneural genes. The Notch pathway then inhibits the expression of proneural genes, which in turn results in the expression of gliogenic signals. With the expression of gliogenic signals, neural stem cells specify to glial progenitor cells becoming either astrocytes or Ols. Figure modified from (Bertrand et al., 2002).

1.3 Oligodendrogenesis

During vertebrate CNS development, glial progenitor cells located in the ventral pMN region give rise to OPCs that start to express transcription factors such as Olig1/2 and Sox10 to proliferate and migrate dorsally in the neural tube, subsequently differentiating into myelinating Ols (Claus Stolt et al., 2002; Li et al., 2007; Lu et al., 2002). Once expression of the transcription factor *nkx2.2* is induced, OPCs stop migrating and start to differentiate into pre-Ols and subsequently towards immature Ols, which extend numerous processes to ensheath segments of multiple axons (Zhou et al., 2001). Eventually, immature Ols mature into myelinating Ols, wrapping and insulating their associated axon segments by producing myelin sheaths (Emery, 2010). One individual Ol can myelinate up to 40 axonal segments (Pfeiffer et al., 1993). OPC development into mature myelinating Ols is accompanied by complex morphological changes of the distinct Ol lineage cells. The process of myelination is dependent on the expression of several myelin-associated proteins such as myelin basic protein (Mbp), proteolipid protein (Plp), myelin protein zero (Mpz/P0), myelin oligodendrocyte glycoprotein (Mog) or myelin-associated glycoprotein (Mag) (Pfeiffer et al., 1993). These transcription factors and proteins serve as specific markers for the distinct cell types towards mature Ols. When this process is disturbed due to cell death, local OPCs are activated and proliferate to maintain a homeostatic balance in the number of OPCs (Hughes et al., 2013). Taken together, the development of the Ol lineage is highly complex and many signaling cascades regulate the single stages of migration, proliferation and differentiation. Vertebrate oligodendrogenesis is shown in **Figure 4**.



1.3.1 Regulators of oligodendrogenesis

Olig2-expressing (olig2⁺) OPCs depend on platelet derived growth factor (PDGF) for proliferation and migration (Richardson et al., 1988). OPCs contain growth-cone like structures to recognize a variety of chemotactic signals guiding them to their final destination (Simpson and Armstrong, 1999). Some types of growth factors, such as vascular endothelial growth factor (VEGF), fibroblast growth factor (FGF) and hepatocyte growth factor (HGF) are known to regulate OPC migration (McMorris and Dubois-Dalcq, 1988; Milner *et al.*, 1997; Yan and Rivkees, 2002; Bribián *et al.*, 2006; Hayakawa *et al.*, 2011, 2012; Murcia-Belmonte *et al.*, 2014).

Once OPCs reach their final destination they start to proliferate to subsequently differentiate into mature myelinating OLs. Several extracellular signals such as BMP4-, muscarinic

acetylcholine (MA), Wnt/ β -catenin-, PDGF-, Prostaglandin E2- and Notch-signaling are known to promote proliferation and to inhibit differentiation (Calver et al., 1998; Deshmukh et al., 2013; Dizon et al., 2011; Fancy et al., 2009; Franklin, 2015; Lee et al., 2015; Reid et al., 2012; Scafidi et al., 2014; Shioh et al., 2017; Wang et al., 1998). The transcription factors Id2, Id4 and Hes5, downstream of these extracellular signals, are known to prevent OPC differentiation (Kondo and Raff, 2000; Norton et al., 1998).

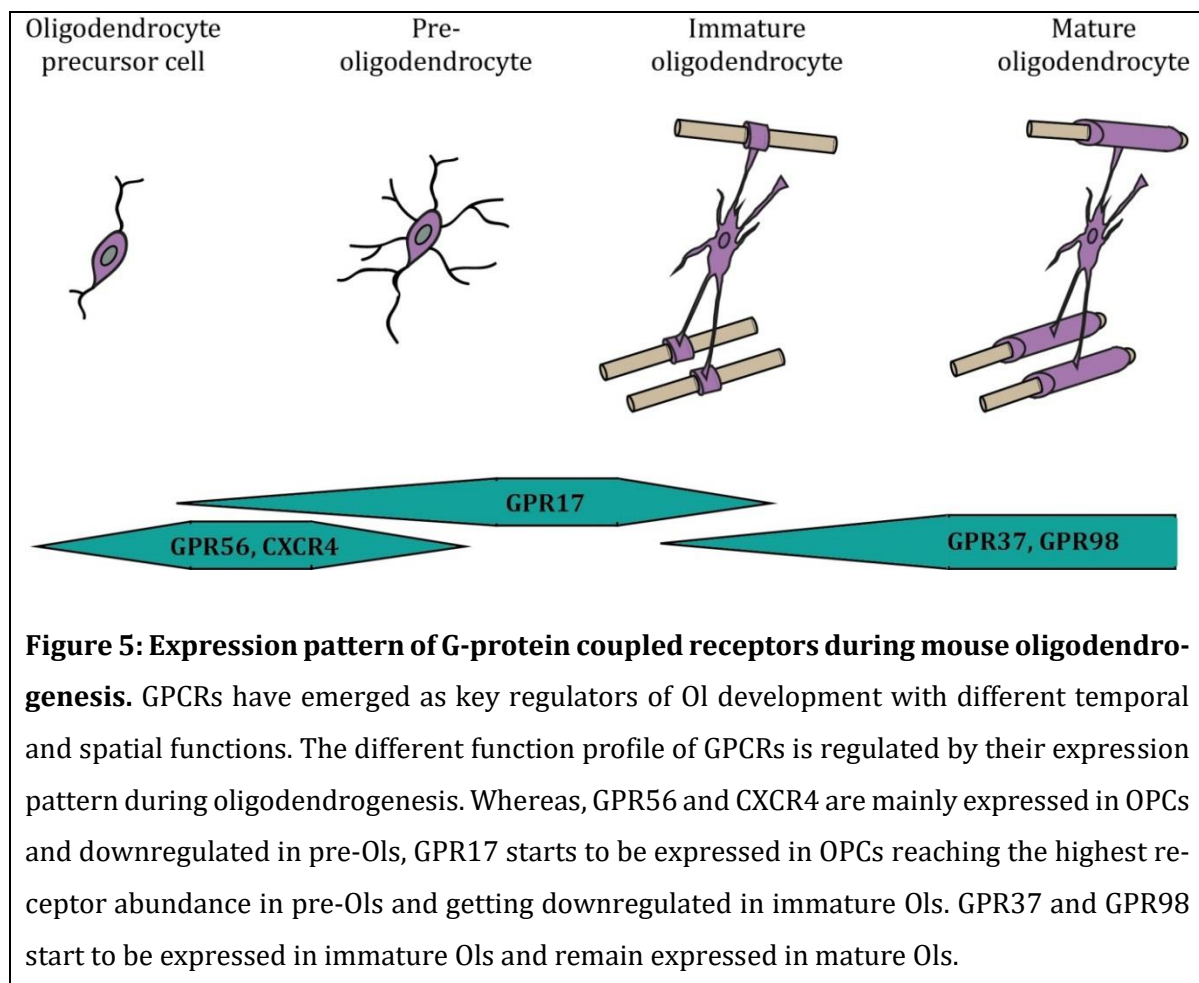
Eventually, other signaling pathways, such as Endothelin 2, insulin-like growth factor 1 (IGF1), Id suppressors or thyroid hormones (TH), initiate OPC differentiation into mature myelinating Ols (Barres et al., 1994; Cai et al., 2011; Ibarrola et al., 1996; Patel et al., 2010; Ye et al., 2007; Yuen et al., 2013). Furthermore, posttranscriptional regulation by microRNAs has been shown to have a pivotal role in Ol differentiation preventing transcription of differentiation inhibitors (Dugas et al., 2010; Zhao et al., 2010). Interestingly, undifferentiated OPCs remain present throughout adulthood to maintain myelin adaptations and repair after disruption of myelin sheaths (Gautier et al., 2015). Therefore, some of the discussed developmental signals may serve as potential therapeutic targets to promote white matter development during adulthood. Regulators of vertebrate oligodendrogenesis are shown in **Figure 4**.

Recently, GPCRs have emerged as key regulators of Ol development with different temporal and spatial functions (Mogha et al., 2016). GPCRs are seven transmembrane (7TM) receptors, whose N-terminal part is extracellularly and the C-terminal part intracellularly located. GPCRs regulate many different intracellular signaling cascades in response to diverse stimuli such as hormones, ions, neurotransmitters, photons and others. 7TM receptors are classified into five superfamilies: glutamate-, rhodopsin-, adhesion-, frizzled- and secretin receptors (Fredriksson et al., 2003). They represent the largest receptor family among pharmaceutical drug targets in mammals (Hauser et al., 2017; Rask-Andersen et al., 2011).

One such GPCR is GPR37, which starts to be expressed in pre-Ols and later in mature Ols. It is considered as a negative regulator of Ol differentiation since loss of GPR37 results in premature Ol differentiation, causing hypermyelination during development and adulthood (Yang et al., 2016). Furthermore, the adhesion GPCR GPR56, which is expressed during early stages of Ol development, has been shown to be a crucial regulator of OPC proliferation and differentiation. Absence of GPR56 causes a reduced number of mature Ol and hypomyelination of axons resulting from decreased OPC proliferation (Ackerman et al., 2015; Giera et al., 2015). At later stages of development another adhesion GPCR GPR98 expressed in myelinating Ol revealed to be a differentiation inhibitor of the Ol lineage *in vitro* (Shin et al., 2013). Similar to GPR37, the orphan receptor GPR17 has been described as a negative regulator of Ol differentiation and myelination in mice. GPR17 starts to be expressed in OPCs, being abundant in pre-Ols but not

detectable in mature Ols in mice (Boda et al., 2011; Chen et al., 2009). Hence, *GPR17* is a GPCR of particular interest in the context of Ol development and myelination and will be introduced in detail in the next chapter. Expression of GPCRs during Ol development is shown in **Figure 5**.

Moreover, several other GPCRs such as KOR, GPR30, sphingosin-1 phosphate receptors (S1P1), Cxcr4 and endothelin receptors are also known to regulate CNS myelin repair, highlighting GPCRs as potential therapeutic targets for demyelinating diseases (Deshmukh et al., 2013; Du et al., 2016; Mei et al., 2014, 2016; Najm et al., 2015).



1.3.2 The orphan G protein-coupled receptor 17 and its role during oligodendrocyte development

GPR17 belongs to the rhodopsin-like 7TM GPCR superfamily and was first characterized by Raport and collaborators in 1996 (Raport et al., 1996). Transcriptome analysis revealed that *GPR17* is one of the most important genes expressed in adult and fetal neuroprogenitor cells (Maisel et al., 2007). Its phylogenetic position is located between P2Y purinergic and cysteinyl

leukotriene receptors (Ciana et al., 2006). Although a lot of research has already been performed investigating the endogenous ligand of GPR17, the results are remaining controversial (Bened-Jensen and Rosenkilde, 2010; Bläsius et al., 1998; Heise et al., 2000; Qi et al., 2013; Simon et al., 2017). Therefore, GPR17 is still considered as an orphan receptor. Intriguingly, a small synthetic molecule MDL29,951 (2-carboxy-4,6-dichloro-1H-indole-3-propionic acid) revealed to be a reproducible and selective agonist of GPR17 in primary rat Ols as well as in heterologous expression systems (Hennen et al., 2013).

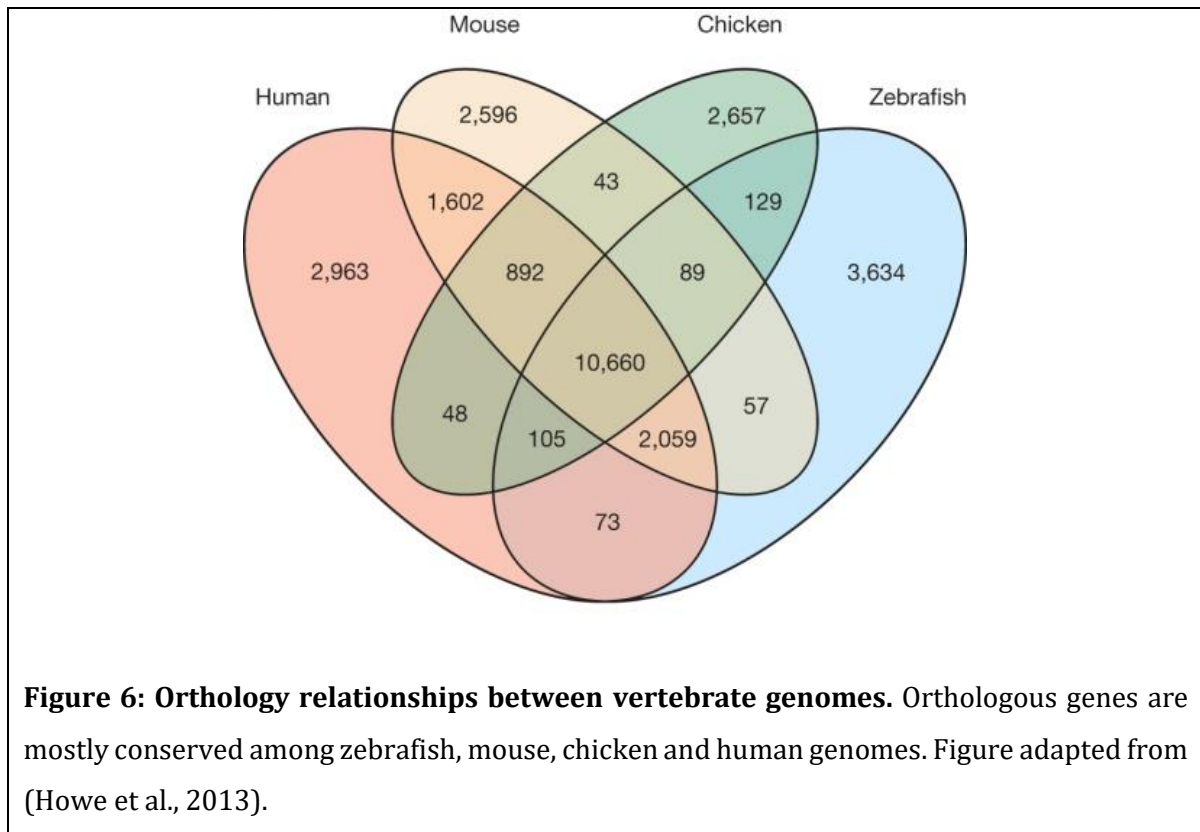
In humans and non-human primates GPR17 exists in two isoforms with different length of their N-terminus, the short- (GPR17-S, 339 amino acids) and the long isoform (GPR17-L, 369 amino acids) (Bläsius et al., 1998). Whereas the expression of the isoform GPR17-S is more abundant in brain and spinal cord compared to GPR17-L, the opposite was observed in heart and kidney. Notably, both isoforms are expressed in organs susceptible to ischemic injury and it has already been shown that GPR17 is involved in the evolution of ischemic brain and traumatic spinal cord injury (Ceruti et al., 2009; Ciana et al., 2006; Lecca et al., 2008). Furthermore, differences in the pharmacological profile could be observed for both isoforms, indicating tissue specific roles for both human isoforms (Bened-Jensen and Rosenkilde, 2010). The expression pattern of GPR17-S is similar to mice and rat GPR17, being detected in OPCs and highly expressed in pre-Ols, but not detectable in mature Ols (Bened-Jensen and Rosenkilde, 2010; Bläsius et al., 1998; Chen et al., 2009; Ciana et al., 2006; Lecca et al., 2008). Expression of GPR17 in neurons still remains controversial (Chen et al., 2009; Lecca et al., 2008; Maisel et al., 2007).

The expression profile of GPR17 and its downregulation during Ol maturation already indicates a spatial and temporal receptor function. Furthermore, *Gpr17* knockout mice show an early onset of differentiation of OPCs, whereas transgenic overexpression prevents Ol development and myelination (Chen et al., 2009). Therefore, GPR17 is a differentiation inhibitor of Ol lineage cells in mice. Similar findings could be observed using primary rat Ols. Activation of GPR17 by MDL29,951 resulted in decreased *mbp* expression levels (Simon et al., 2016). Notably, GPR17 is highly abundant within active white matter plaques of MS patients as well as in drug-induced mouse models of demyelinating diseases (Ceruti et al., 2009; Chen et al., 2009; Lecca et al., 2008; Zhao et al., 2012). Moreover, genetic absence of *Gpr17* prevents demyelination and fosters remyelination in a murine autoimmune model of MS indicating GPR17 as a promising therapeutic target to foster remyelination (Ou et al., 2016).

1.4 The zebrafish

Within the phylum Chordata, zebrafish (*Danio rerio*) belong to the class Actinopterygii and the family Cyprinidae. Zebrafish is a freshwater teleost of South-East Asian origin. The majority of zebrafish genes are conserved across other vertebrate species (**Figure 6**). Notably, 71.4 % of human genes have at least one zebrafish orthologue and 69 % of zebrafish genes have at least one human orthologue, making zebrafish a robust vertebrate model system applicable to study human diseases and biology or to perform pharmacological drug screens (Driever et al., 1994; Howe et al., 2013).

Zebrafish produce a large number of offspring that develop rapidly *ex utero*. Following fertilization, a zebrafish egg develops into a freely swimming animal within three days, and after five days post fertilization (dpf) embryogenesis is completed and the larvae exhibit most of the mammalian organs (Kimmel et al., 1995). The small size and their translucent nature during embryogenesis makes zebrafish an excellent model for *in vivo* live imaging and whole mount protein and RNA visualization. Consequently, many transgenic zebrafish reporter lines were generated that express fluorescent exogenous proteins under the control of specific transcription factors to investigate tissue or cell specific events (Preston and Macklin, 2015). Moreover, external fertilization and development of zebrafish allow feasible genetic manipulation by direct injection into fertilized eggs. Therefore, many genetical modifying techniques have been adapted to zebrafish, such as the Tol2 transposon system, the modified Bacterial Artificial Chromosome system (BAC), the GAL4/UAS binary transcription system, and the knockout methodologies Zinc Fingers, TALENs and CRISPR Cas (Blackburn et al., 2013; Bussmann and Schulte-Merker, 2011; Campbell et al., 2013; Davison et al., 2007; Kwan et al., 2007; Suster et al., 2011; Urnov et al., 2010). For more precise spatial and temporal control of gene expression, techniques such as heat shock promoter-driven activation of transcription and Cre-mediated systems, have also been adapted to zebrafish (Thummel et al., 2005; Zhan and Gong, 2010). Partial knock down of proteins can be easily performed by injection of translation or splice blocking antisense morpholinos (Bill et al., 2009).



1.4.1 Oligodendrocyte development, myelination and remyelination in zebrafish

Notably, several studies have demonstrated that the fundamental structure of myelin, Ol specific markers and myelination regulating transcription factors such as Nkx2.2, Sox10, Olig1 and Olig2 are highly conserved between fish and mammals (Kucenas et al., 2008; Monk and Talbot, 2009; Raphael and Talbot, 2011). All important myelin proteins such as Mbp, Mpz/P0 and Plp are expressed in zebrafish (Bai et al., 2011; Nawaz et al., 2013; Schweitzer et al., 2006). Furthermore, several novel myelin proteins have been found in zebrafish, such as ClaudinK, Zwilling-A, Zwilling-B and 36k (Münzel et al., 2012; Schaefer and Brösamle, 2009). However, some differences between zebrafish and mammalian myelin have been reported. Whereas Mpz/P0 exclusively has been found in the CNS in mammals, it has also been identified in the PNS and CNS in zebrafish. Moreover, no paralogue of 36k, a major component of zebrafish myelin, has been found in mammals (Morris et al., 2004; Waehneltdt and Jeserich, 1984).

In zebrafish Ols derive from olig2⁺ neural precursor cells inside the pMN domain of the neural tube within the ventral spinal cord, similar to the mammalian oligodendrogenesis (Park et al., 2002; Shin et al., 2003). Here, Sonic Hedgehog and notch signaling also regulate OPC specification and development (Schebesta and Serluca, 2009). During the first 24-30 hpf, neural stem cells specify to OPCs. Approximately at 50 hpf OPCs start to migrate dorsally out of the ventral

Introduction

spinal cord searching for their axon to myelinate (Kirby et al., 2006). During migration OPCs move rostrally and caudally attaching and detaching axon tracks while extending and retracting their numerous processes. With time lapse imaging it has been shown that individual OPCs are sensitive to their surrounding environment avoiding contact with other OPCs (Kirby et al., 2006). Therefore, it is hypothesized that there exists a defined density of OPCs. With the up-regulation of the transcription factor *nkx2.2a*, starting approximately at 2.5 dpf, differentiation of OPCs is initiated (Kucenas et al., 2008). At 3 dpf first mature Ols are present in the dorsal part of the ventral spinal cord expressing myelin associated proteins such as ClaudinK to form nascent myelin. Furthermore, Ols seem to have an intrinsic plasticity, responding to adjacent signals to assess the required amount of myelin (Almeida et al., 2011). Within a 5 hour window after formation of their first nascent internode, individual Ols form their full subset of internodes (Czopka et al., 2013). At 7 dpf first compact myelin sheaths are found in zebrafish (Brösamle and Halpern, 2002). Oligodendrogenesis continues approximately a month, whereas myelination constantly proceeds into adulthood in zebrafish (Jung et al., 2010; Park et al., 2007). Ol development during zebrafish embryogenesis is shown in **Figure 7**.

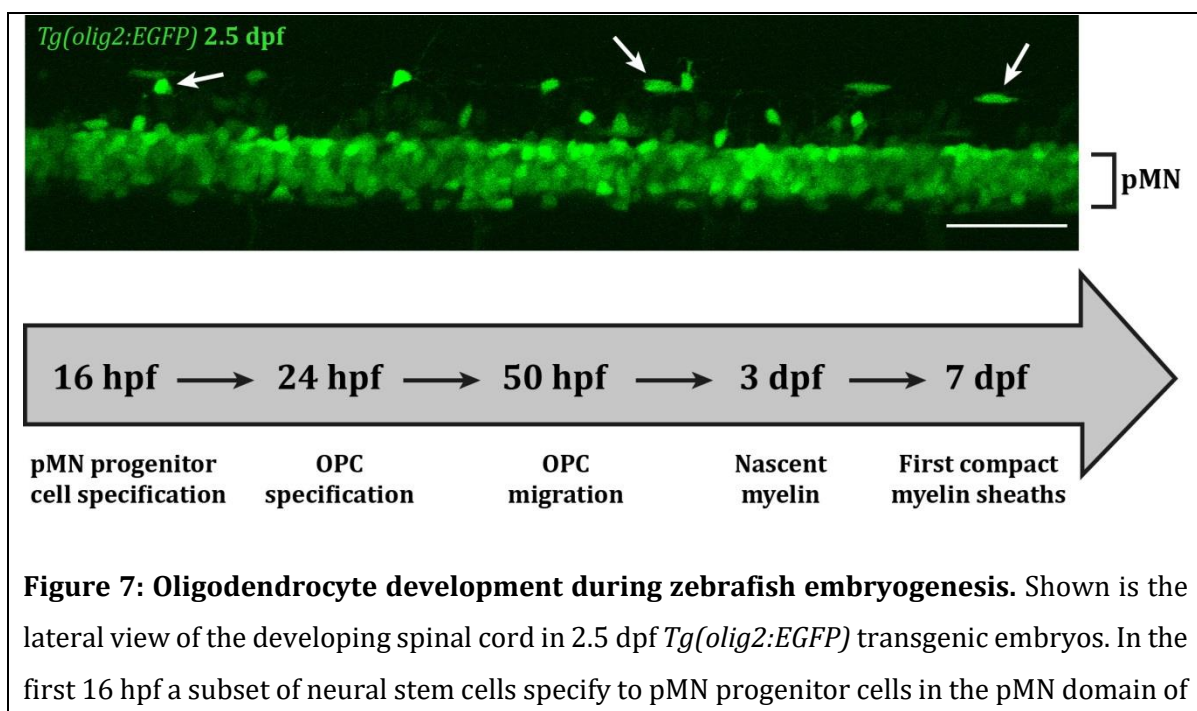


Figure 7: Oligodendrocyte development during zebrafish embryogenesis. Shown is the lateral view of the developing spinal cord in 2.5 dpf *Tg(olig2:EGFP)* transgenic embryos. In the first 16 hpf a subset of neural stem cells specify to pMN progenitor cells in the pMN domain of

the ventral spinal cord. PMN progenitor cells give rise to proliferative OPCs during the next 8 hours. Approximately at 50 hpf OPCs start to migrate dorsally out of the pMN domain. Once they find their target to myelinate, migration stops and OPCs start to differentiate into mature Ols. First nascent myelin is detectable at 3 dpf, whereas first compact myelin is detectable only at 7 dpf. Ol lineage cells are shown with arrows. Scalebar is 50 μ m. Figure modified from (Preston and Macklin, 2015).

Zebrafish have the extraordinary ability to regrow entire organs after damage (Shi et al., 2015). In contrast to mammals, where remyelination largely fails, larval and adult zebrafish exhibit the remarkable talent to fully regenerate damaged axons after spinal cord injury (Becker and Becker, 2008; März et al., 2011). One of the reasons for that difference could be that zebrafish do not form a glial scar after nervous damage (Goldshmit et al., 2012). A glial scar is an inhibitory environment that prevents maturation of OPCs resulting in failed remyelination (Huebner and Strittmatter, 2009). When mature Ols and myelinated axons are laser ablated in the dorsal part of the zebrafish spinal cord, nearby anterior, posterior and ventral OPCs start to proliferate and migrate within the ablated region remyelinating the regrowing axons within two weeks (Karttunen et al., 2017).

1.4.2 Zebrafish as a powerful model organism to study CNS myelination and remyelination

The process of myelination and remyelination with complex intercellular interactions between Ol lineage cells, axons, microglia, astrocytes and the vasculature is difficult to simulate in cell culture systems, making *in vivo* model organisms the gold standard for longitudinal studies of myelination and remyelination. A substantial issue with investigating myelination *in vivo* is that myelination is the last major event during CNS development and lasts over a long time, making the investigation of such a complex intercellular process technically challenging in rodent models. Whereas robust myelination in mice starts at birth and continues during the first month, the process of axonal ensheathment occurs within the first week after fertilization in zebrafish (Baumann and Pham-Dinh, 2001; Brösamle and Halpern, 2002). Their high number of rapidly developing offspring dramatically shortens the time that is needed to study myelination *in vivo* while increasing the amount of data at the same time. Moreover, the translucent nature and the availability of many fluorescent reporter lines developing outside the mother, make zebrafish an advantageous and powerful model to study myelination and remyelination non-invasively by real-time microscopy (Preston and Macklin, 2015). The

Introduction

accessibility of different fluorescent reporter lines that label subsets of Ol cell bodies and/or their myelin sheaths provide for specific investigation of myelination in intact tissue complexity (Preston and Macklin, 2015).

Besides laser ablation there are many other techniques to provoke demyelination and induce remyelination in zebrafish, such as the chemical demyelination with lysophosphatidylcholine or the use of transgenic expression of nitro reductase in Ols (Chung et al., 2013; Münzel et al., 2014). Notably, zebrafish possess the full complement of immune cells and an immune response similar to rodent EAE models can be simulated by immunization with a homogenate of the CNS (zCNS) and Complete Freund's Adjuvant (CFA) (Gray et al., 2011; Langenau et al., 2004; Quintana et al., 2010). For the above reasons zebrafish has emerged as a handy, inexpensive but powerful tool to study myelination and remyelination *in vivo* (Buckley et al., 2008; Chung et al., 2013; Czopka, 2016; Driever et al., 1994; Kazakova et al., 2006; Kirby et al., 2006; McCurley and Callard, 2010; Münzel et al., 2012; Preston and Macklin, 2015).

1.4.3 Zebrafish: a tool for *in vivo* drug discovery

The translucent nature, the small size and the high number of offspring developing ex utero make zebrafish a popular *in vivo* model to perform large scale genetic and chemical screens (Buckley et al., 2010; Driever et al., 1996; Kazakova et al., 2006; Kokel and Peterson, 2011; Pichler et al., 2003; Rennekamp and Peterson, 2015; Zon and Peterson, 2005). Large scale screenings are easy to handle using zebrafish larvae because compounds can be taken up by the embryos after addition to their aqueous environment at specific developmental time points. Additionally, the toxicity of drugs can be easily assessed at the same time by inspecting the development of treated larvae. With the use of Ol lineage specific fluorescent reporter lines, zebrafish has emerged as a powerful screening model to test potential pro-myelinating drugs for the treatment of demyelinating diseases (Buckley et al., 2010; Early et al., 2018; Preston and Macklin, 2015). For example, the use of transgenic lines with GFP expression, such as *Tg(olig2:EGFP)*, *Tg(claudinK:EGFP)*, *Tg(mbp:EGFP)*, *Tg(mbp:CAAX-EGFP)* and *Tg(nkx2.2a:mEGFP)*, is an established method to quantify chemical or genetic treatments affecting oligodendrogenesis and myelination by quantifying the respective number of dorsal cells and comparing them to control treatment.

1.5 Aim of this study

The process of remyelination fails in patients with MS and currently there is no pharmaceutical therapy promoting remyelination. Notably, GPR17 an Ol differentiation inhibitor is upregulated in demyelinated lesions of MS patients and inhibition of GPR17 in a murine autoimmune model of MS promotes remyelination (Chen et al., 2009; Ou et al., 2016). Thus, inhibition of GPR17 provides a promising therapeutic approach to promote remyelination in patients with MS. Complex biological processes like (re-)myelination are difficult to recapitulate *in vitro*. Therefore, the development of novel therapies promoting remyelination, require *in vivo* examination within animal models. Drugs emerging from preclinical studies in animal MS models are often ineffective in human clinical trials, thus highlighting the need for “humanized” animal models (Baker and Amor, 2015).

For the above reasons, aim of this study is to exploit zebrafish with its experimental advantages for the establishment of a humanized *in vivo* platform capable of identifying specific inhibitors of human GPR17 as therapeutic compounds promoting remyelination in patients with MS. Therefore, this study intends to investigate the role of Gpr17 in zebrafish in order to generate “humanized” zebrafish lines that express either the human GPR17 or a human/zebrafish chimeric GPR17. The chimeric GPR17 contains the human extracellular and transmembrane regions with the human ligand binding domain and the intracellular loops of zebrafish Gpr17. By humanizing Gpr17 in zebrafish we are aiming to provide a screening tool to find GPR17 inhibitors with higher chances of success in human clinical trials.

Until now, performing large chemical screens affecting myelination or remyelination in zebrafish have been very laborious and time-consuming. An automated *in vivo* screening

Introduction

system would not only simplify and fasten screens for antagonists of GPR17 but would also be of great interest for research groups that screen drugs affecting OI development. Therefore, this thesis also deals with the establishment of an automated, generally applicable and straight-forward imaging system for the rapid screening of potential compounds affecting human GPR17 in zebrafish larvae.

2 Materials

2.1 Chemicals

Chemicals	Company/Sources	Product number
(4-(2-hydroxyethyl)-1-piperazineethanesulfonic acid) (HEPES)	VWR	441487M
10x Tris/Glycine/SDS	Biorad	1610772
6x DNA Loading buffer	Thermo Fisher Scientific	R0611
Agarose LE	Biozym	840004
Agarose Type IX-A, Ultra-low Gelling Temperature	Sigma-Aldrich	A2576
Ampicillin sodium	Sigma	A0166
Ampuwa water	Ampuwa	09016871/100
Buffer Tango	Thermo Fisher Scientific	BY5
Chloroform	PanReac Applichem	A1585
Cutsmart buffer	NEB	#B7204S
DEPC water	Roth	T143.3
Dimethyl sulfoxide (DMSO)	Sigma	D8418
Disodium phosphate		
dNTPs 100mM solutions	Thermo Fisher Scientific	R0182
DreamTaq™ buffer	Thermo Fisher Scientific	B65
Dulbecco's Phosphate-Buffered Saline (DPBS)	Gibco by Life Technologies	14190-094
EDTA-disodium	Serva	39760.01
Ethanol absolute	PanReac Applichem	A1613
Ethidium bromide 1 %	Sigma Aldrich	46067
Ethyl 3-aminobenzoate methane sulfonate (MS222)	Fluka Analytical	A5040
Formamide	Sigma Life Science	47671
GANT61	Sigma Life Science	G9048
GeneRuler 1 kb DNA ladder 250 to 10000 bp	Fisher Scientific GmbH	SM0311

Materials

GeneRuler 100 bp plus DNA ladder	Fisher Scientific GmbH	SM0321
GeneRuler Ultra Low range DNA ladder	Fisher Scientific GmbH	SM1211
Glycerol	Merck	104093
Green GC Phusion Buffer	NEB	F539L
Heparin sodium salt from porcine	Sigma-Aldrich	104093
Intestinal mucosa		
Instant Ocean Sea Salt	Instant Ocean	SS15-10
Isopropyl alcohol	Calroth	6752.4
Magnesium sulphate heptahydrate	Merck	1.05886.1000
Methanol	PanReac Applichem	131091.161
Methylene blue	Merck Darmstadt	6040
Mineral oil	Sigma	M5904
N-Phenylthiourea (PTU)	Sigma	P7629
Normal Goat Serum	Sigma Aldrich	G9023
Nuclease-free water	Qiagen	129144
Paraformaldehyde	Sigma-Aldrich	158127
Phenol red	Sigma-Aldrich	P0290
Phusion HF buffer	Thermo Fisher Scientific	F518
Potassium dihydrogen phosphate		
Potassium chloride	Fluka Chemika	351861/1
Protease from <i>Streptomyces griseus</i> XIV	Sigma-Aldrich	P5147
Proteinase K	PanReac AppliChem	A3830,0100
SKP-C25	Xcessbio	M60136-2s
Sodium chloride	AppliChem	A2942,1000
SSC buffer 20x	Gibco by life technologies™	15557-044
Trichostatin A (TSA)	Sigma Aldrich	T8552
Tris-HCl	Calroth	9090.3
TRIzol Reagent	Ambion by life technologies™	T9424
Tween 20	Sigma Aldrich	P9416

2.2 Enzymes

Enzyme	Company	Product number
DreamTag® DNA Polymerase	Thermo Fisher Scientific	EP0701
MseI	New England Biolabs®	R0525S
Phusion®	Thermo Fisher Scientific	F5305
TatI	Thermo Fisher Scientific	ER1291

2.3 Buffer and solution-Recipes

100 ml 1M HEPES

HEPES	23.8 g
dH ₂ O	100 ml

Adjust pH with 1N NaOH to 7.2.

100 ml 0.5M HEPES

1M HEPES	50 ml
dH ₂ O	50 ml

2.5 liters of 3x Danieau

2.9M NaCl	150 ml
60mM Ca(NO ₃) ₂	75 ml
70mM KCl	75 ml
0.5M HEPES	75 ml
40mM MgSO ₄ ·7H ₂ O	75 ml
dH ₂ O	2050 ml

10 liters of 0.3x Danieau

3x Danieau	1 L
dH ₂ O	9 L

1 liter of 0.3x Danieau + methylene blue

500x methylene blue	2 ml
0.3x Danieau	998 ml

1 liters of 0.3x Danieau + PTU

50x PTU	20 ml
0.3x Danieau	980 ml

100 ml 1M PO₄ buffer

1M Na ₂ HPO ₄	80 ml
1M NaH ₂ PO ₄	20 ml

Adjust pH to 7.3

Materials

500 ml 10X PBS

NaCl	40.0 g
KCl	1.0 g
1M PO ₄ Buffer	100.0 ml
dH ₂ O	400 ml

200 ml 4 % PFA

PFA	8.0 g
MilliQ water	180 ml

After dissolving at 60°C add 20 ml 10x PBS and adjust the pH to 7.4 with 1N NaOH.

50 ml 75 % MeOH in PBS for dehydration

MeOH	37.5 ml
10x PBS	12.5 ml

50 ml 50 % MeOH in PBS for dehydration

MeOH	25 ml
10x PBS	25 ml

50 ml 25 % MeOH in PBS for dehydration

MeOH	12.5 ml
10x PBS	37.5 ml

100 ml Immunohistochemistry (IHC) Tris buffer

Tris Base	2.8171 g
DEPC water	100 ml

Adjust pH to 9 with 1N HCL

1L 100mM IHC Sodium phosphate buffer

Na ₂ HPO ₄	10.9 g
NaH ₂ PO ₄	3.1 g
DEPC water	1 L

Adjust pH to 7.4

100 ml IHC PBTx

TritonX100	800 µl
100mM IHC sodium phosphate buffer	75 ml

10 ml IHC NGS/BSA/PBTx blocking solution

Normal goat serum	1 ml
Bovine serum albumin	0.2 g

10 ml IHC NGS/BSA/PBTx antibody blocking solution

Normal goat serum (NGS)	200 µl
Bovine serum albumin(BSA)	0.2 g
IHC PBTx	10 ml

2.4 Antibodies

2.4.1 Primary antibodies

Antibody	Species	Company	Product number
Acetylated tubulin	mouse	Sigma-Aldrich	T7451
Cleaved caspase 3	rabbit	Cell Signaling Technology	9661
GFP	rabbit	Invitrogen	A11122
PCNA	mouse	Sigma Aldrich	P8825
SV2	mouse	DSHB	AB_2315387

2.4.2 Secondary antibodies

Antibody	Species	Company	Product number
Anti-guinea pig Alexa Fluor 546	goat	Molecular Probes	A11074
Anti-mouse Alexa Fluor 546	goat	Life Technologie	A11030
Anti-mouse-HRP	goat	Jackson Immuno Research	115-035-003
Anti-rabbit Alexa Fluor 488	goat	Life Technologie	A11034
Anti-rabbit-HRP	goat	Jackson Immuni Research	111-035-144

2.5 Oligonucleotides

2.5.1 Oligonucleotides for RNAscope

Name	Sequence	Company	Company
Dr-gpr17	Targeting 171-1105 of XM_005165958.3	Acdbio by Bio- Techne GmbH	300031
Dr-si-dkey-96n2.3	Targeting 81-1044 of XM_001341260.4	Acdbio by Bio- Techne GmbH	320269-C3
RNAscope® Probe- EGFP-C2		Acdbio by Bio- Techne GmbH	400281-C2
RNAscope® Nega- tive Control Probe DapB-C3		Acdbio by Bio- Techne GmbH	310043-C3

2.5.2 Oligonucleotides for sequencing and genotyping *gpr17* knockout lines

Name	Sequence
Gpr17-F1	CTTGCTGCCCAACCAGTCCA
Gpr17-R1	AGCGAGGAGGTAAGACGGTT
F5_gen0_Fwd	AACTGGAGGTCATTGGCC
F5_gen0_Rev	CATACGGTTGAGCCATTGAC

2.5.3 Morpholino oligonucleotides

Name	Sequence	Concentration	Company
<i>gpr17</i> MO	GTTCTGTCAAGGAG- GACTCCATTT (ZDB-GENE-100922-133)	2.54 mg 300 nmol M=8465	Gene Tools, LLC
Control MO	CCTCTTACCTCAG- TTACAATTTATA	0.833 mg 100 nmol M=8328	Gene Tools, LLC

2.6 Plasmids

Name	Size (bp)	Company/Host
3HA-hGPR17 in pcDNA3.1+	1151	Research group of Prof. Dr. Evi Kostenis, Institute of Pharmaceutical Biology, University of Bonn, Germany
3HA-zfGpr17 in pcDNA3.1+	1155	Research group of Prof. Dr. Evi Kostenis, Institute of Pharmaceutical Biology, University of Bonn, Germany
3HA-h+zfGpr17 in pcDNA3.1+	1110	Research group of Prof. Dr. Evi Kostenis, Institute of Pharmaceutical Biology, University of Bonn, Germany
tdTomato in pBluescriptII SK	1428	Clontech Laboratories

2.7 Zebrafish lines

Name	
TU wildtype fishline	EZRC, KIT
TL wildtype fishline	EZRC, KIT
AB wildtype fishline	EZRC, KIT
Brass wildtype fishline	EZRC, KIT
<i>Tg(claudinK:EGFP)</i>	(Münzel et al., 2012)
<i>Tg(nkx2.2a:mEGFP)</i>	(Kirby et al., 2006; Kucenas et al., 2008)
<i>Tg(mbp:CAAX-EGFP)</i>	(Almeida et al., 2011)
<i>Tg(mbp:EGFP)</i>	(Almeida et al., 2011)
<i>Tg(olig2:EGFP)</i>	(Shin et al., 2003)
<i>Tg(-8.4ngn1:GFP)</i>	(Blader et al., 2003)
<i>Mut5(gpr17)^{-/+}</i> fishline	Nanjiing Sanjay Medical Technology, China

2.8 Commercial Assays

Assay/Kit	Company	Product number
DyNAmo® Flash Probe qPCR Kit	Thermo Fisher Scientific	F-455S
iScript™ cDNA synthesis Kit	Bio-Rad Laboratories	170-8890
mMessage mMachine™ T7 Ultra Kit	Invitrogen by Thermo Fisher Scientific	AM1345
NucleoBondR Xtra Maxi	Macherey-Nagel	740414.10
NucleoSpin Gel and PCR Clean-UP	Macherey-Nagel	740609.250
Nucleospin RNA clean up kit	Macherey-Nagel	740948.50
Qubit RNA HS Assay Kit	Molecular Probes by Life Technologies™	Q32855
RNAscope Fluorescent Multiplex Reagent Kit	Acdbio by Bio-Techne GmbH	320850
pGEM®-T Easy Vector Systems I	Promega	A1360
TRIzol RNA Isolation	Invitrogen	15596018

2.9 Consumables and other used materials

Consumables	Company	Product number
1.5 ml Tubes	Sarstedt	72.690
2 ml Tubes	Eppendorf	211-2120
96 Well glass bottom plate	Cellvis	P96-1.5H-N
EppendorfR LoBind microcentrifuge tubes	Sigma Aldrich	Z666548
EppendorfR LoBind microcentrifuge tubes	Sigma Aldrich	Z666556
Falcon tubes 50 mL	Greiner Bio-One	227263
Falcon tubes 15 mL	Greiner Bio-One	188272
Melek's whiskers	Öznur Yilmaz	-
Microloader 20 µl	Eppendorf	5.242.956.003
Multiply®-µStrip Pro 8-Strip	Sarstedt	72.991.002

Parafilm™	Labomedic	1447011
Pastette® Extended Fine Tip Mini	Alpha Laboratories Limited	Lw4231
Pasteur pipette, glass	Labomedic	447016
Pasteur plast pipette	Ratio lab GmbH	2600111
PCR tubes	Starlabs	B1402-5500
Petri dish	Greiner Bio One	633180
Petri dish, small	Greiner Bio One	EL46.1
Pipette tips, 2.5µl	Sartstedt	720025
Pipette tips, 10µl	Sartstedt	720031
Pipette tips, 200µl	Sartstedt	70.760.002
Pipette tips, 1000µl	Sartstedt	70.762
Precellys Bulk beads for 500pp Zirconium oxide beads	PEQLAB Biotechnologie	KT03961-1-103.BK
UVette	30106300	Eppendorf
Whatman paper	Biometra	GB005

2.10 Software and algorithm

Name	Company/Version
Adobe Illustrator	Adobe/Version 23.0.3
CFX Manager	Biorad
Fiji is just ImageJ	ImageJ/Version 1.52i
ImSpector	LaVision/Version
Microsoft Excel	Microsoft Corporation/Version 2010
Microsoft Word	Microsoft Corporation/Version 2010
Prism	Graphpad/Version 6
qBase+	Biogazelle NV
Serial Cloner	Serial Basics/Version 2.6.1
SnapGene	SnapGene/Version 4.3.2
ZF-MigratingCells.kala	Perkin Elmer

2.11 Equipment

Equipment/Type	Company	Product number
AREX heating magnetic stirrer	VELP Scientific	-
Balances TE 64 (precision balance) TE 6101	Satorius	BL310
CFX96™ Real-Time System	Bio-Rad Laboratories	185-5196
Dual-Stage Class Micropipette Puller	Narishige	PC-10
Eppendorf BioPhotometer®D30	Eppendorf	6133000001
Eppendorf µCuvette® G1.0	Eppendorf	6138000018
EnSight™ multimode plate reader	Perkin Elmer	HH34000000
Eppendorf ThermoMixer	Eppendorf	5436
Geldoc 2000	Bio-Rad Laboratories	-
Incubator IN	Memmert	ASTM304
Innova 4000 Incubator	New Brunswick Scientific	8261-30-1007
Micromat	AEG	-
Microscope Stemi	Zeiss	Stemi 508
Mikro 200R centrifuge	Hettich Zentrifugen	-
MPPI-3 Pressure Injector	Applied Scientific Instrumentation, Inc.	-
Nikon AZ100	Nikon	-
Nikon Digital Sight DS-U3	Nikon	-
Nikon Digital Sight DS-Qi1Mc	Nikon	-
PerfectSpin Mini	PEQLAB Biotechnologie	91-PSPIN-M

PlateFuge™ Microplate Microcentrifuge	Benchmark Scientific	C2000
PowerPac Basic	Bio-Rad Laboratories	-
Precellys 24	PEQLAB Biotechnologie	91-PCS24
Two photon microscope	LaVision	Trimscope II
Qubit® 2.0 Fluorometer	Life Technologies	Q32866
Seven Compact pH- electrode	Mettler Toledo	-
Sub Aqua 2 Plus water bath	Grant	-
T100 Thermal Cycler	1861096	Bio-Rad Laboratories
Thermal Cycler 2720	Applied Biosystems	4359659
Unimax 1010	Heidolph	-
Vortex Mixer	VELP Scientific	F202A0173

3 Methods

3.1 Zebrafish maintenance

According to the guidelines for the laboratory use of zebrafish (Westerfield 2007), adult zebrafish were maintained at 28°C with a light/dark cycle of 14/10 hours in the zebrafish facility of the Institute of Anatomy at the University of Bonn. To mate zebrafish, a pair of male and female zebrafish were transferred and separated by a divider in a mating tank the evening before. The next morning the dividers were removed at 9 am to get fertilized embryos with similar age. After collecting the fertilized eggs, embryos were reared at 28°C in 0.3x Danieau's buffer supplemented with 0.00001 % methylene blue solution until 24 hpf. From 24 hpf embryos were reared in 0.3x Danieau's buffer or when used for imaging in 0.3x Danieau's buffer supplemented with 0.003 % phenylthiourea (PTU) to prevent pigmentation. All experiments were performed according to the Belgium and European laws (Ethical commission protocols ULg1076 and ULg624).

3.2 DNA extraction

For sequencing or genotyping of zebrafish larvae, DNA was extracted by dissolving the embryo with 20 µl of 50 mM MeOH for 20 minutes at 95°C with agitation. After cooling down the extracted DNA 2 µl of 1M Tris-HCl (1:10) was added and the DNA was stored at -20°C. For sequencing or genotyping of adult zebrafish, a tiny part of the fin of the respective fish were cut and dissolved as described before. Therefore, the fish were anesthetized beforehand using 1x MS222 in 0.3x Danieau.

3.3 Genotyping and sequencing of adult and larval zebrafish

For genotyping as well as for sequencing of adult and larval zebrafish, the respective DNA region needs to be amplified beforehand. DNA of zebrafish was extracted as described in 3.6 and DNA amplification was performed using polymerase chain reaction (PCR).

3.3.1 Polymerase chain reaction

PCR is an enzymatic method to selectively amplify target DNA of a given DNA template. Hereby, short oligonucleotide primers are designed to flank the target DNA region (forward and reverse primer). Upon binding of the primers, a DNA polymerase generates and amplifies the complementary DNA region of the template by primer extension in the 3' direction. The

extension of the growing DNA strand is achieved by the DNA polymerase incorporating complementary base pair dNTPs into the growing strand. Approximately 35 cycles of heating and cooling are necessary for the different reactions occurring during the PCR. A melting temperature of 95°C to break DNA double strands initiates each PCR cycle. By cooling down again the respective primer annealing temperature is reached and the primers can bind to the target DNA region. Subsequent heating up to 72°C leads to optimal reaction temperature for the DNA polymerase to generate the respective complementary DNA strand during the last step of each individual cycle. The total volume of PCR reaction mixture was adjusted to 25 µl. Primers were ordered from Sigma Aldrich and dissolved at a stock concentration of 100 µM. The individual primer annealing temperature (T_m) was calculated with Thermo Fisher Scientific T_m calculator tool.

3.3.2 Sequencing of *gpr17* knockout fish

Fins of zebrafish were cut and assigned to the respective fish. Afterwards, DNA was extracted (3.6) and a PCR was performed (3.7.1) to amplify the region of the mutated DNA with a size of ~800 bp. The PCR reaction mix contained 1 µM forward- and reverse primer (*gpr17*-F1 and *gpr17*-R1), 1x Dream Taq Buffer 10x, 0.25 mM dNTPs, 1.25 units Dream Tag Polymerase and 2.5 µl DNA template. The PCR program was set up to 25 cycles starting with an initial denaturation with 3 minutes at 95°C. Each PCR cycle started with 30 seconds at 95°C followed by 30 seconds of primer annealing at 71°C and a final elongation step of 1 minute at 72°C. After the last cycle an elongation reaction of 10 minutes at 72°C was performed and the PCR product was finally cooled down to 12°C. Afterwards, the amplified target DNA was cleaned up using the NucleoSpin Gel and PCR Clean-UP Kit (Macherey Nagel) and sent to Eurofins for Sanger sequencing. DNA sequence analysis was performed using SnapGene version 4.3.2.

3.3.3 Genotyping of *gpr17* knockout fish

A genotyping protocol for the *gpr17* knockout line *Mut5* was established as follows. After extraction of DNA of fins of adult zebrafish or whole larvae a PCR mix containing 1 µM forward- and reverse primer (F5-geno_Fwd1 and F5-geno_Rev1), 1x Dream Taq Buffer 10x, 0.25 mM dNTPs, 1.25 units Dream Tag Polymerase and 2.5 µl DNA template. The PCR program for genotyping of *Mut5* was set up to 25 cycles starting with an initial denaturation with 3 minutes at 95°C. Each PCR cycle started with 30 seconds at 95°C followed by 30 seconds of primer annealing at 63°C and a final elongation step of 1 minute at 72°C. After the last cycle an elongation reaction of 10 minutes at 72°C was performed and the PCR product was finally cooled down to 12°C. The amplified target DNA was separated on a 2 % agarose gel for at least 20 minutes

Methods

at 80 V. Wild type DNA resulted in a 267 base pairs (bp) band in the gel, whereas homozygous *Mut5* DNA with a deletion of 43 bp resulted in a 224 bp band in the gel. Heterozygous DNA resulted in two bands at 267 bp and 224 bp.

3.4 TA- Cloning

First, we extracted DNA (3.2) of *Mut5*^{+/+} and amplified *gpr17* via PCR (3.3.2). To ligate the *gpr17* insert with the linearized pGEM®-T Easy vector we followed the protocol of Promega's pGEM®-T Easy vector System I.

3.5 Microinjections of zebrafish embryos

All injection experiments were performed with self-drawn glass capillaries injecting into the yolk of one- or two-cell stage embryos. For proper injection, embryos were fixed by placing them into the notches of an agarose mold. To adjust the concentration of the agent the injection volume was calibrated in mineral oil by fine-tuning the diameter of the injected droplet with a calibration slide. Depending on the diameter of the injected droplet the volume and the concentration of the agent were calculated using the formula Fig.8.

$$V_{\text{injection}} = \frac{4}{3} \times \pi \times \left(\frac{\text{diameter droplet } \mu\text{m}}{2} \right)^3 = x \mu\text{m}^3$$

$$1 \mu\text{m}^3 = 1 \times 10^{-9} \mu\text{L}$$

$$x \mu\text{m}^3 \times 10^{-9} \frac{\mu\text{L}}{\mu\text{m}^3} = y \mu\text{L} = y * 10^3 \text{ nL}$$

$$n = c \times V = \text{concentration of working solution } \frac{\text{mol}}{\text{L}} \times (y * 10^3 \text{ nL}) \times 10^{-9} \text{ L} = z \text{ mol}$$

$$m = n \times M = z \text{ mol} \times M \frac{\text{g}}{\text{mol}} = w \text{ g}$$

Figure 8: Calculation of the injected amount of agent. X is the injected volume [μm^3] depending on the calibrated diameter of the droplet [μm]. Y is the injected amount of agent in nL depending on the injected volume x [μm]. Z is the injected amount of agent in mole depending on the injected volume y and on the concentration of the working solution of agent of the respective agent. W is the injected mass[g] of agent.

3.5.1 Morpholino injections

The antisense oligonucleotide morpholino (MO) *gpr17* MO were designed with Gene Tools, LLC to block the translation of *gpr17* (Reinof, 2014). The lyophilized *gpr17* MO (300 nmol)

and the control morpholino (CoMO, 100 nmol) were dissolved in Ampuwa water and stored as a stock solution with 2 mM at room temperature. For injection, a 20 μ l working solution with a concentration of 0.25 mM of *gpr17* MO or CoMO was prepared, containing 2 μ l phenolred, 1 μ l 10x Cutsmart buffer, 14.5 μ l Ampuwa water and 2.5 μ l *gpr17* MO or CoMO stock solution. Prior to injection the working solutions were heated for five minutes at 65°C and subsequently loaded into a micropipette. According to the calibration of Philip Reinoß the diameter of the injected droplet was adjusted to 135 μ m resulting in a droplet volume of 1.3 nL containing 2.75 ng *gpr17* MO or CoMO (Reinoß, 2014).

3.5.2 RNA injections

3.5.2.1 RNA synthesis

ThermoFisher's mMessage Machine Kit T7 Ultra Kit® was used for the *in vitro* synthesis of *gpr17*, *hGPR17*, *h+zfGpr17* and control *tdTomato* RNA. Before the *in vitro* transcription, the plasmids of the different constructs were linearized using XhoI for *gpr17*, *hGPR17* and *h+zfGpr17* and MfeI for the *tdTomato* plasmid. After following the protocol, the RNAs were precipitated with lithium chloride and quantified with the Qubit RNA HA Assay Kit®. The RNAs were frozen as aliquots at -80°C.

3.5.2.2 Rescue experiments

3.5.2.2.1 Morpholino rescue

To maintain the same conditions as in the *gpr17* MO injection experiments during the MO rescue experiments, a new 0.5 mM *gpr17* MO and CoMO stock solution was prepared containing 2 μ l CutSmart, 4 μ l phenolred, 5 μ l 2 mM *gpr17* MO or CoMO stock solution and 9 μ l Ampuwa water. For the MO and CoMO injection a 0.25 mM working solution of 2.5 μ l 5 mM *gpr17* MO or CoMO mixed with 2.5 μ l Ampuwa water were prepared (2.75 ng MO or CoMO). The 0.5 mM MO stock solution was mixed with the *hGPR17*, *h+zfGpr17* and *tdTomato* RNA and filled up to 5 μ l with Ampuwa water, so that 1.3 nL injection volume (droplet diameter of 135 μ m) contains of 500 pg RNA and 2.75 ng *zf-gpr17* MO. *gpr17* MO, CoMO and rescue solutions were heated to 65°C for five minutes and subsequently injected into one- or two-cell stage embryos of *Tg(olig2:EGFP)*. As a control for proper injection and comparison *tdTomato* RNA was used. The translation of the respective RNAs is not blocked by the MO. The spinal cord segments 4-10 of the injected fish were imaged at 3 dpf and dorsal olig2⁺ cells were counted using “Fiji is just ImageJ”.

Methods

3.5.2.2.2 *Gpr17* knockout rescue

According to Figure 8 the RNA stock solutions of *gpr17*, *hGPR17*, *h+zfGpr17* or *tdTomato* were mixed with 1 µl phenolred and filled up to 5 µl with Ampuwa water so that the resulting solutions contain 200 pg of RNA within an injection volume of 1.8 nL (droplet diameter of 150 µm). The injection solutions were injected into one- or two-cell stage embryos of *gpr17^{-/-} Tg(olig2:EGFP)* and *gpr17^{+/+} Tg(olig2:EGFP)*. As a control for proper injection and comparison *tdTomato* RNA was used. The injected *gpr17* RNA contains a HA-tag. Therefore, the MO can not bind to the complementary RNA sequence anymore. The spinal cord segments 4-10 of the injected fish were imaged at 3 dpf and dorsal *olig2⁺* cells were counted using “Fiji is just ImageJ”.

3.5.2.2.3 Overexpression

RNA overexpression injections were performed like described in 3.6.2.2.2 in *Tg(olig2:EGFP)*.

3.6 Whole-mount fluorescent labeling techniques

3.6.1 Fixation and dehydration of zebrafish larvae

To keep tissue integrity and to preserve native protein fluorescence of the respective reporter fish lines prior to RNAscope or immunohistochemistry (IHC) experiments, larvae were fixed in 4 % PFA with a pH of 7.4 for two hours at room temperature (RT) followed by three washing steps with 1x PBS for 15 minutes. Subsequently, fixed larvae were dehydrated with increasing concentrations of 25 %, 50 %, 75 % and 100 % Methanol (MeOH) in 1x PBS for 15 minutes each. After the last washing step larvae were stored in fresh MeOH at -20°C for 2 hours before proceeding with the respective experiment.

3.6.2 Whole-mount in situ hybridization using RNAscope

The RNAscope Multiplex Fluorescent Assay is designed to detect up to three different mRNAs simultaneously in various tissue with subcellular resolution. The principle is based on the complementary hybridization of small antisense oligonucleotides (single Z probe) to the mRNA of interest. If two pairs of Z-probes binding next to each other (double Z pair), they can be hybridized by four successively binding scaffolding oligonucleotides (AMP1, AMP2, AMP3 and AMP4) leading to the attachment of individual fluorophores to the specific mRNA. Several different double Z-pairs are binding along the mRNA of interest amplifying the fluorescent

signal. The single Z-probes were designed by Acdbio. The following protocol was modified for the use on zebrafish larvae from (Gross-Thebing et al., 2014).

3.6.2.1 Modified RNAscope protocol

2 to 5 dpf larvae were fixed and dehydrated as described in 3.2. After removing the MeOH, larvae were air-dried for approximately 15 minutes in 2 ml tubes. Afterwards, larvae need to be permeabilized for 45 minutes by adding 50 μ l Pretreat 3 solution. The removal of Pretreat 3 solution is followed by a series of three washings with 1 ml 1x PBS supplemented with 0.01 % Tween. Then 50 μ l of the pre-warmed antisense oligonucleotides Dr-gpr17 or Dr-si-dkey-96n2.3, each combined with RNAscope® Probe-EGFP-C2, are added to the larvae and incubated overnight at 40°C. Antisense probes can be recovered and reused. The next morning larvae need to be washed three times with 0.2x SSC supplemented with 0.01 % Tween (0.2x SSCT) for 15 minutes at RT. Then larvae were fixed again in 1 ml 4 % PFA for 10 minutes at RT. Fixation solution was removed and larvae were washed three times with 1 ml 0.2x SSCT. Subsequently 0.2x SSCT was replaced with 50 μ l AMP1 and incubated for 45 minutes at 40°C followed by three washing steps with 1 ml 0.2x SSCT for 15 minutes at RT. Afterwards, 50 μ l AMP2 was added to the larvae and incubated for 25 minutes at 40°C. Afterwards, larvae were washed three times with 1 ml 0.2x SSCT for 15 minutes at RT. Then Larvae were incubated in 50 μ l AMP3 for 35 minutes at 40°C and washed three times in 1 ml 0.2x SSCT for 15 minutes at RT. Eventually larvae were incubated with 50 μ l AMP4 for 25 minutes at 40°C, subsequently washed three times with 1 ml 0.2x SSCT and stained with 50 μ l DAPI overnight at 4°C. The next day larvae were rinsed three times with 1 ml 1x PBS, mounted in 0.25 % low melting agarose and imaged with a two-photon microscope.

3.6.3 Whole-mount immunohistochemistry

Whole-mount IHC is an antibody-based method to visualize proteins within intact tissue complex. The individual protein is recognized by a specific binding first antibody. Fluorescent signal amplification is based on the specific binding of a fluorescent labeled second antibody recognizing the first antibody. For visualization of the individual proteins the Genetex-Whole-mount IHC protocol for zebrafish embryos was modified and applied to the following experiments.

3.6.3.1 Immunohistochemistry protocol

Prior to the experimental procedure larvae need to be fixed and dehydrated as described in 3.2. To start the whole-mount IHC zebrafish larvae have to be rehydrated throughout a series of 75 %, 50 %, 25 % MeOH in 1x PBST and subsequently washed three times with 1x PBST for 5 minutes at RT. Antigen retrieval to break methylene bridges of the fixation was initiated with a washing step with 150 mM Tris buffer (pH=9.0) for 5 minutes at RT followed by the incubation of the larvae in fresh Tris buffer for 15 minutes at 70°C. Afterwards, larvae were washed two times with 1xPBST for 5 minutes at RT. Larvae permeabilization was performed using proteinase K with a final concentration of 5 µg/ml in 1xPBST for 90 minutes at RT. A postfixation with 4 % PFA for 20 minutes at RT was used to stop digestion. Postfixation is followed by 5 washing steps with 1xPBST for 5 minutes at RT. Afterwards, larvae were pre-incubated with IHC-NGS/BSA/PBTx blocking solution (2.3) for 4 hours at 4°C. Antibodies (2.4.1) were diluted in IHC-NGS/BSA/PBTx antibody blocking solution (2.3) and incubated for three days at 4°C. SV2 antibody (DSHB) was diluted 1:250, MbpA antibody (Thermo Fischer Scientific) 1:200, acetylated tubulin antibody (Sigma-Aldrich) and GFP (Invitrogen) antibodies were diluted 1:500. First antibody incubation was stopped with five washing steps with 1xPBTx (2.3) for 1 hour at RT. Subsequently, larvae were incubated with the individual second antibody, diluted 1:1000 in IHC-NGS/BSA/PBTx antibody blocking solution (2.3), protected from light for two days at 4°C. Incubation were stopped and unbound antibody were removed with 6 washing steps for 15 minutes and 5 washing steps for 5 minutes with 1xPBST at RT followed by a postfixation with 4 % PFA for 20 minutes at RT. Fixation solution was removed with five washing steps with 1xPBST for 5 minutes. Samples were stored protected from light in 1xPBST at 8°C overnight. The next day samples were mounted in low melting agarose (3.3) and laterally imaged as described in 3.4. Image processing was performed using Fiji ImageJ.

3.6.4 Immunohistochemistry of larvae sections

IHC staining of zebrafish spinal cord paraffin sections were performed by Dr. Anna Sophia Japp (Institute of Neuropathology, Medical Centre, University of Bonn) on Ventana Benchmark XT Immunostainer (Roche Ventana, Darmstadt, Germany). Therefore 2 dpf old zebrafish were anesthetized and fixed in 4 % PFA and stored at 4°C. Afterwards, larvae were embedded in paraffin and the sections were counter stained with hematoxylin. They were then stained with the respective antibodies (anti-Pcna (Sigma Aldrich) 1:1000, anti-Cleaved caspase 3 (Cell signaling Technologies) 1:200). Images were taken with Nikon AZ100 microscope and processed with Fiji ImageJ.

3.7 Compound treatment

All treatments were performed by adding the drugs to the aqueous environment of the larvae, which were reared in a light cycle incubator at 28.5°C. Prior to the treatment, 1 dpf old embryos were enzymatically dechorionated with 2 mg/ml pronase in 0.3x Danieau supplemented with 0.003 % PTU. After three washing steps with 0.3x Danieau supplemented with 0.003 % PTU embryos were transferred into small petri dishes filled with the individual compound in a total volume of 3 ml of 0.3x Danieau supplemented with 0.003 % PTU. The compound solutions were renewed every day.

3.7.1 GANT 61 treatment

A stock solution of 10 mM GANT 61 in DMSO was prepared. At 30 hpf embryos were bathed in 10 μ M GANT61 in 0.3x Danieau supplemented with 0.003 % PTU. The same concentration of DMSO (0.1 %) was used as a control.

3.7.2 SKP-C25 treatment

A stock solution of 10 mM SKP-C25 in DMSO was prepared. At 2 dpf embryos were exposed to 2 μ M SKP-C25 in 0.3x Danieau supplemented with 0.003 % PTU. The same concentration of DMSO (0.02 %) was used as a control.

3.7.3 Trichostatin A treatment

Embryos were treated with 100ng/ml Trichostatin A (TSA). The same concentration of Methanol (0.2 %) was used as a control.

3.8 Two-photon imaging of zebrafish

3.8.1 Mounting of zebrafish

Zebrafish younger than 3 dpf were dechorionated using 2 mg/ml pronase in 0.3x Danieau for approximately 10 minutes with strong agitation at RT. After three washing steps with 0.3x Danieau larvae were laterally mounted using 1.25 % low melting agarose containing 5 % MS222 enabling two-photon imaging without movement.

3.8.2 Two-photon imaging

For two-photon imaging a scan head based laser-scanning microscope TriMScope (LaVision, BioTec, Bielefeld, Germany) equipped with a 20x water-immersion objective lens (NA1.0, W Plan-Apochromat, Zeiss) and a tunable TiSa laser (InSight™ Deepsee™, Spectra-Physics, Santa Clara, USA) was used. For two-photon imaging only Danieau + PTU-treated fish without skin pigments were used. After mounting the fish in low melting agarose images of zebrafish spinal cord segments 4-10 were acquired as a z-stack (z-step 2µm) with a field of view of 449 µm x 111µm and a resolution of 2730 x 678 pixel resulting in image properties with 0.16 µm per pixel. Image analysis and processing were performed using Fiji ImageJ.

3.9 Automated Ensight™ imaging protocol

3.9.1 Imaging settings for proper detection of *Tg(olig2:EGFP)*

To achieve sharp images of the whole fluorescent spinal cord, the plate reader has to take images of different focus height and combine them to a sharp maximum projection. Six foci plane offsets in a range from 0 to 250 µm are sufficient to gain the whole larva in focus. A bright-field image is necessary for the “ZF-MigratingCells.kala” algorithm to identify the presence of a single larva in each well by calculating pixel texture values. To properly detect larvae of *Tg(olig2:EGFP)* and their fluorescent spinal cord we adjusted the imaging settings of the Kaleido™ software of the plate reader according to **Table 1**. The imaging settings can only be used when using the Cellvis 96-well glass bottom plate (0.17±0.005 mm). For other plates the settings have to be adjusted.

Table 1. Imaging settings for proper detection of *Tg(olig2:EGFP)* in the Kaleido™ software.

Name of the Channel	Excitation Wavelength [nm]	Excitation Power [%]	Exposure Time [ms]	Additional Focus Offset [μm]	Global Focus Height [μm]	Real Focus Offset for Channel [μm]
GFP0	465	100	50	0	+25	25
GFP50	465	100	50	50	+25	75
GFP100	465	100	50	100	+25	125
GFP150	465	100	50	150	+25	175
GFP200	465	100	50	200	+25	225
GFP250	465	100	50	250	+25	275
Brightfield	465	4	4	0	+25	25

3.9.2 Larvae positioning protocol

Lateral views of zebrafish are required to count cells in the dorsal spinal cord making the positioning a critical step in zebrafish imaging. Therefore, we developed a fast positioning protocol to force each larva of the 96-well plate into its lateral position (**Figure 13A**). The positioning protocol starts with the manual transfer of single fish needs into each well of the 96-well plate. Afterwards, larvae need to be anesthetized with 6 μM MS222 in each well using a multi-well pipette. Larva then needs to be centered in each well using a small pipet tipp. Notably, the centering is the most important step during the positioning protocol. To force down each larva on the bottom of each well a short centrifugation of the whole 96-well plate with 8g for 5 seconds is necessary. Eventually, the 96-well plate can be placed into the EnSight™ multimode plate reader using the “soft plate movement” function.

3.9.3 Automated image analysis algorithm

The algorithm was designed with Norbert Garbow from the Perkin Elmer company to firstly detect the borders of each well of the 96-well plate. Next the algorithm identifies the zebrafish circumference based on a texture analysis of the bright field channel. This object search depends on texture threshold settings, one of the algorithms input parameters (**Table 2**). The algorithm then searches for the most prominent spine-like structure by detecting the region with the highest fluorescence intensity in the maximum contrast projection of the six foci planes as the ventral spinal cord. The detection of the fluorescence intensity is based on fluorescence threshold settings and can also be adjusted in the input parameters of the algorithm. Based on the ventral spine detection the region of interest (ROI) to search for dorsal olig2⁺ cells is defined as a 33 μm wide area above the spinal cord. Within this ROI fluorescent spot-like objects that fulfill the fluorescent contrast requirements, a definable input parameter of the algorithm, are identified and counted as cells.

Table 2. Input parameters of the image analysis algorithm in the Kaleido™ software.

Input parameter	Meaning	Value for <i>Tg(olig2:EGFP)</i>
Contrast Threshold to identify Fish Larvae in Bright-field	Regions with higher texture value within a well are detected as “covered by an object” (zebrafish). Regions with lower texture value are not detected as an object.	28
Spine Detection: Length of Orientation Filter	Combines the discontinuous parts of the ventral spinal cord. For low GFP expression of the spine of other transgenic lines “medium” or “large” may provide a better detection of the spine.	Short
Minimum Fluorescence Contrast of Migrating Cells	Contrast threshold with a range of 0-1. Cells with lower fluorescent contrast are excluded from counting.	0.2
Cell Density: Averaging Length in Search Region [µm]	Possible values: 100, 200, 400, 800. A sliding window of the here defined width is used to determine a cell number per length.	400
Well Detection: Channel	Channel used for the detection of the region of interest.	Automatic
Well Detection: Excluded Well Margin	A width to exclude the outer rim of the well. Can be used to exclude artifacts visible at the well border	20
Well Detection: Mode	Standard or Fast. Value defining the calculation time of the algorithm	Standard
Well Detection: Well Dimensions	If set to “manual” the well size parameter can be defined by the inputs below.	Automatic
Well Detection: Well Shape	The shape of the well that is detected by the algorithm. Round or square. That depends on the type of plate.	Round
Well Detection: Well Diameter	Diameter [mm] of the well detection of the algorithm. If set to a value >8mm the complete image is analysed, no well detection is performed.	6.6

3.10 Quantification and analysis

3.10.1 Cell counting

In vivo images of zebrafish spinal cord segments 4-10 were acquired as stacks with the two-photon microscope as described in 3.4. Zebrafish were anesthetized and mounted in low melting agarose prior to imaging as described in 3.3. With Fiji ImageJ the single images were

stacked as a z-stack maximum projection. Images were blinded before cell counting. To count cells the Fiji ImageJ Cell counter plugin (Author: Kurt De Vos, University of Sheffield) was used. Cells in the dorsal part, that were not touching the ventral spinal cord, were defined as dorsal cells.

3.10.2 Measurement of the mean fluorescence intensity of the ventral spinal cord

In vivo images zebrafish spinal cord segments 4-10 were acquired as stacks with the two-photon microscope as described in 3.4. Zebrafish were anesthetized and mounted with 195 μ l 1.25 % low melting agarose supplemented with 5 μ l MS222 prior to imaging as described in 3.3. Imaging was performed with the same experimental adjustment for all experiments, such as 4 % laser power for the morphant experiments, 2 % laserpower (new laser was installed) for the mutant experiments and the same volume of low melting agarose. With Fiji ImageJ the single images were stacked as a z-stack average projection and the mean fluorescent intensity of the ventral spinal cord were measured by using the measurement function of Fiji ImageJ.

3.10.3 Statistical analysis

All the graphs with their statistical analysis were generated and performed with GraphPad Prism version 6.0. All experiments were repeated at least in three independent experiments with a different number of zebrafish, unless otherwise mentioned. For all quantitative experiments D'Agostino-Pearson omnibus normality test was performed to check the distribution of the values. In case of Gaussian distribution, the parametric t-test was used for statistical analysis. If the values were not normally distributed the non-parametric Mann-Whitney U test was applied. All error bars of the experiments investigating the role of *gpr17* are shown as standard error of the mean (SEM), unless otherwise mentioned. All error bars of the experiments validating the automated imaging system are shown as standard deviation (SD), unless otherwise mentioned. The height of each bar represents the mean value of each group. Asterisks in the graphs show: ns when $P > 0.05$, * when $P \leq 0.05$, ** when $P \leq 0.01$, *** when $P \leq 0.001$ and **** when $P \leq 0.0001$.

4 Results

4.1 The G protein-coupled receptor Gpr17 in zebrafish

Before investigating whether a humanized zebrafish can be used as an *in vivo* compound screening system, the function of endogenous Gpr17 in zebrafish has to be clarified. Therefore, the following chapter will deal with the spatial and temporal expression profile of *gpr17* in zebrafish larvae.

4.1.1 *Gpr17* mRNA expression in zebrafish

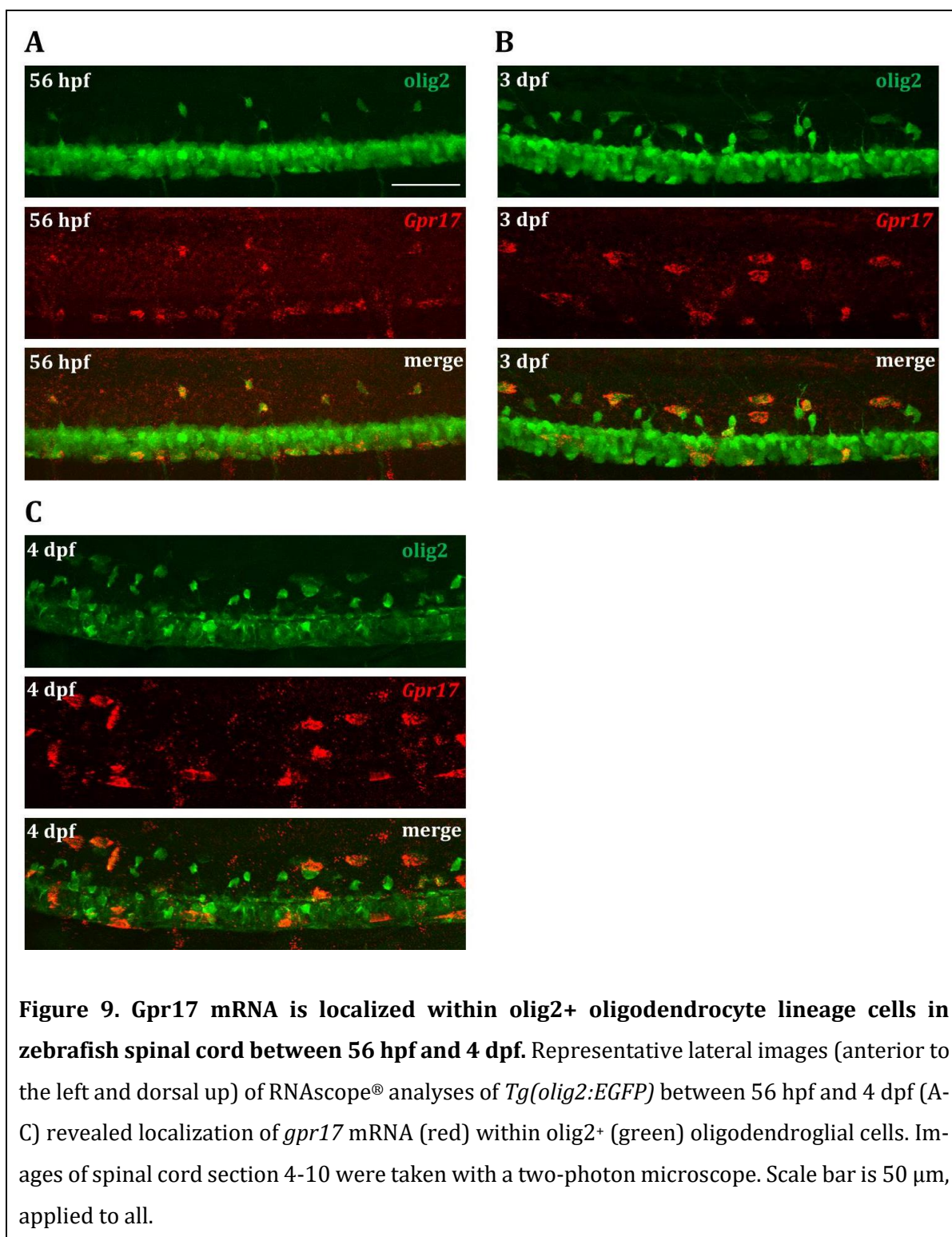
By performing a BLAST/BLAT search with the Ensemble genome browser 97, we identified the *gpr17* gene on chromosome 6 and a potential paralogue si:dkey-96n2.3 (*gpr17B*) on chromosome 24 in zebrafish. By using Clustal Omega's multiple alignment analysis we found a 57.3 % homology of zebrafish Gpr17 protein and a 43.4 % homology of Gpr17B protein with the human GPR17-S protein.

Whereas data in mice demonstrate that *gpr17* is expressed in OPCs and pre-Ols during embryogenesis, expression data in zebrafish only indicated *gpr17* expression in the spinal cord (Chen et al., 2009; Schmitt, 2019). Therefore, cell specific expression of *gpr17* in the spinal cord of zebrafish still remained unknown. To this end, a novel *in situ* hybridization (ISH) assay called RNAscope®, allowing the investigation of mRNA expression at cellular level was modified for the use on zebrafish larvae.

4.1.1.1 *Gpr17* mRNA is expressed in olig2⁺ oligodendrocyte lineage cells in zebrafish

RNAscope® technology revealed robust expression of *gpr17* from 56 hpf to 4 dpf in olig2⁺ cells in *Tg(olig2:EGFP)*, which express EGFP in *olig2* expressing Ol lineage cells (**Figure 9A-C**). The transcription factor *olig2* is expressed in all Ol lineage cells during oligodendrogenesis, making it difficult to distinguish between the different subpopulations of oligodendroglia. Therefore, the analysis of different timepoints together with the usage of different reporter lines expressing GFP under the promotor of more specified transcription factors or proteins are necessary to distinguish between the various oligodendroglia subpopulations. *Gpr17* mRNA expression was observed in all dorsal olig2⁺ cells at 56 hpf. Since neuronal progenitor cells start to specify into OPCs at approximately 30 hpf and first dorsal mature Ols arise at 3 dpf, we concluded that *gpr17* is expressed in OPCs during zebrafish oligodendrogenesis (Preston and Macklin, 2015).

Moreover, we could not detect any *gpr17B* mRNA expression in zebrafish and we will therefore not focus on this variant in the present thesis.



4.1.1.2 *Gpr17* mRNA is expressed in pre-oligodendrocytes in zebrafish

To investigate whether *gpr17* mRNA is also expressed in pre-Ols we performed the RNAscope® assay in *Tg(nkx2.2a:mEGFP)* at 2.5 dpf. *Nkx2.2a* is a transcription factor expressed in pre-Ols promoting differentiation of OPCs into mature Ols (Kucenas et al., 2008). We found robust localization of *gpr17* mRNA within *nkx2.2a*⁺ pre-Ols in *Tg(nkx2.2a:mEGFP)* larvae (**Figure 10**).

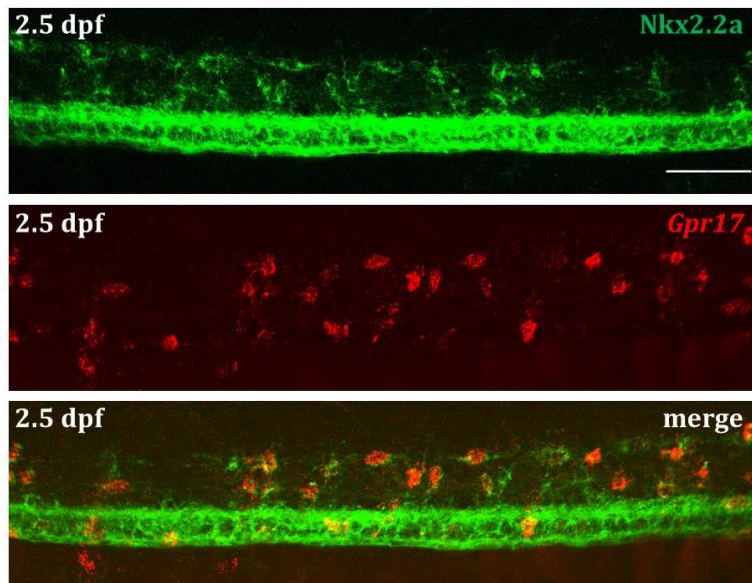
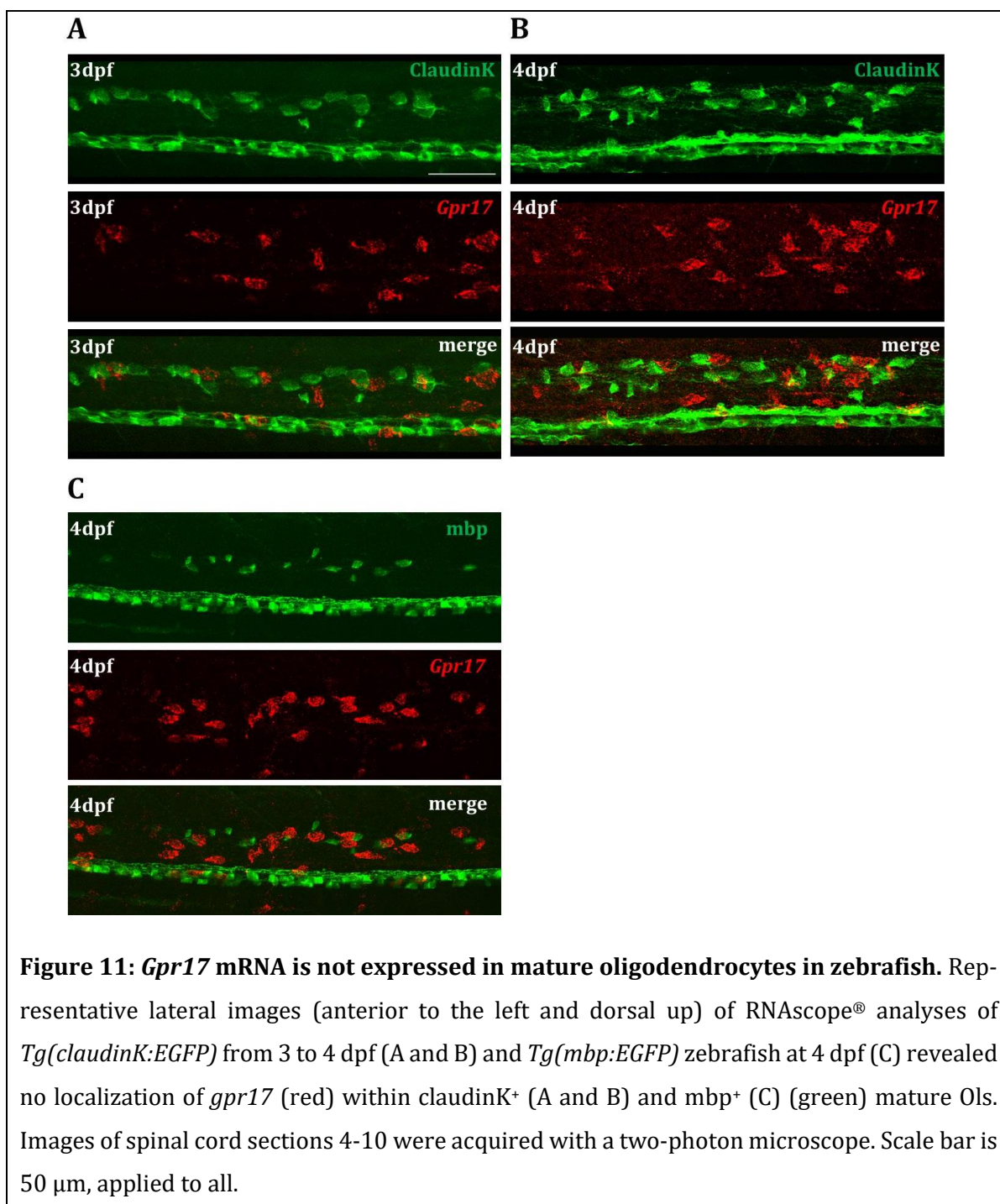


Figure 10: *Gpr17* mRNA is expressed in pre-oligodendrocytes in zebrafish. Representative lateral images (anterior to the left and dorsal up) of RNAscope® analyses of *Tg(nkx2.2a:mEGFP)* at 2.5 dpf revealed localization of *gpr17* mRNA (red) within *nkx2.2a:mEGFP*⁺ (green) pre-Ols. Images of spinal cord section 4-10 were taken with a two-photon microscope. Scale bar is 50 μ m, applied to all.

4.1.1.3 *Gpr17* mRNA is not expressed in mature oligodendrocytes in zebrafish

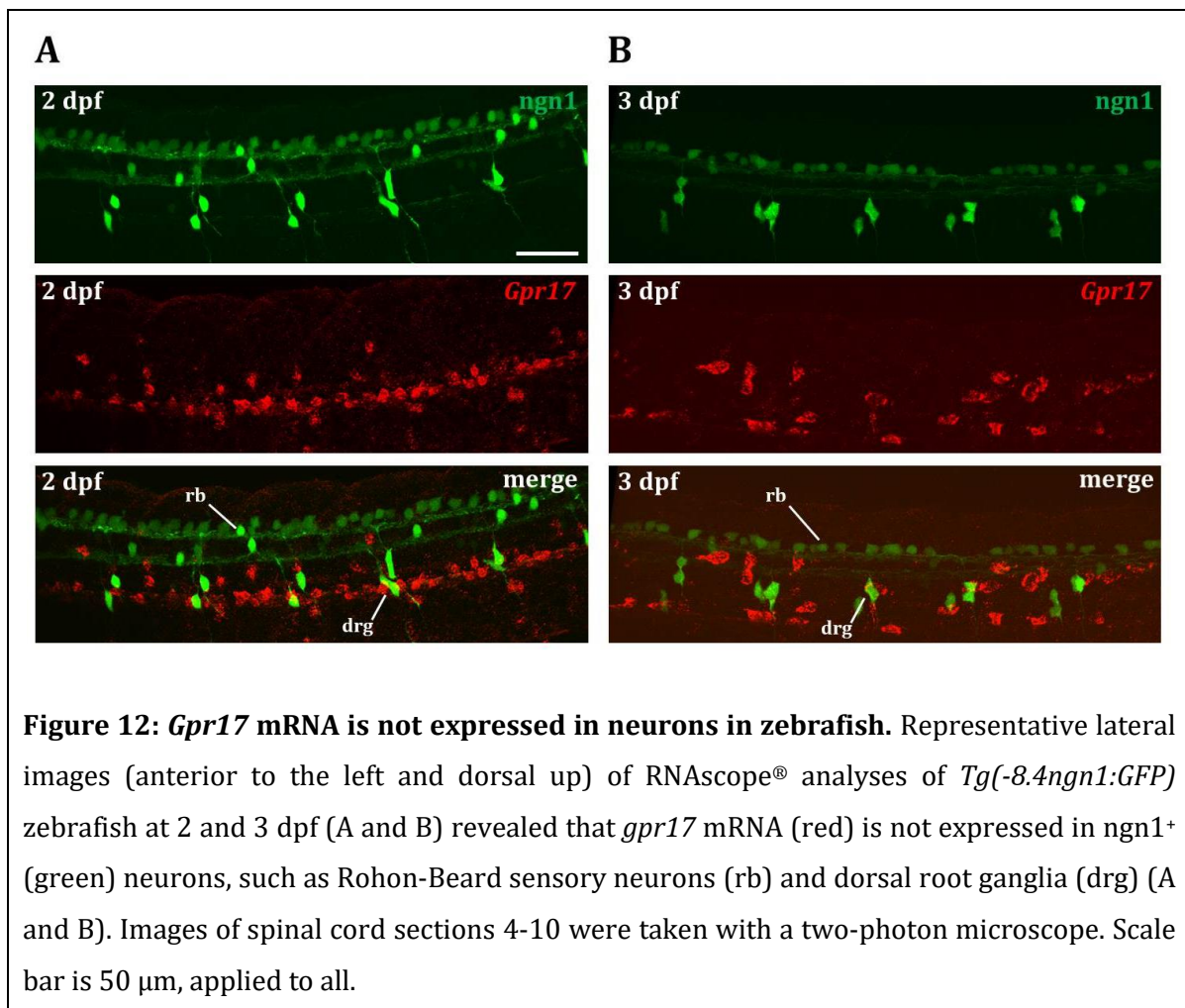
Notably, at 3 dpf, when first mature Ols are present, *olig2*⁺ cells emerged that lack *gpr17* mRNA (**Figure 9B**). To investigate whether *gpr17* is expressed in mature Ols we performed the RNAscope® assay in *Tg(claudinK:EGFP)* at 3 and 4 dpf and in *Tg(mbp:EGFP)* larvae at 4 dpf. *ClaudinK* is a tight junction protein that starts to be expressed in mature Ols in zebrafish (Münzel et al., 2012). *Mbp* is one of the major components of the myelin sheath and is therefore expressed in mature myelinating Ols. We could not observe any localization of *gpr17* mRNA within either GFP⁺ mature Ols of *Tg(claudinK:EGFP)* or in GFP⁺ mature Ols of *Tg(mbp:EGFP)* zebrafish (**Figure 11A-C**). Although *gpr17* mRNA appears to be located in *claudinK*⁺ and *mbp*⁺ cells in the representative compressed stack of the images, we could not observe any *gpr17*

localization within the respective cells when we analysed individual Z-sections of the acquired Z-stack as well as 3D-animations of these stacks. The appearance of a co-localization between *gpr17* and GFP in the compressed stack was due to an artifact of projecting different cells from multiple Z-sections into a single compressed image. Altogether, our data demonstrate that *gpr17* is expressed in OPCs and pre-Ols but not in mature Ols in zebrafish and therefore reflect the expression profile reported in mice (Bened-Jensen and Rosenkilde, 2010; Bläsius et al., 1998; Chen et al., 2009; Ciana et al., 2006; Lecca et al., 2008).



4.1.1.4 *Gpr17* mRNA is not expressed in neurons in zebrafish

To investigate the controversial expression pattern of *gpr17* in neurons (Chen et al., 2009; Lecca et al., 2008; Maisel et al., 2007), we performed the RNAscope® assay in *Tg(-8.4ngn1:GFP)* zebrafish (Blader et al., 2003) to detect both *gpr17* mRNA and neurogenin1 positive cells (*ngn1*⁺). The bHLH transcription factor neurogenin1 (*ngn1*) is expressed in Rohon-Beard sensory neurons (*rb*), hindbrain interneurons, clusters of neuronal precursors in the neural plate and in dorsal root ganglia (*drg*). We observed no *gpr17* mRNA expression within *ngn1*⁺ neurons at both 2 and 3 dpf in zebrafish spinal cord (**Figure 12A, B**), consistent with the findings previously reported in mice (Chen et al., 2009), in which no *gpr17* expression was found in neurons.



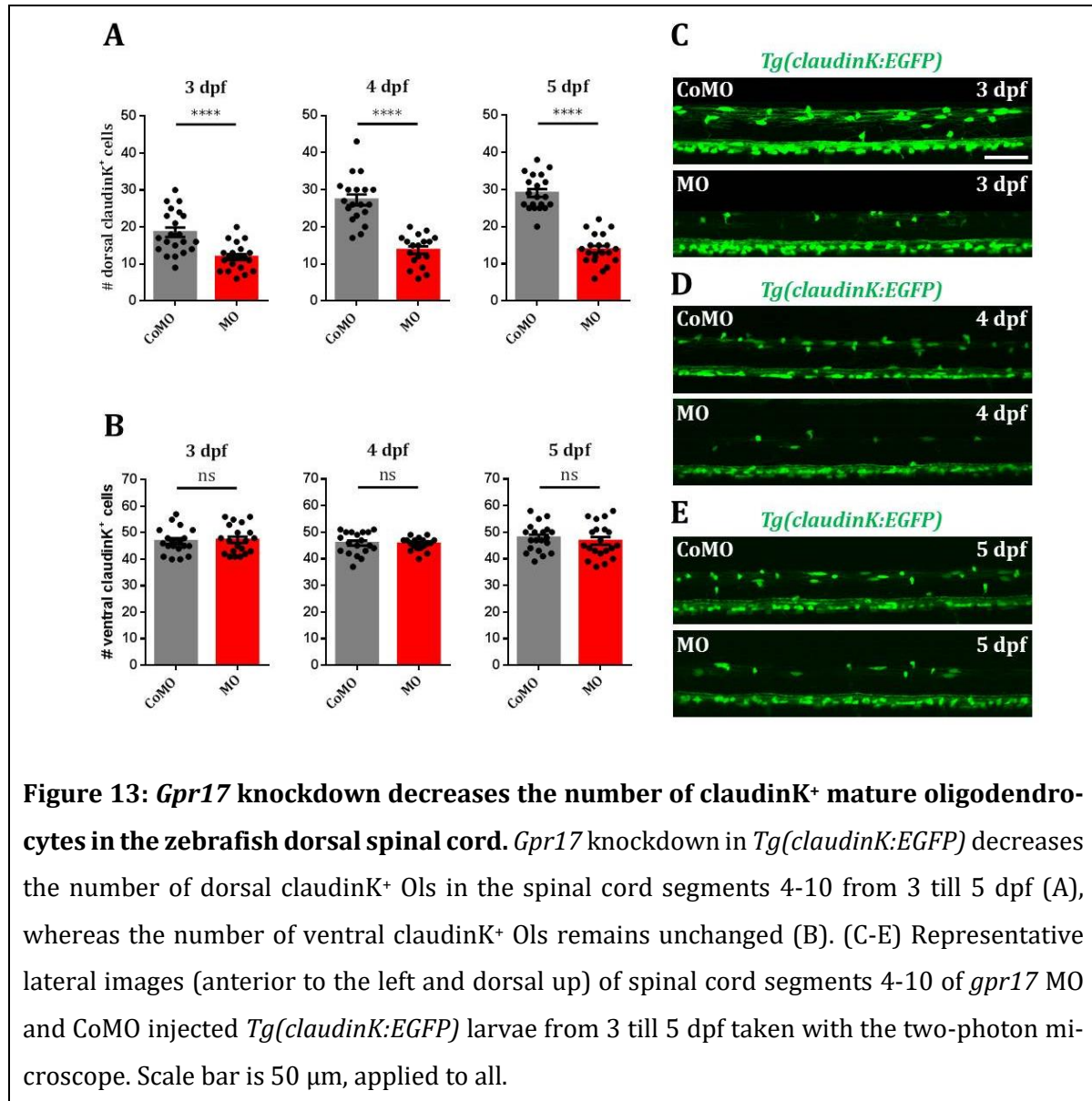
4.1.2 The functional role of Gpr17 in zebrafish

After clarifying the temporal and spatial expression of *gpr17* mRNA, we next investigated the functional role of Gpr17 in zebrafish. Therefore, we questioned whether Gpr17 affects Ol development and myelination in zebrafish in the same manner that has been observed in mice. To this end, we carried out *gpr17* morpholino (MO) knockdown and *gpr17* knockout experiments.

4.1.2.1 *Gpr17 knockdown decreases number of mature oligodendrocytes in the zebrafish dorsal spinal cord.*

To perform *gpr17* knockdown experiments, a short morpholino-modified antisense oligonucleotide was designed, which complementarily binds to a specific region of the target RNA, thereby blocking *gpr17* translation. We injected *gpr17* morpholino (MO) and control morpholino (CoMO) into the single-cell stage of different zebrafish reporter lines and investigated Ol development using different imaging techniques. *gpr17* MO specificity has been previously shown by RNA rescue injections into *gpr17* MO injected zebrafish (Schmitt, 2019).

To investigate the role of Gpr17 during Ol maturation, we initially performed MO knockdown experiments in *Tg(claudinK:EGFP)* and *Tg(mbp:EGFP)* embryos from 3 till 5 dpf, when first mature Ols are present in the dorsal spinal cord of zebrafish. When we quantified dorsal claudinK⁺ cells in the spinal cord of *Tg(claudinK:EGFP)* morphants, we found a significant reduction in the number of claudinK⁺ mature Ols from 3 till 5 dpf compared with CoMO injected fish (**Figure 13A**). By contrast, we found no change in the number of ventral claudinK⁺ Ols in the spinal cord of morphant *Tg(claudinK:EGFP)* compared to control injected larvae (**Figure 13B**).



Similarly, we found a significantly decreased number of dorsal and unchanged number of ventral *mbp*⁺ mature Ols in the spinal cord of MO injected *Tg(mbp:EGFP)* larvae from 4 till 5 dpf relative to control injected zebrafish (Figure 14A, B). This demonstrates that upon *gpr17* knockdown, Ol maturation in the dorsal spinal cord is impaired, whereas it remains unchanged in the ventral spinal cord indicating no general impairment of Ol development caused, for example, by increased apoptosis, decreased proliferation or defective differentiation.

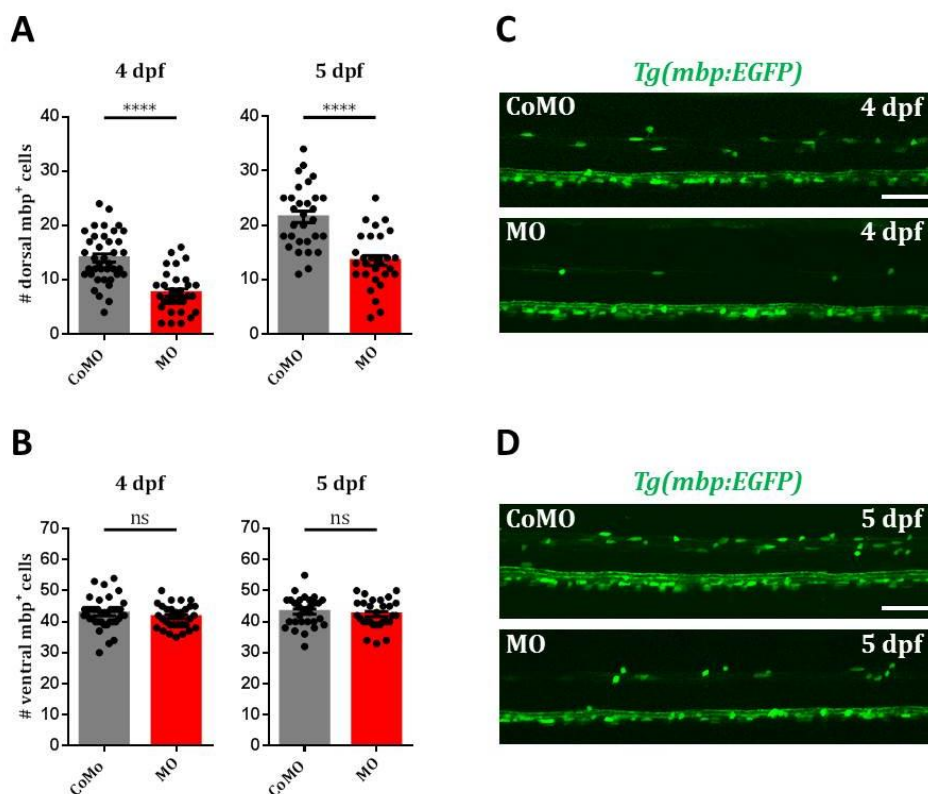


Figure 14: *Gpr17* knockdown decreases the number of mbp⁺ mature oligodendrocytes in the zebrafish dorsal spinal cord. *Gpr17* knockdown in *Tg(mbp:EGFP)* decreases the number of dorsal mbp⁺ Ols in the spinal cord segments 4-10 from 4 till 5 dpf (A), whereas the number of ventral mbp⁺ Ols remains unchanged (B). (C, D) Representative lateral images (anterior to the left and dorsal up) of spinal cord segments 4-10 of *gpr17* MO and CoMO injected *Tg(mbp:EGFP)* larvae from 4 till 5 dpf taken with the two-photon microscope. Scale bar is 50 μ m, applied to all.

4.1.2.2 Migration of olig2⁺ oligodendrocyte precursor cells is impaired after *gpr17* knockdown.

To investigate whether knockdown of *gpr17* is specifically affecting dorsal Ol maturation or also early OPC development and migration, we performed MO experiments in *Tg(olig2:EGFP)* larvae. The automated image analysis system used to generate several of the following results will be explained in detail in chapter 4.3. *Gpr17* knockdown in *Tg(olig2:EGFP)* resulted in a significantly decreased number of olig2⁺ Ol lineage cells in the whole dorsal spinal cord from 3 till 5 dpf compared with CoMO injected fish (**Figure 15A**). Since olig2 is expressed in the whole Ol lineage and at 3 dpf all subtypes of Ol lineage cells are present in the dorsal spinal cord, we performed time-lapse imaging of *gpr17* MO and CoMO injected *Tg(olig2:EGFP)* between 50 and 74 hpf. Compared with CoMO injected fish, we found a significant reduction of

Results

olig2⁺ OPCs after *gpr17* knockdown during early embryonic development, when only OPCs are present in the dorsal spinal cord (<2.5 dpf) (**Figure 15B**).

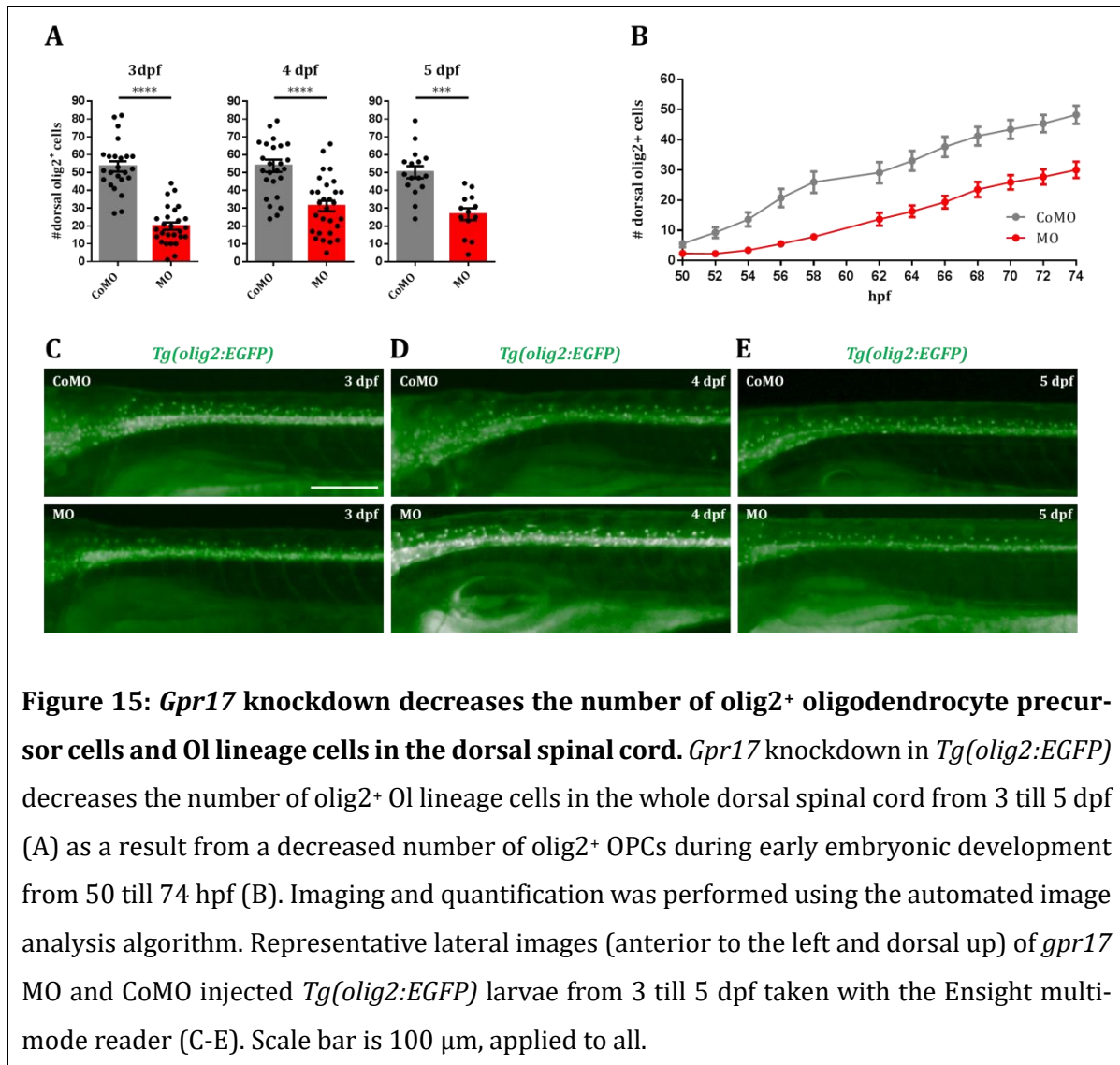
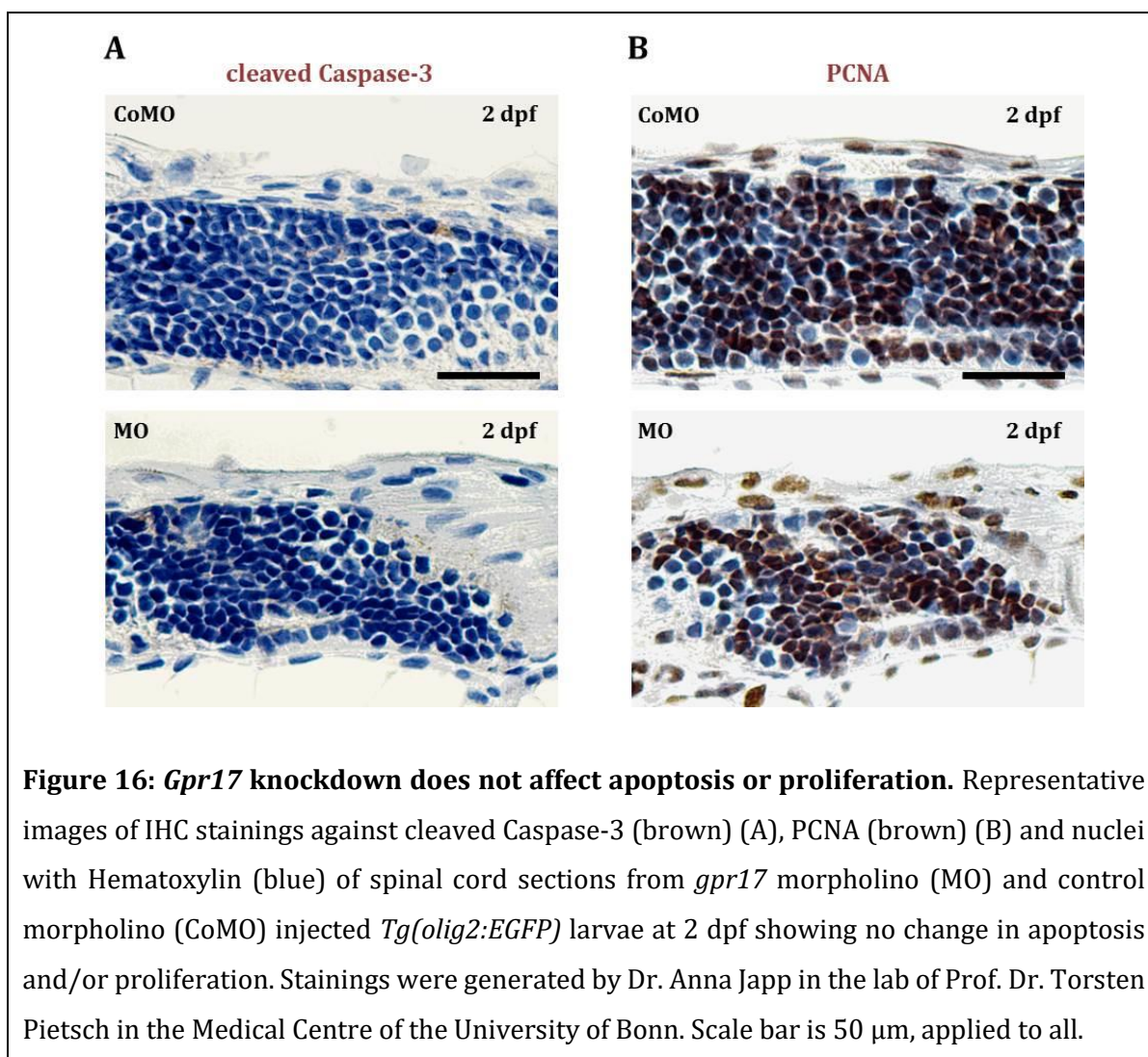


Figure 15: *Gpr17* knockdown decreases the number of olig2⁺ oligodendrocyte precursor cells and Ol lineage cells in the dorsal spinal cord. *Gpr17* knockdown in *Tg(olig2:EGFP)* decreases the number of olig2⁺ Ol lineage cells in the whole dorsal spinal cord from 3 till 5 dpf (A) as a result from a decreased number of olig2⁺ OPCs during early embryonic development from 50 till 74 hpf (B). Imaging and quantification was performed using the automated image analysis algorithm. Representative lateral images (anterior to the left and dorsal up) of *gpr17* MO and CoMO injected *Tg(olig2:EGFP)* larvae from 3 till 5 dpf taken with the Ensignt multi-mode reader (C-E). Scale bar is 100 μ m, applied to all.

Altogether, our data demonstrate that the knockdown of *gpr17* results in a reduced number of dorsal olig2⁺ OPCs and, consequently, in a reduced number of dorsal mature claudinK⁺ and mbp⁺ Ols in zebrafish spinal cord, raising the question about which possible causes could explain the observed phenotype.

4.1.2.3 *Gpr17* knockdown does not impair general or neuronal development, apoptosis or proliferation in zebrafish larvae.

To investigate whether *gpr17* MO injection decreases the number of Ol lineage cells by unspecific effects, such as increased cell death (apoptosis), decreased proliferation, impaired larval general or neuronal development, we performed several different experimental approaches. First, we stained *gpr17* MO and CoMO injected *Tg(olig2:EGFP)* larvae at 2 dpf for the apoptosis marker cleaved Caspase-3 and for the proliferation marker Proliferating cell nuclear antigen (PCNA). The number of cells positively labelled for cleaved Caspase-3 (**Figure 16A**) and PcnA (**Figure 16B**) were not increased after *gpr17* knockdown compared to CoMO injected larvae, ruling out an alteration of apoptosis or proliferation as a reason for the decreased number of OPCs and mature Ols in the dorsal spinal cord.



Results

Neither did we observe alterations of animal size or general development by time-lapse imaging between 50 and 74 hpf (**Figure 17A, B**), nor any defects in neuronal development by staining with established markers for the neural network, such as acetylated tubulin and synaptic vesicular protein 2 (SV2), ruling out gross unspecific effects of *gpr17* MO injection (**Figure 17C, D**).

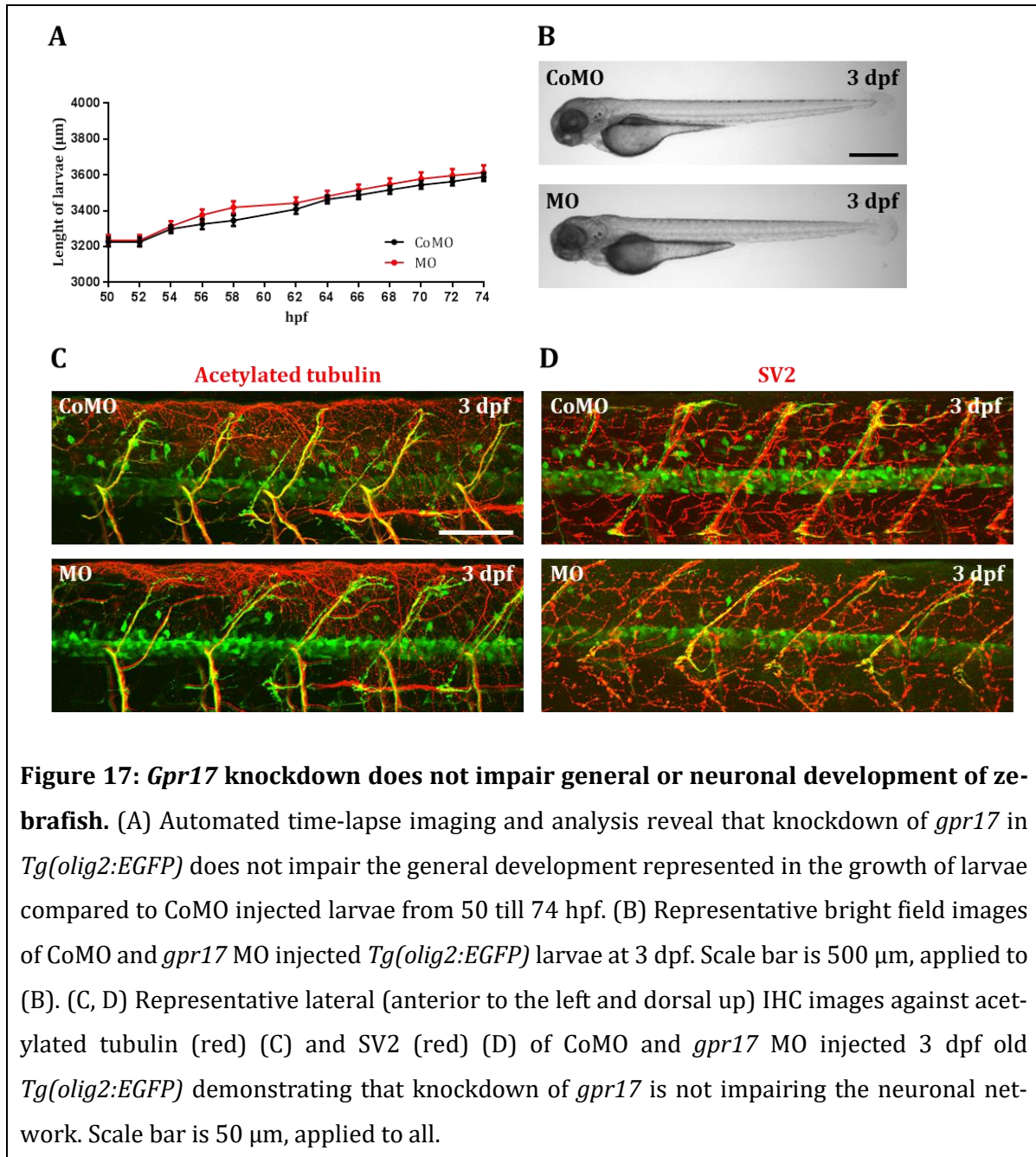
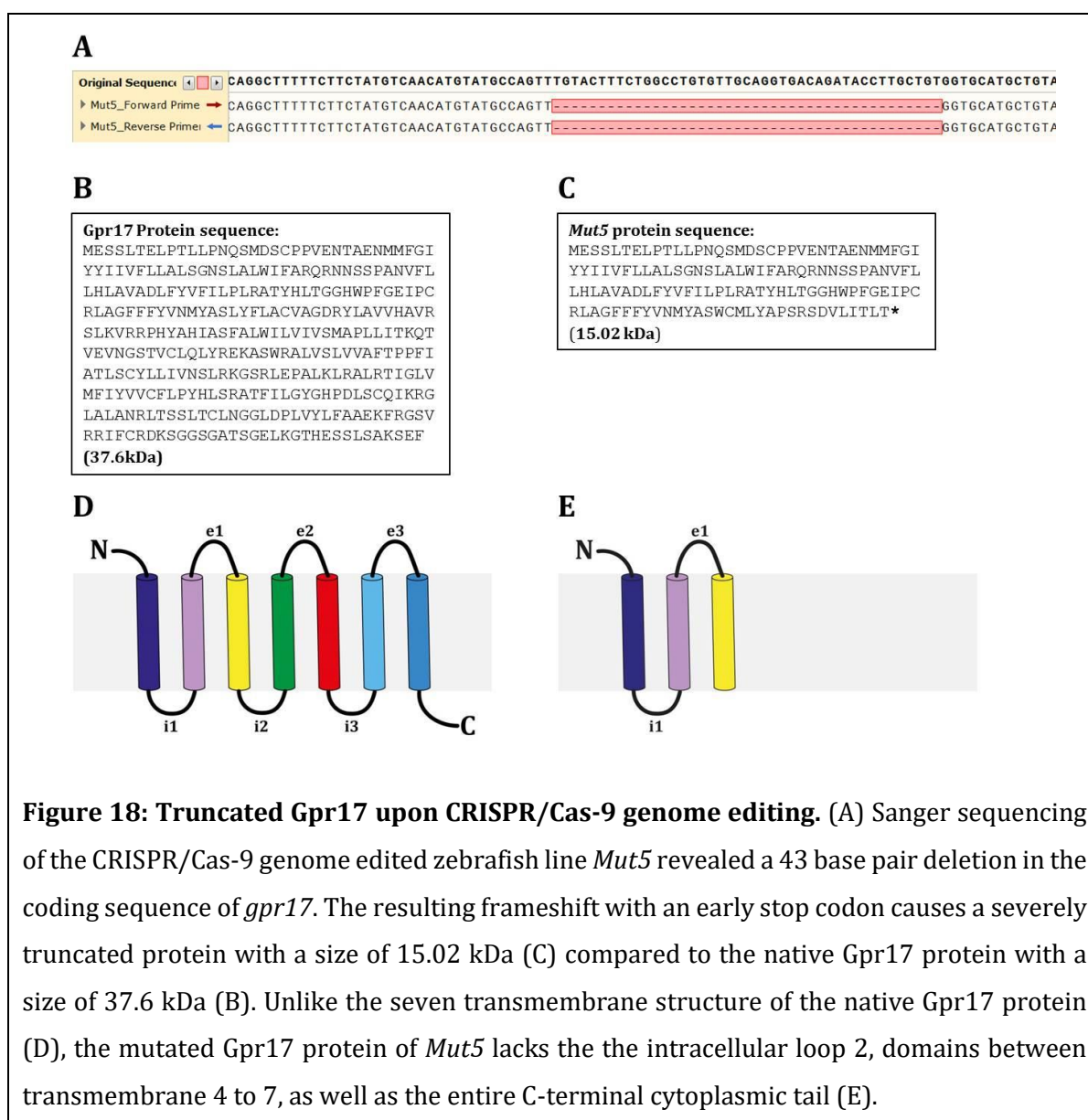


Figure 17: *Gpr17* knockdown does not impair general or neuronal development of zebrafish. (A) Automated time-lapse imaging and analysis reveal that knockdown of *gpr17* in *Tg(olig2:EGFP)* does not impair the general development represented in the growth of larvae compared to CoMO injected larvae from 50 till 74 hpf. (B) Representative bright field images of CoMO and *gpr17* MO injected *Tg(olig2:EGFP)* larvae at 3 dpf. Scale bar is 500 µm, applied to (B). (C, D) Representative lateral (anterior to the left and dorsal up) IHC images against acetylated tubulin (red) (C) and SV2 (red) (D) of CoMO and *gpr17* MO injected 3 dpf old *Tg(olig2:EGFP)* demonstrating that knockdown of *gpr17* is not impairing the neuronal network. Scale bar is 50 µm, applied to all.

4.1.2.4 *Gpr17* knockout fish

To confirm the specificity of the MO knockdown experiments and to obtain further evidence for the functional role of *Gpr17* during OI development, Nanjing Sanjay Medical Technology in China generated several potential *gpr17* knockout fish by CRISPR/Cas-9 technology. Upon genome editing, a 43 bp deletion in the coding sequence of *gpr17* was identified in the fish *Mut5*, causing a severely truncated protein due to the resulting frameshift with an early stop codon (**Figure 18A-C**). The mutated *Gpr17* protein of *Mut5* lacks the intracellular loop 2, all regions between the transmembrane domains 4 and 7, as well as the entire C-terminal cytoplasmic tail (**Figure 18E**). Additionally, we extracted RNA from *Mut5* and confirmed the respective mutation within the complementary DNA by Sanger sequencing. Therefore, we consider *Mut5* as a putative *gpr17* knockout zebrafish line.

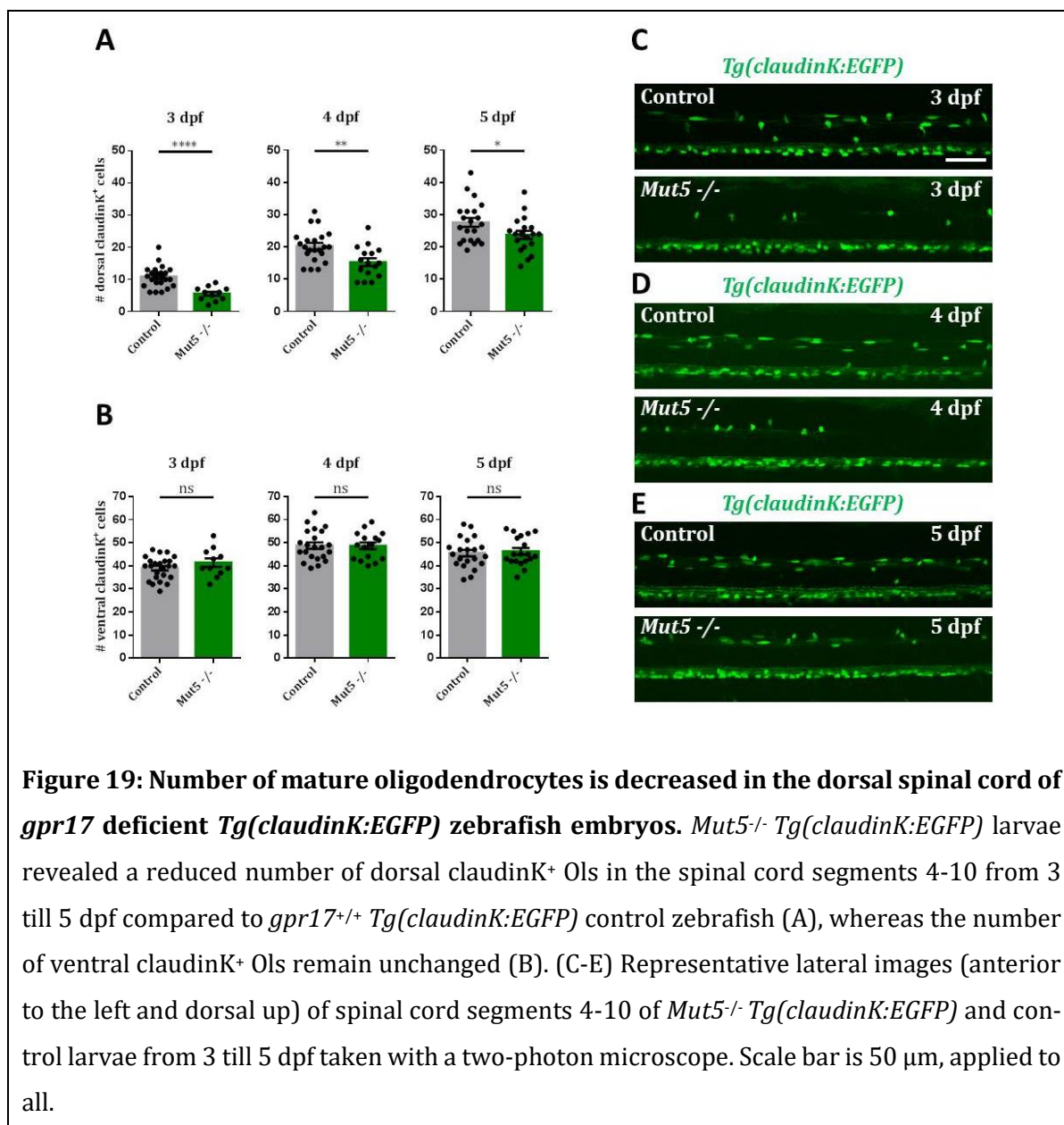


Results

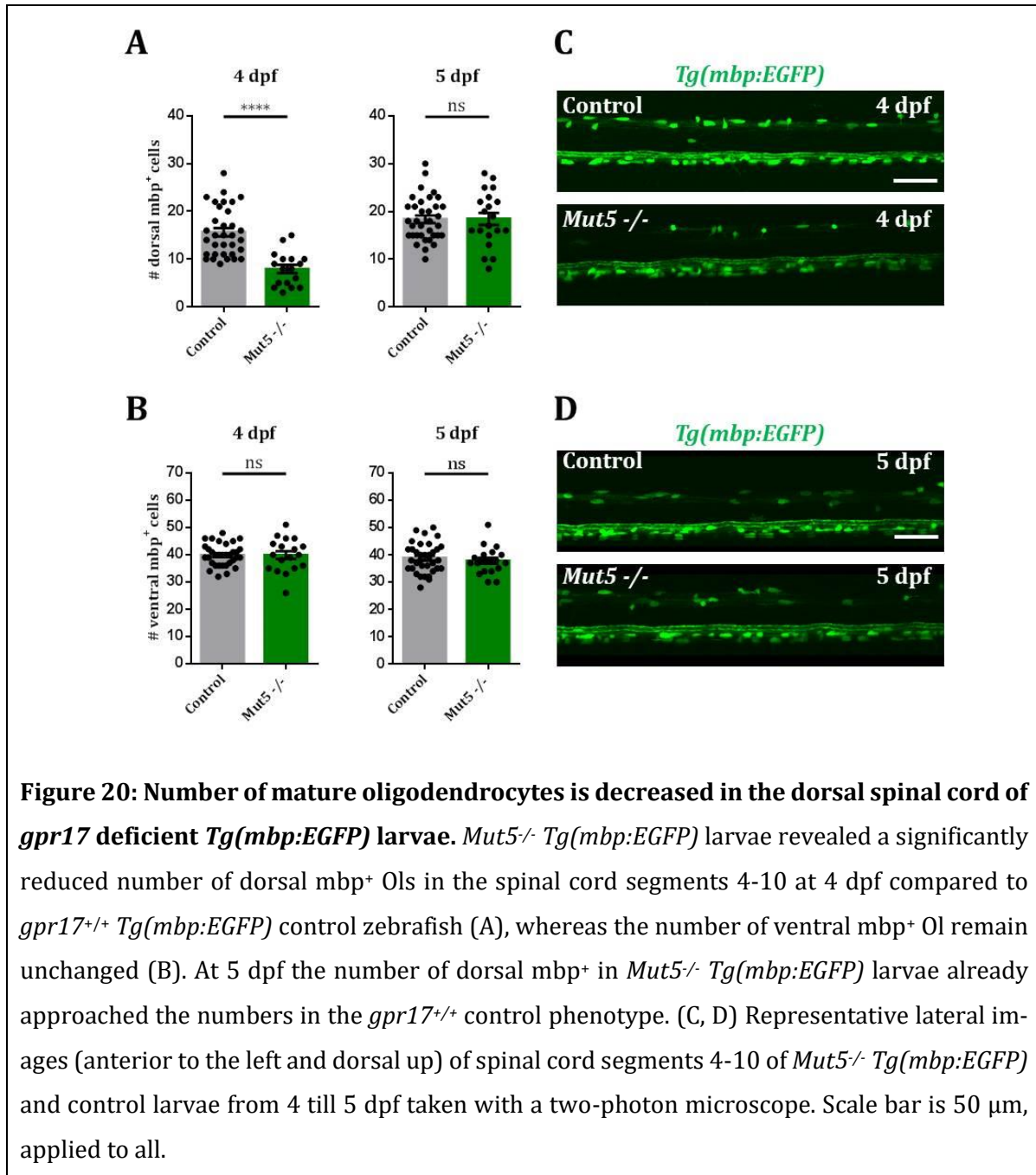
Similar to *Gpr17*^{-/-} mice, homozygous *Mut5* (*Mut5*^{-/-}) zebrafish are viable, show no behavioral abnormalities and produce viable offspring. Adult *gpr17*^{-/-} fish were then crossed into the respective transgenic fluorescent reporter lines to generate *gpr17*^{+/-} fish. The respective *gpr17*^{+/-} reporter lines were then inbred and their offspring, including wt, *gpr17*^{-/-} and *gpr17*^{+/-} individuals, were used for imaging. After image analysis the respective zebrafish were then genotyped. With this experimental approach, we ensured that possible off-target effects upon genome editing are also analysed in the respective wt controls, therefore making the obtained data comparable.

4.1.2.5 Mature oligodendrocyte numbers are decreased in the dorsal spinal cord of *gpr17* deficient zebrafish affecting dorsal myelination.

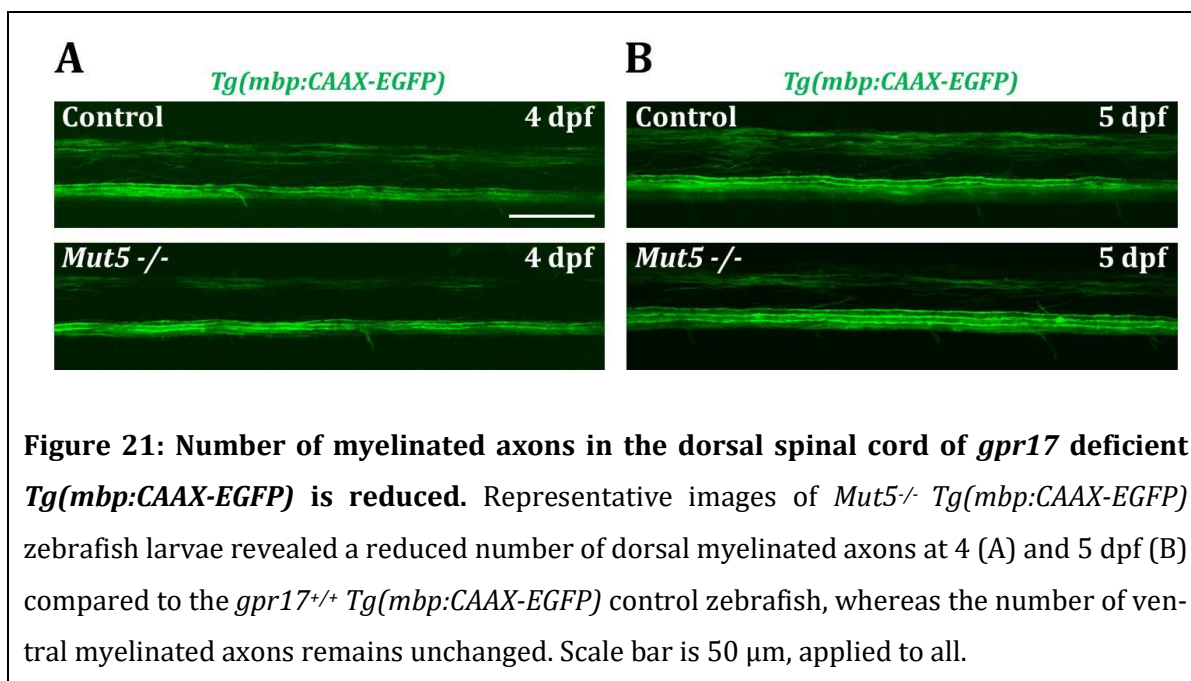
To determine whether *gpr17* knockout affects Ol maturation in a similar manner as we observed after *gpr17* knockdown, we imaged *Mut5*^{-/-} *Tg(claudinK:EGFP)* and *Mut5*^{-/-} *Tg(mbp:EGFP)* larvae versus the respective *gpr17*^{+/+} control reporter line. When we quantified claudinK⁺ cells in the dorsal spinal cord of *Mut5*^{-/-} *Tg(claudinK:EGFP)* larvae, we found a significant reduction in the number of mature Ols from 3 till 5 dpf compared with control larvae (**Figure 19A**). We did not observe any difference in the number of claudinK⁺ cells in the ventral spinal cord from 3 till 5 dpf, suggesting no general impairment of Ol development in *gpr17* deficient zebrafish larvae (**Figure 19B**). Unlike to the knockdown experiments, Ol development in *gpr17*^{-/-} *Tg(claudinK:EGFP)* larvae tends to approach the control phenotype with increasing age, indicating existence of compensatory mechanisms in *gpr17*^{-/-} zebrafish.



Likewise, a significant decrease in the number of dorsal and an unchanged number of ventral mbp⁺ mature Ols in the spinal cord of *Mut5*^{-/-} *Tg(mbp:EGFP)* larvae relative to *gpr17*^{+/+} *Tg(mbp:EGFP)* larvae were found at 4 dpf (**Figure 20A, B**). Interestingly, at 5 dpf a significant difference in the number of dorsal mbp⁺ Ols in *Mut5*^{-/-} *Tg(mbp:EGFP)* and *gpr17*^{+/+} larvae could not be detected anymore.



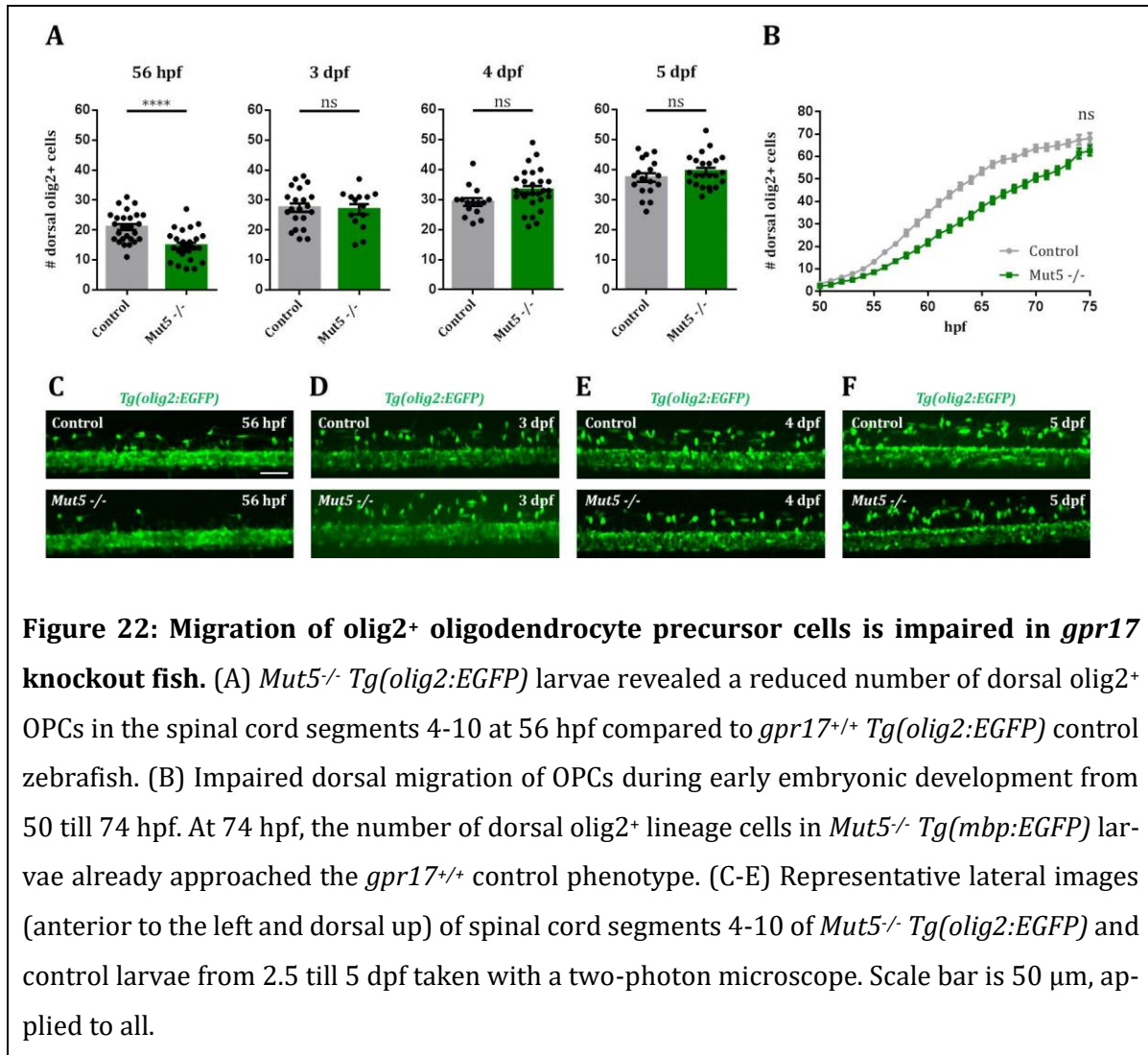
As a logic consequence of the reduced number of dorsal mature Ols, we found a reduced number of myelinated axons in the dorsal part of the spinal cord of *gpr17* deficient *Tg(mbp:CAAX-EGFP)* relative to control larvae at 4 and 5 dpf (**Figure 21A, B**). In contrast, we observed an unchanged number of myelinated axons in the ventral spinal cord of *Mut5*^{-/-} *Tg(mbp:CAAX-EGFP)* compared to control fish (**Figure 21A, B**).



Thus, consistent with our findings in *gpr17* morphants, during early development in *gpr17* deficient zebrafish, Ol maturation is affected in the dorsal spinal cord, but not in the ventral spinal cord, which suggests no general impairment of Ol development.

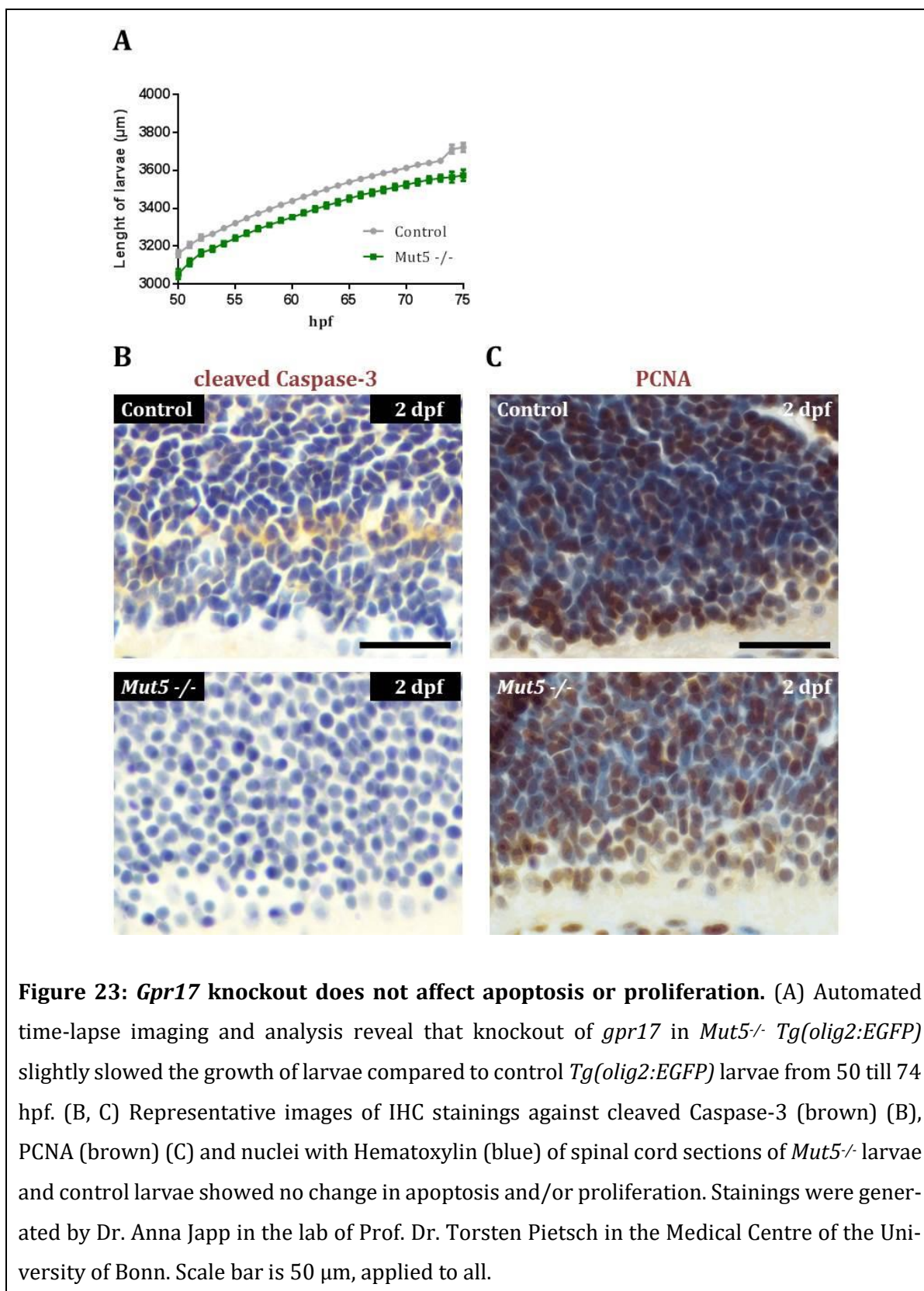
4.1.2.6 Migration of olig2⁺ oligodendrocyte precursor cells is impaired in *gpr17* knock-out fish.

To investigate whether *gpr17* knockout specifically affects dorsal Ol maturation or, as observed in *gpr17* morphants, early OPC development and migration, we started to image the offspring of *gpr17^{+/+} Mut5 Tg(olig2:EGFP)* at early times and genotyped the respective larvae afterwards. In *Mut5^{-/-} Tg(olig2:EGFP)*, we found significantly decreased numbers of olig2⁺ OPCs in the dorsal spinal cord compared with *Mut5^{+/+} Tg(olig2:EGFP)* control larvae at 56 hpf (**Figure 22A**). Moreover, we observed a reduced migration of olig2⁺ OPCs into the dorsal area of the spinal cord when performing time-lapse imaging with the offspring from *Mut5^{-/-} Tg(olig2:EGFP)* and *Tg(olig2:EGFP)* control larvae (**Figure 22B**). Therefore, consistent with the *gpr17* knockdown, *gpr17* knockout also results in a reduction of dorsal OPCs in the early beginning of Ol development in zebrafish. However, from 3 dpf the number of dorsal olig2⁺ Ol lineage cells in *Mut5^{-/-} Tg(olig2:EGFP)* larvae started to catch up with numbers observed in control zebrafish (**Figure 22A, B**), again indicating some compensation mechanism in *gpr17^{-/-}* zebrafish.



4.1.2.7 *Gpr17* knockout is specific and does not impair apoptosis, proliferation or neuronal development

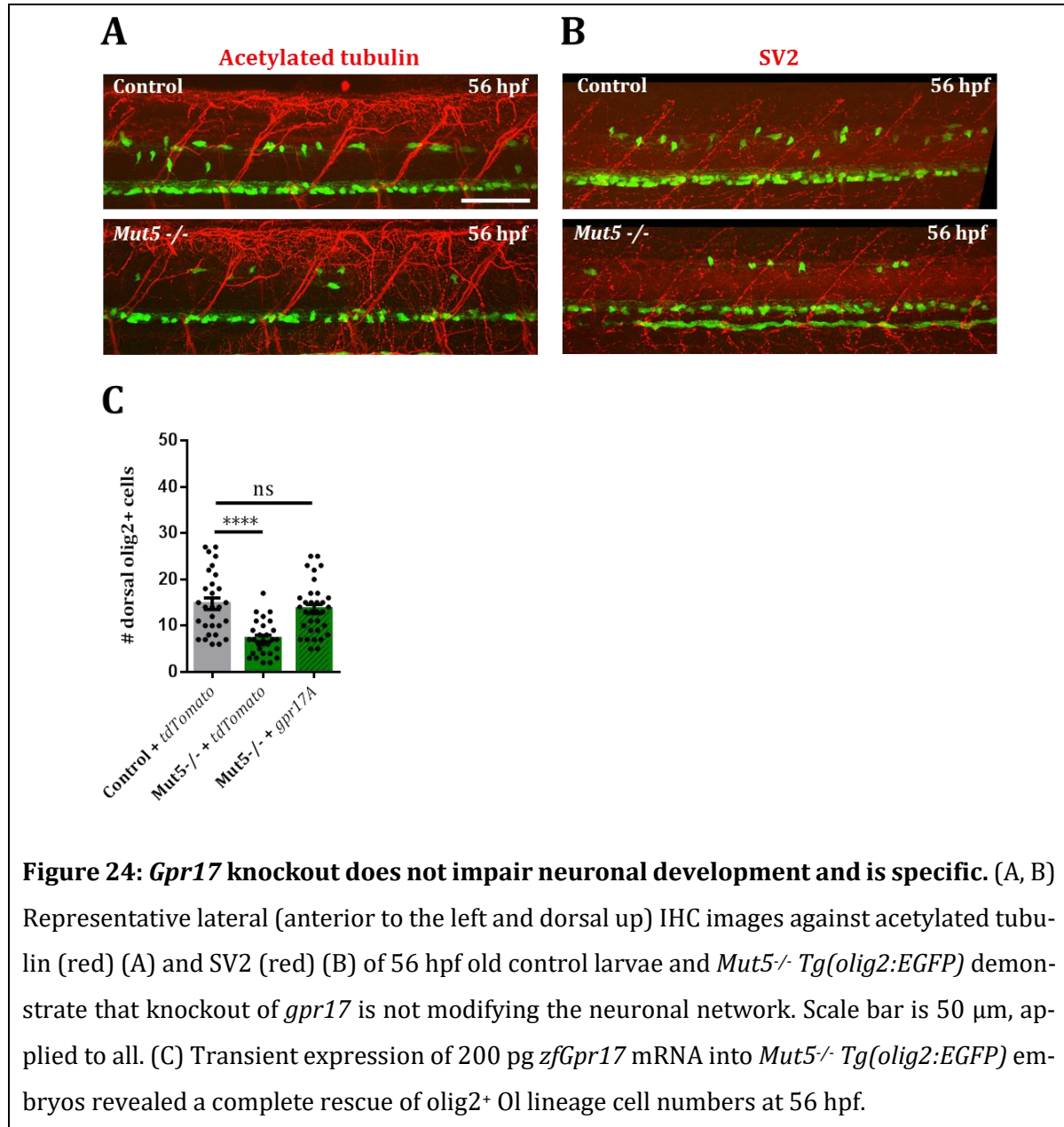
We next analysed whether *gpr17* gene editing decreases the number of Ol lineage cells by un-specific effects, such as increased cell death (apoptosis), decreased proliferation, altered larval general or neuronal development. We observed a slightly slower growth of *Mut5^{-/-} Tg(olig2:EGFP)* larvae compared to control *Tg(olig2:EGFP)* larvae from 50 till 75 hpf (**Figure 23A**). Nevertheless, immunohistochemistry analyses of *Mut5^{-/-}* and *gpr17^{+/+}* control larvae at 2 dpf for the apoptosis marker cleaved Caspase-3 (**Figure 23B**) and for the proliferation marker PCNA (**Figure 23C**) showed that the number of cells positively labelled for both markers was not altered after *gpr17* gene editing compared to control larvae. These findings ruled out alterations of apoptosis or proliferation as reasons for the reduced number of OPCs and mature Ols in the dorsal spinal cord.



Furthermore, immunostaining analyses to detect acetylated tubulin and SV2 were comparable between *Mut5^{-/-}* and control larvae, indicating no defects in neuronal development (**Figure 24A, B**). Altogether, our immunohistochemistry analyses discard the possibility of gross

Results

unspecific effects upon CRISPR/Cas-9 genome editing. Notably, we were able to rescue the *gpr17* knockout phenotype by injecting *gpr17* mRNA into the single-cell stage eggs of *Mut5*^{-/-} *Tg(olig2:EGFP)* larva, thus confirming the *gpr17* knockout specificity (**Figure 24C**).

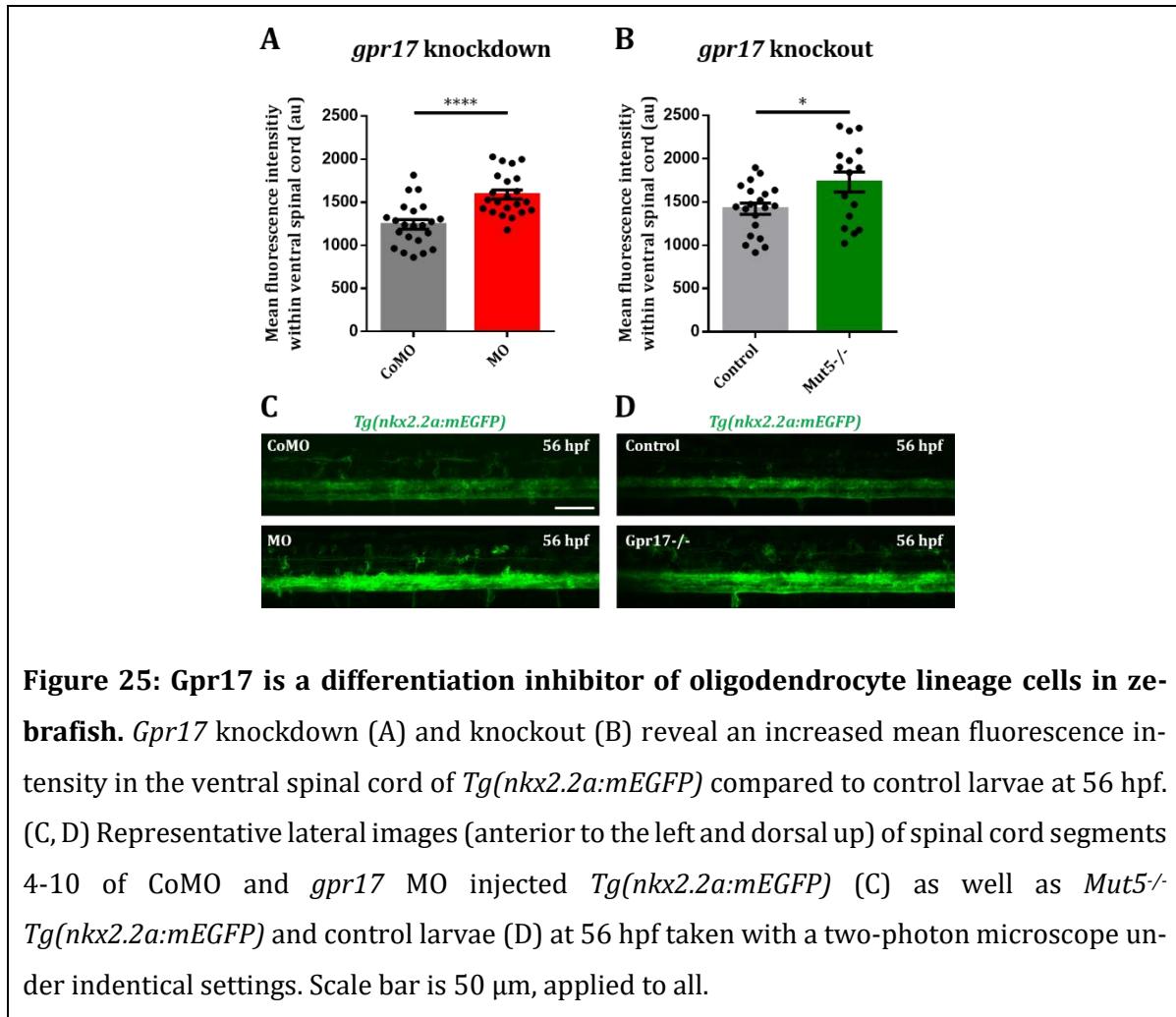


In summary, the results obtained with *gpr17* knockout zebrafish are consistent with our findings in *gpr17* MO morphants, displaying a reduction in the number of both migrating OPCs and migrated mature Ols in dorsal spinal cord upon *Gpr17* inactivation. This reduction is not due to unspecific off-target effects of either *gpr17* MO morphants or *gpr17* deficient zebrafish. Interestingly, whereas the partial knockdown of *gpr17* does not lead to a compensation of the observed phenotype, *gpr17* mutants tend to compensate it over time, suggesting a potential

transcriptional regulation in the highly regenerative zebrafish to counteract the deficiency of *gpr17*.

4.1.2.8 *Gpr17* is a differentiation inhibitor of oligodendrocyte lineage cells in zebrafish

To examine the effects of *gpr17* deletion more directly, we performed *gpr17* MO knockdown experiments in *Tg(nkx2.2a:mEGFP)* larvae. *Nkx2.2a* is a transcription factor expressed in axon-associated pre-Ols that enter the terminal differentiation pathway (Kucenas et al., 2008). *Gpr17* MO injection resulted in a significant increase of fluorescence intensity in the ventral spinal cord of *Tg(nkx2.2a:mEGFP)* compared with control injected larvae at 56 hpf (**Figure 25A**). Consistent with this observation, we also found a significant increase of fluorescence intensity within the ventral spinal cord of *Mut5^{-/-} Tg(nkx2.2a:mEGFP)* compared with control larvae (**Figure 25B**). These data indicate that in the absence of *Gpr17* OPCs prematurely differentiate into pre-Ols in zebrafish ventral spinal cord, thus increasing the amount of pre-Ols while decreasing OPC numbers. Consequently, this reduction in ventral OPCs diminishes the number of available OPCs that migrate into the dorsal spinal cord. Taken together, our findings define *Gpr17* as an inhibitor of oligodendroglial differentiation in zebrafish since its absence accelerates the progression of OPCs to pre-Ols.



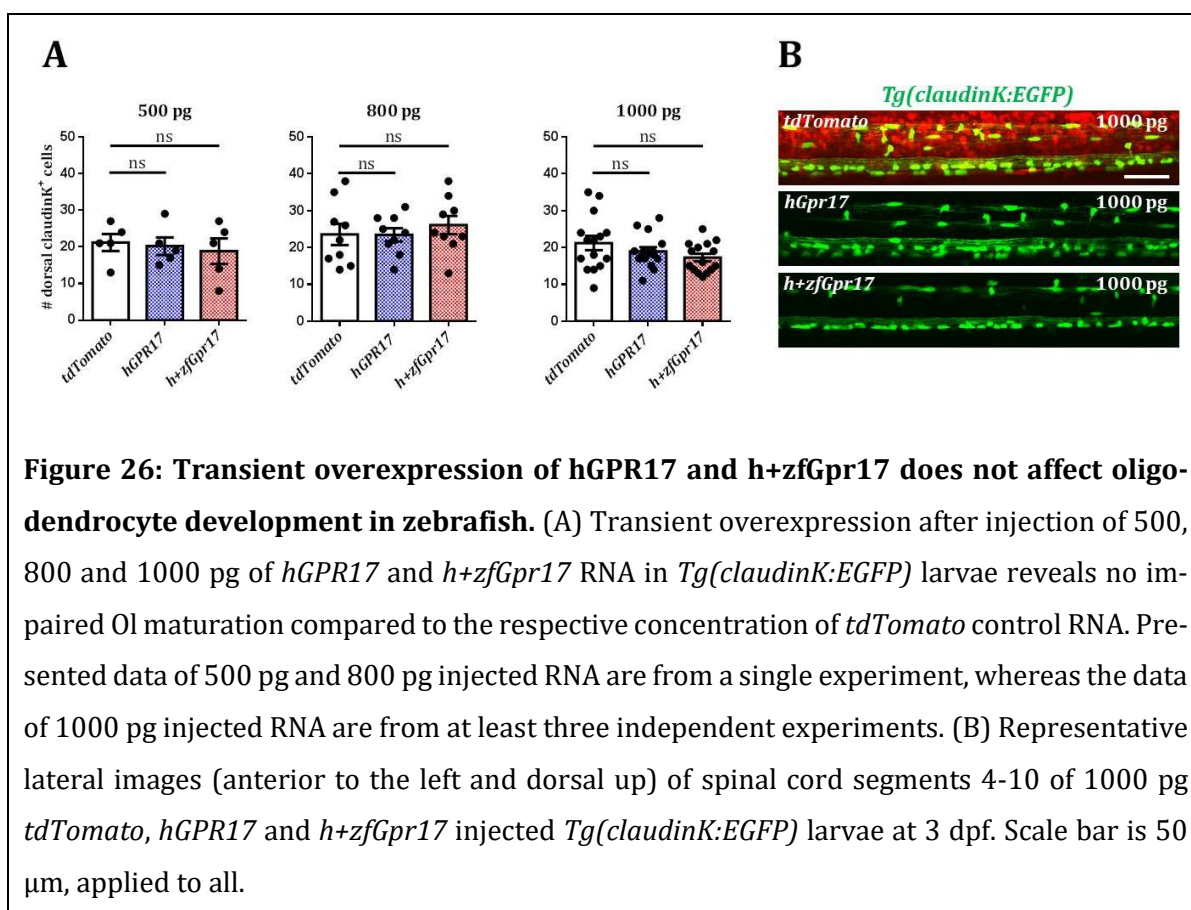
In summary, our data demonstrate that the role of Gpr17 as a negative regulator of Ol differentiation is conserved between zebrafish and mammals. Therefore, we envisage that a zebrafish functionally expressing a human or chimeric Gpr17 receptor may serve as a model organism for myelination research and for establishment of an *in vivo* compound screening platform.

4.2 A humanized zebrafish as a model organism for human disease research

Having clarified the expression and function of Gpr17 in zebrafish, we then investigated whether the human GPR17 receptor (hGPR17) can be functionally expressed in zebrafish. Because the zebrafish and the human Gpr17 proteins only share a 43.4 % homology, which could compromise the expression of hGPR17 in zebrafish, we have also designed a chimeric GPR17 receptor (h+zfGpr17), consisting of the extracellular and transmembrane regions of the hGPR17 receptor together with the intracellular loops of the zebrafish receptor. Expression and functionality of h+zfGpr17 have already been confirmed *in vitro* (Schmitt, 2019).

4.2.1 Transient overexpression of *hGPR17* and *h+zfGpr17* do not affect oligodendrocyte development in zebrafish

To investigate the functionality of *hGPR17* and *h+zfGpr17* *in vivo*, we transiently overexpressed both receptors in zebrafish by injecting different amounts of the respective RNAs into single cell stage eggs of *Tg(claudinK:EGFP)* larvae. *TdTomato* RNA was injected as a control, proving the efficacy of the injection and excluding non-specific injection effects. We observed strong red fluorescent *tdTomato* expression after injection with all different RNA concentrations, thus assuming efficient expression of *hGPR17* and *h+zfGpr17* as well (**Figure 26B**). Similar to the transient overexpression of the native zebrafish *Gpr17* receptor (Schmitt, 2019), changes in the number of dorsal *claudinK*⁺ Ols after transient overexpression of *hGPR17* and *h+zfGpr17* compared to *tdTomato* control injected zebrafish at 3 dpf were not present, ruling out unspecific effects of both receptors in zebrafish (**Figure 26A, B**).



4.2.2 hGPR17 and h+zfGpr17 are functional in zebrafish

To investigate whether hGPR17 and h+zfGpr17 are functionally expressed in zebrafish we performed rescue experiments by injecting the respective mRNA into single stage eggs of either *gpr17* MO injected *Tg(olig2:EGFP)* or *Mut5^{-/-} Tg(olig2:EGFP)* larvae. Quantification of the number of dorsal olig2⁺ Ol lineage cells at 3 dpf displayed a partial rescue in both *hGPR17* and *h+zfGpr17* injected *gpr17* morphants relative to control morpholino (**Figure 27A**). Furthermore, a complete rescue in *hGPR17* and *h+zfGpr17* injected *Mut5^{-/-} Tg(olig2:EGFP)* larvae was observed at 56 hpf (**Figure 27B**).

Altogether, our data indicate that both hGPR17 and h+zfGpr17 are functional in zebrafish. These findings support the concept of developing a humanized zebrafish as a model organism for human disease research, which could be used as tool to screen in zebrafish for drugs inhibiting human GPR17 that would successfully foster remyelination in humans.

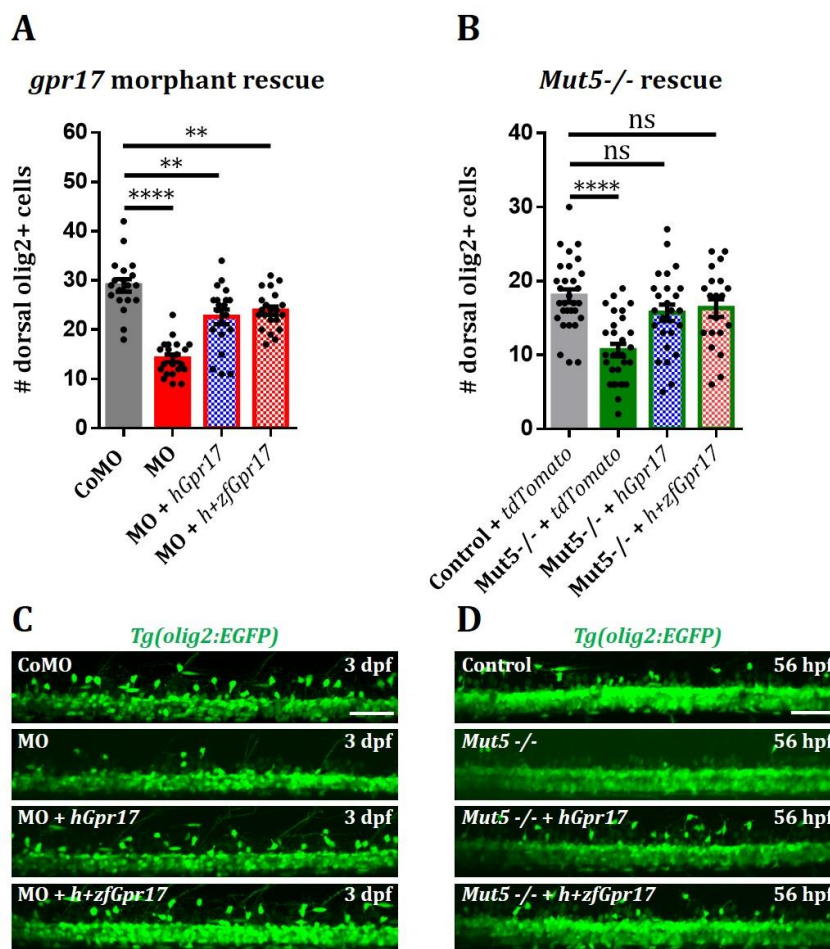


Figure 27: hGPR17 and h+zfGpr17 are functional in zebrafish. Transient expression after injection of 500 pg *hGPR17* and *h+zfGpr17* mRNA into *gpr17* MO injected *Tg(olig2:EGFP)* and 200 pg in *Mut5*^{-/-} *Tg(olig2:EGFP)* larvae revealed a partial rescue of dorsal olig2⁺ Ol lineage cells in *gpr17* morphants at 3 dpf (A) and a complete rescue in *Mut5*^{-/-} *Tg(olig2:EGFP)* larvae at 56 hpf (B). Representative lateral images (anterior to the left and dorsal up) of spinal cord segments 4-10 of CoMO, *gpr17* morphants and 500 pg *tdTomato*, *hGPR17* and *h+zfGpr17* injected *gpr17* morphants at 3 dpf (C) and *Mut5*^{-/-} *Tg(olig2:EGFP)* larvae at 56 hpf (D). Scale bar is 50 μ m, applied to all.

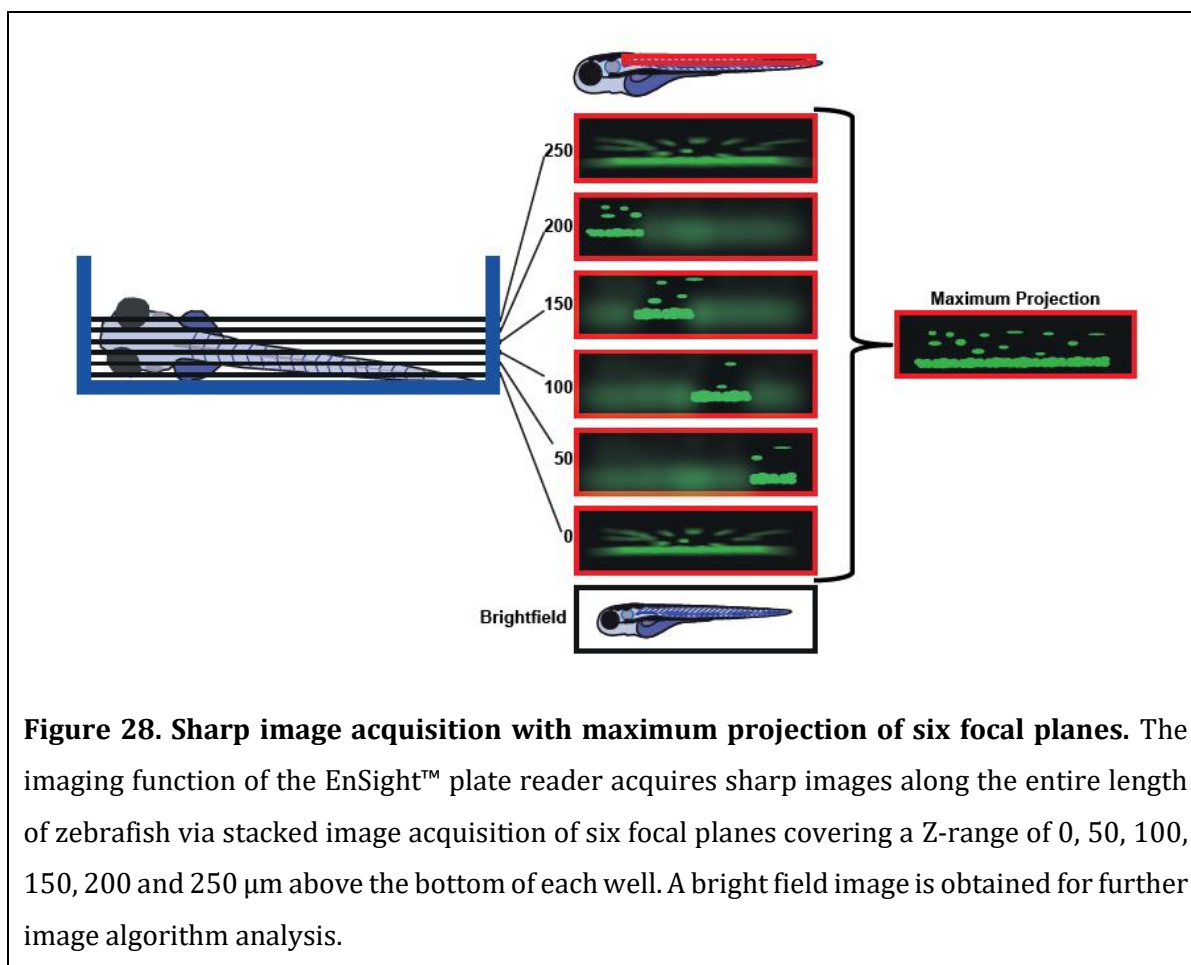
4.3 A novel plate reader-based automated high throughput *in vivo* imaging and analysis platform to investigate oligodendrocyte development in living zebrafish larvae

To facilitate the search for inhibitors of human GPR17 in zebrafish, an automated screening system would be mandatory, preferably as a high throughput *in vivo* imaging and analysis platform. Therefore, we decided to perform spinal cord imaging using the Perkin Elmer's EnSight™ multimode plate reader, which was initially developed to perform different *in vitro* high-throughput imaging and analysis applications. The EnSight™ reader images multi-well plates at high speed with low signal-to-background noise using both laser-based autofocus for fast setup and solid-state light sources (LEDs) for short illumination times. An automated highly sensitive scientific-grade complementary metal oxide semiconductor (sCMOS) camera enables image acquisition of fluorescence and bright-field images at high speed with high resolution. Moreover, the associated Perkin Elmer Kaleido™ software supports several modes of image analysis and allows the implementation of custom-made image analysis algorithms.

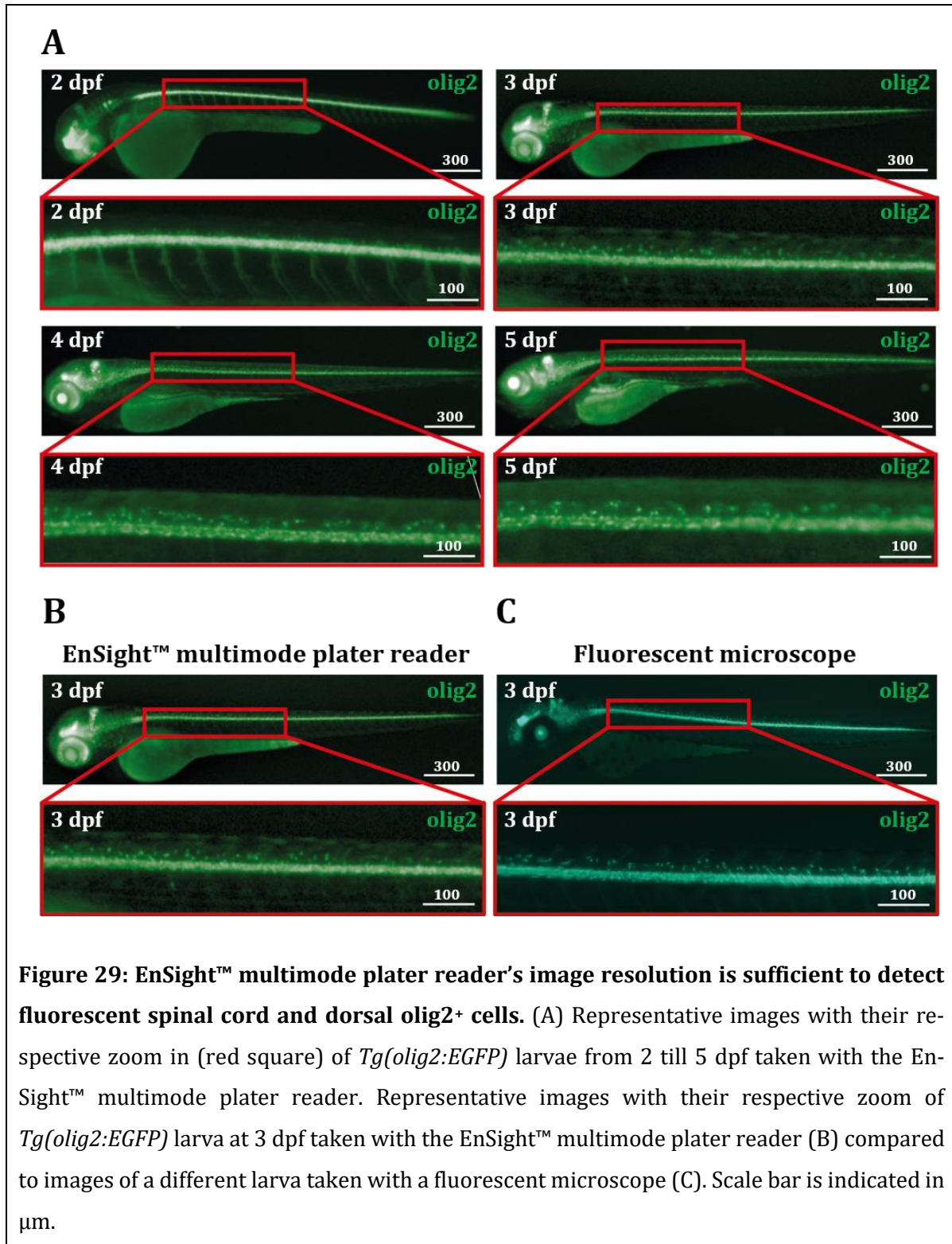
To establish our automated *in vivo* image and analysis system, we employed the zebrafish line *Tg(olig2:EGFP)*, which has been used as a valid Ol reporter line to screen for compounds that affect the recruitment of Ol lineage cells during myelination (Buckley et al., 2010; Shin et al., 2003). *Olig2*⁺ cells migrate to the dorsal part of the spinal cord during early larval development where they start to differentiate by default at 2.5 dpf and mediate the early myelination of dorsal neurons starting at 3 dpf. Changes in proliferation and recruitment of OPCs have been shown to alter the number of dorsal mature Ols and consequently affect myelination (Early et al., 2018). We therefore chose 3 dpf as a suitable timepoint to validate our system with already established compounds.

4.3.1 EnSight™ multimode plate reader's image resolution is sufficient to detect fluorescent spinal cord and dorsal *olig2*⁺ cells

A zebrafish larva has a considerable three-dimensional thickness and is not positioned flat at the bottom due to its voluminous yolk sac, impeding proper image acquisition with the EnSight™ plate reader. To acquire a sharp image along the entire length and thickness of the zebrafish larva, we implemented stacked image acquisition of six focal planes covering a range of 0 to 250 μm above the bottom of each well (**Figure 28**). An additional bright field image of the well was acquired for further confirmation of the presence of a single larva within each well.



In initial tests, we imaged *Tg(olig2:EGFP)* from 2 till 5 dpf in a 96-well plate using the imaging mode of the EnSight™ reader. For all the developmental stages we found a sufficient image resolution enabling the visualization of both the fluorescent ventral spinal cord and the fluorescent dorsal olig2⁺ cells (**Figure 29A**). We also observed an image quality that is comparable to images acquired with a fluorescent microscope (**Figure 29B, C**). Thus, resolution and signal-to-noise ratio of images obtained with the EnSight™ plate reader are sufficient for single olig2⁺ cell detection, providing the EnSight™ plate reader as a promising platform for automated high-throughput *in vivo* screening of compounds that alter OI recruitment.



4.3.2 Kaleido's™ novel image analysis algorithm automatically detects zebrafish larva, its fluorescent spinal cord and dorsal olig2⁺ cells

Given the high image resolution, we aimed to develop an automated image analysis algorithm together with Perkin Elmer to detect the spinal cord of the larvae and subsequently quantify the number of dorsal olig2⁺ cells and other morphometric output parameters.

Therefore, our algorithm was designed to firstly confirm the presence of a single larva within each well by means of the bright field image and a subsequent automatic contrast-based pixel texture analysis that delineates the edges of the animal. Afterwards, the algorithm automatically detects the ventral spinal cord by selecting the region with the highest fluorescent intensity in the fluorescent stacked images. After outlining the ventral spinal cord, the algorithm sets the region of interest (ROI) as a 33 μm wide area above the ventral spinal cord. Within this dorsal ROI the algorithm identifies cells based on fluorescent contrast, such that fluorescent spot-like objects are defined as dorsal olig2⁺ cells. We also implemented in the algorithm an adjustable threshold, definable by a minimum fluorescent contrast parameter, to avoid false positive cell detection and also to adapt the algorithm to different fluorescence intensities of different reporter lines. In initial tests we observed that our algorithm successfully detects the zebrafish body circumference, the fluorescent spinal cord and also dorsal olig2⁺ cells (**Figure 30 A,B**).

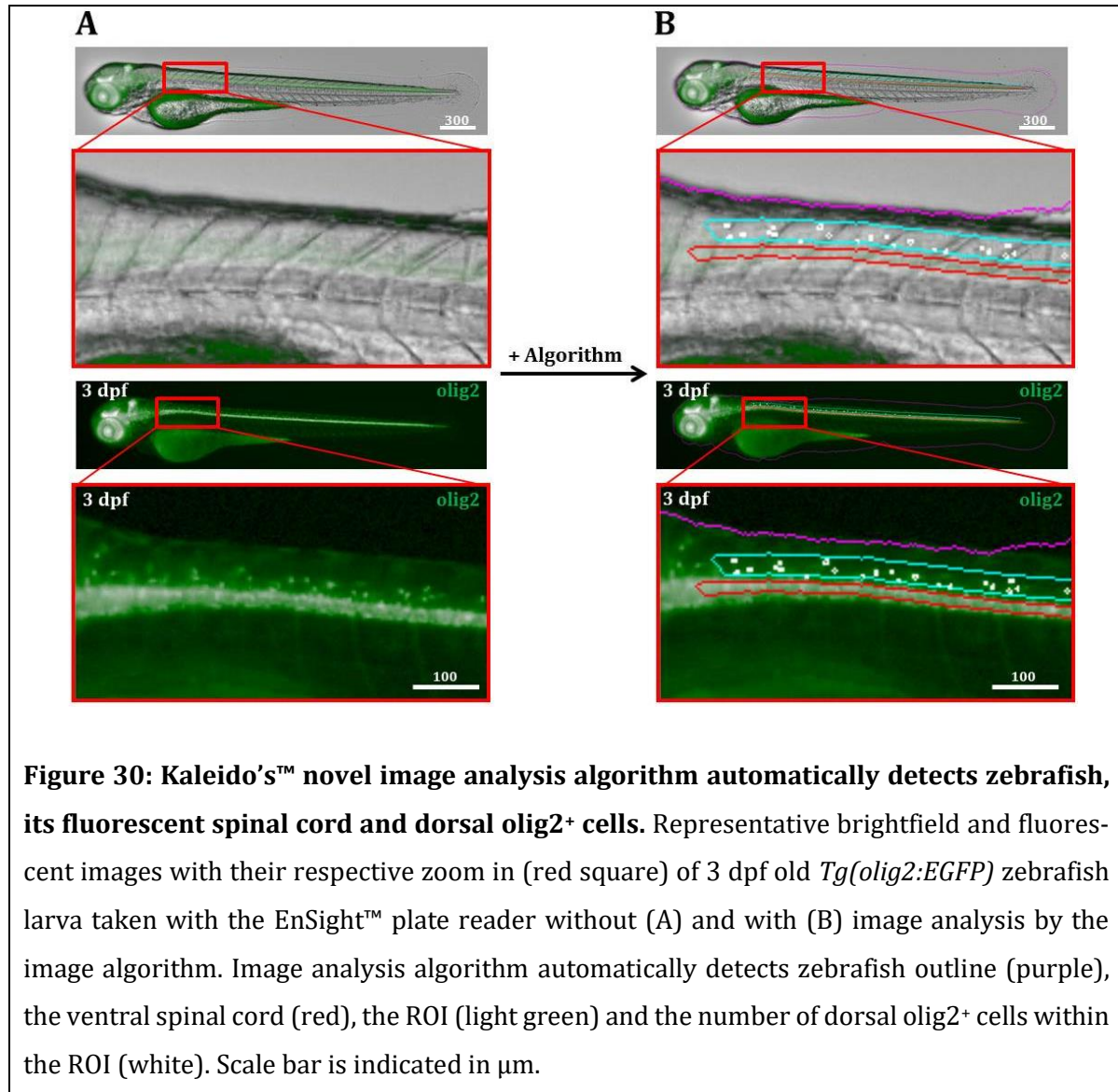


Figure 30: Kaleido's™ novel image analysis algorithm automatically detects zebrafish, its fluorescent spinal cord and dorsal olig2⁺ cells. Representative brightfield and fluorescent images with their respective zoom in (red square) of 3 dpf old *Tg(olig2:EGFP)* zebrafish larva taken with the EnSight™ plate reader without (A) and with (B) image analysis by the image algorithm. Image analysis algorithm automatically detects zebrafish outline (purple), the ventral spinal cord (red), the ROI (light green) and the number of dorsal olig2⁺ cells within the ROI (white). Scale bar is indicated in μm.

In addition to the number of dorsal olig2⁺ cells, our image analysis algorithm provides a number of additional measurements useful for more widespread applications related to drug screenings, other research interests and data validation (**Figure 31A**). For example, the morphometric quantification of the length of zebrafish serves as important information about possible toxic side effects of drugs.

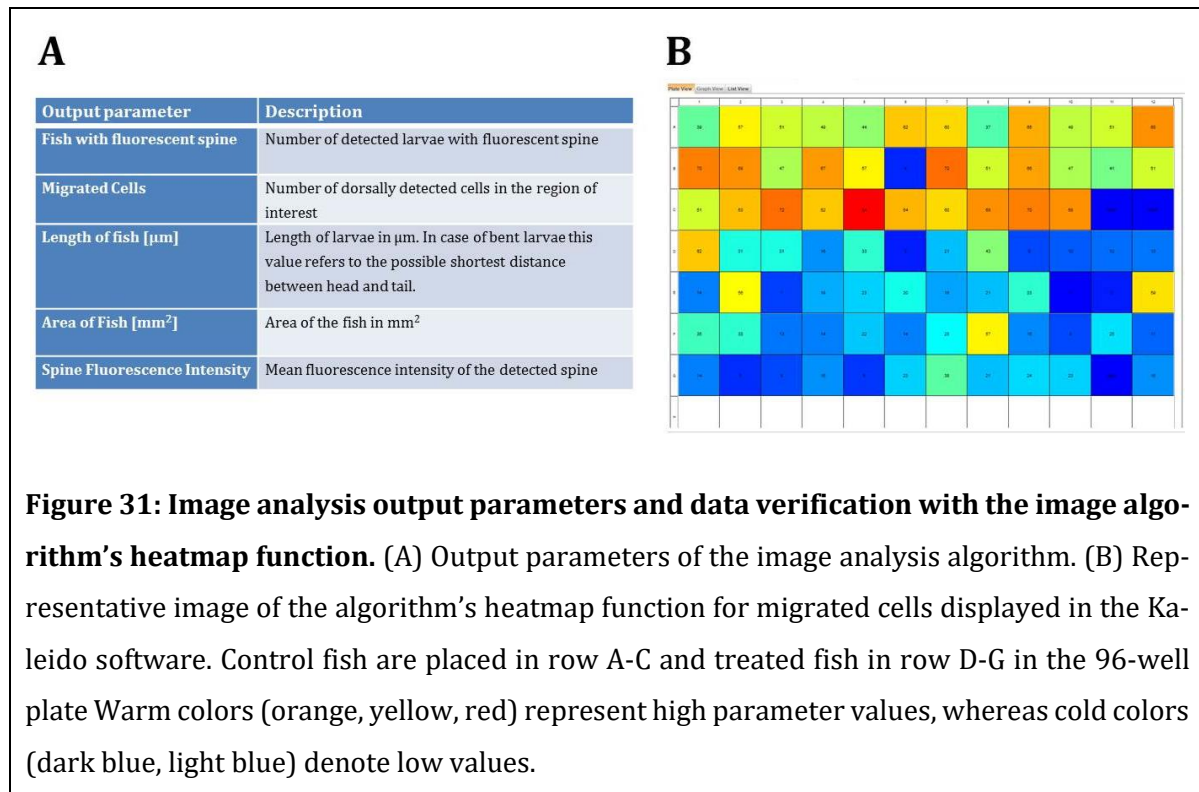
4.3.3 Data verification with the image algorithm's heatmap function

One of the critical steps during automated image analysis is the verification of the acquired data. For this purpose, we included in our image analysis algorithm quality control checks based on additional parameters, such as ventral spinal cord length and fluorescence intensity, which allows easy identification of non-fluorescent or poorly positioned fish.

The implemented algorithm presents different output parameter values in a heatmap-like fashion for an entire 96-well plate in the Kaleido software user interface, assisting in color-based identification of outliers (**Figure 31B**). The image of an identified outlier may be retrieved for further manual in-depth examination. Two major reasons leading to low values are easily detected and excluded: non-fluorescent larvae and poorly positioned larvae.

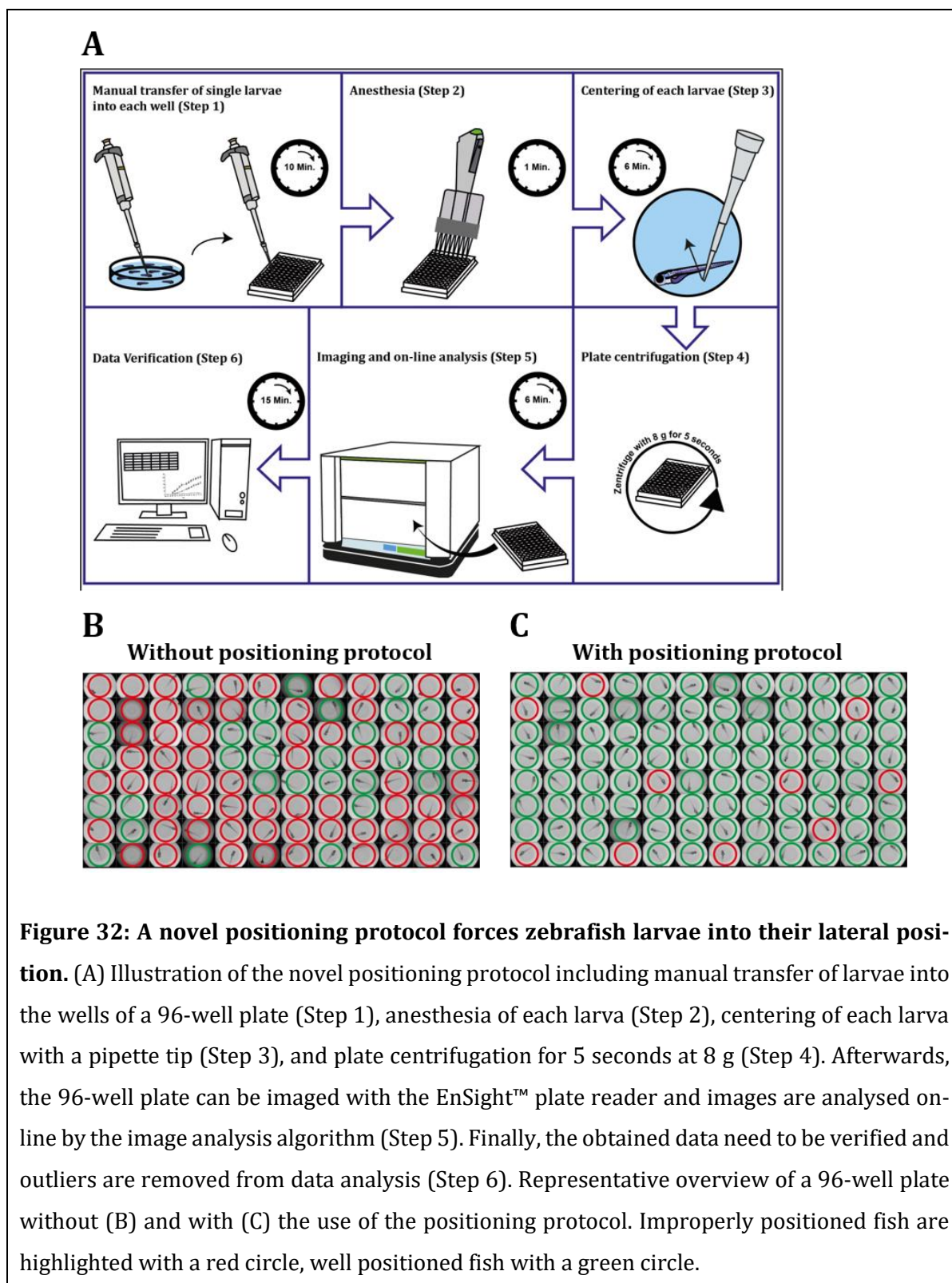
Normally non-fluorescent fish are excluded from data analysis automatically by the algorithm. Occasionally the algorithm detects a spinal cord-like structure due to the autofluorescence of the yolk. As a consequence, the ROI to detect dorsal olig2⁺ cells is in a wrong position and the algorithm will not detect any “Migrating cells”. Because false detection of a spinal cord due to autofluorescence of the yolk always results in a very compressed and small spinal cord-like structure, the parameters “Spine Fluorescence Intensity” and “Length of the Spine [μm]” exhibit unusually low values. Thus, when all three parameters “Migrating cells”, “Spine Fluorescence Intensity” and “Length of the Spine [μm]” exhibit unusually low values with Kaleido’s heatmap function, a non-fluorescent fish was falsely detected as fluorescent.

Larvae that either adhere to the bottom of the well with the yolk up or down (i.e. not laterally positioned) or larvae that are positioned laterally but tilted cannot be analysed properly by the algorithm and need to be excluded. To exclude such results, larvae displaying incoherent values of the parameter “Migrating cells” and “Area of the fish” in the heatmap should be re-evaluated in the individual images.



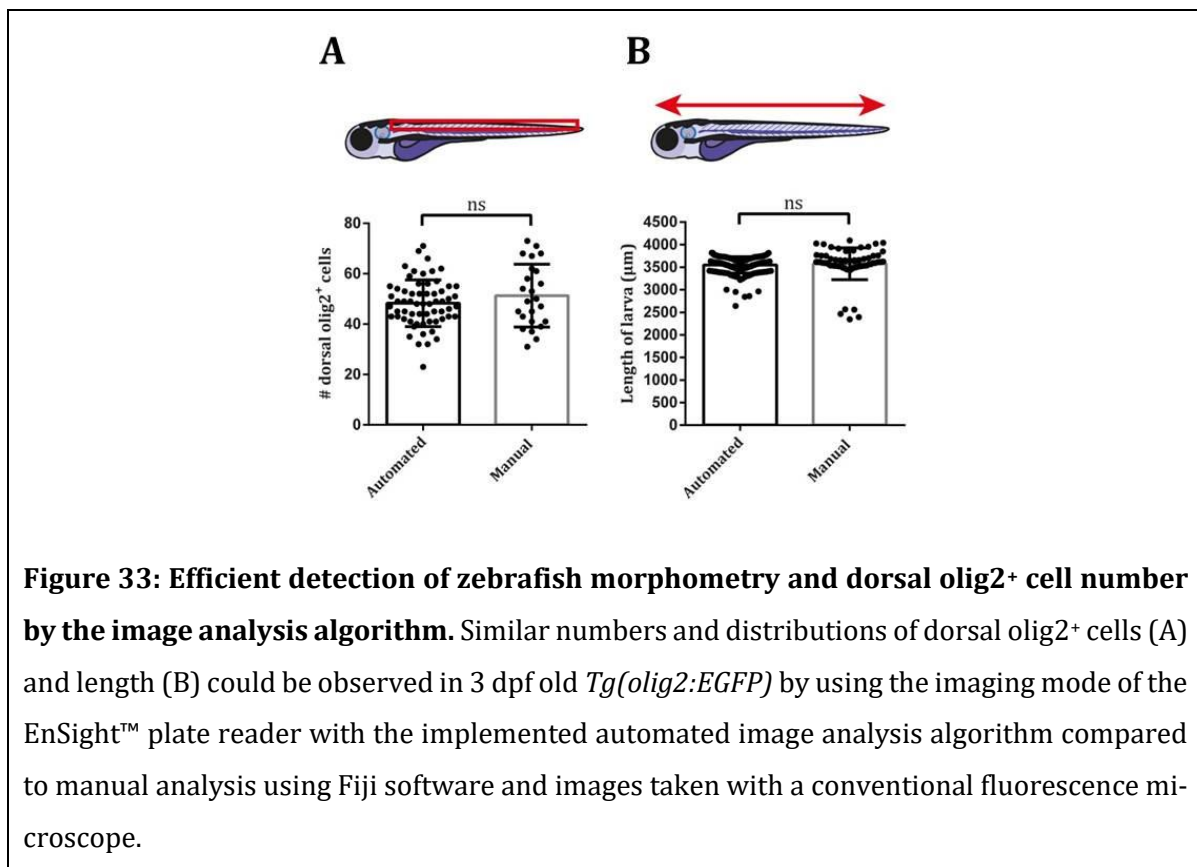
4.3.4 A novel positioning protocol forces zebrafish larvae into their lateral position

Because lateral views of the zebrafish are required to count cells in the dorsal spinal cord their positioning is a critical step in zebrafish imaging. Therefore, larvae need to be anesthetized and laterally placed flat on the bottom of each well. However, we found that only half of the larvae were positioned in the right orientation after placing them into the wells of a 96 well-plate (**Figure 32B**). Consequently, we established a new positioning protocol which includes the manual transfer, anesthesia, well-centering of single fish in each well and a short centrifugation of the 96 well-plate (**Figure 32A**). By developing this novel positioning protocol, we increased the number of correctly positioned fish up to 95 % (**Figure 32C**).



4.3.5 Efficient detection of zebrafish morphometry, fluorescent spinal cord and dorsal olig2⁺ cell number by the image analysis algorithm

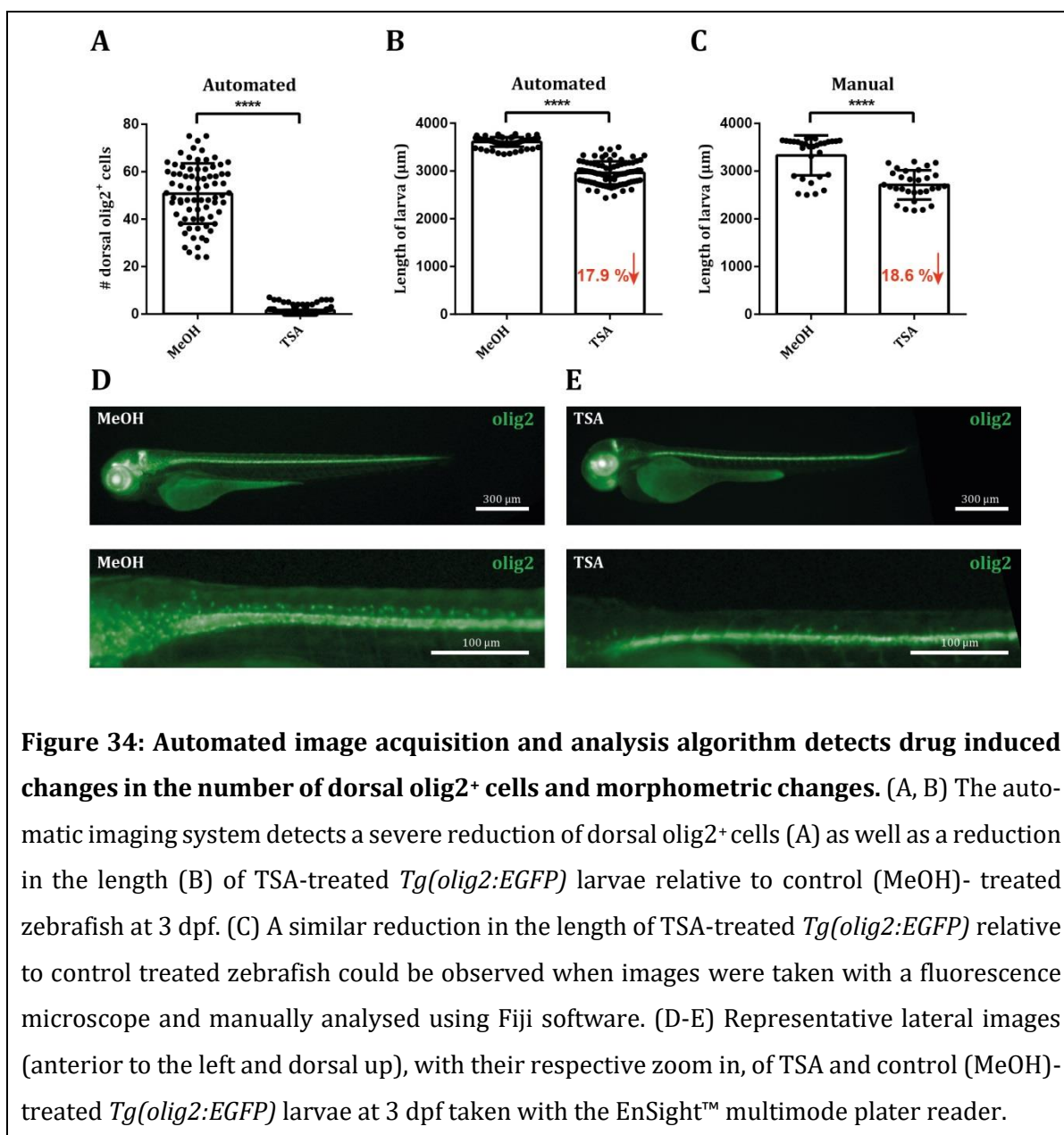
Having developed an efficient imaging and positioning protocol with an automated image algorithm, we examined whether the automatically obtained data mirror the manually analysed images taken with a fluorescent microscope. Hence, initial experiments were conducted with *Tg(olig2:EGFP)* zebrafish line and data were compared at 3 dpf. Manual and automated measurement of dorsal olig2⁺ and length of zebrafish resulted in similar values and distributions, suggesting a high sensitivity of our novel automated image analysis algorithm comparable to manual image analysis (**Figure 33A, B**).



4.3.6 Automated image acquisition and analysis algorithm detects drug induced changes in the number of dorsal olig2⁺ cells and morphometry

To demonstrate that our screening system detects compound-induced changes in dorsal olig2⁺ cells and length of zebrafish, *Tg(olig2:EGFP)* larvae were treated with Trichostatin A (TSA) and image analysis was performed at 3 dpf. TSA is a histone deacetylase (HDAC) inhibitor, formerly shown to inhibit formation and differentiation of OPCs (Takada and Appel, 2010). Indeed, our automated image analysis algorithm detects only few olig2⁺ Ol lineage cells in the

dorsal spinal cord of TSA-treated larvae compared to control-treated fish (**Figure 34A**). We could also detect a reduction (17.9 %) in the length of TSA-treated fish compared to control-treated larvae (**Figure 34B**). To further validate our system, we also manually analysed images of TSA and vehicle-treated fish taken with a stereo microscope. We found an 18.6 % length reduction of TSA-treated fish compared to control-treated fish with the manual analysis (**Figure 34C**), consistent with the length reduction observed by the automated analysis and thus confirming the accuracy of our screening system.



To estimate the power of our method detecting more subtle changes in the number of dorsal olig2⁺ oligodendroglial cells, *Tg(olig2:EGFP)* were exposed to GANT61 and SKP-C25. GANT61

Results

decreases Ol numbers (Almeida et al., 2018a) by inhibiting Gli1/2, which is a downstream effector of the Shh signaling pathway required for Ol generation (Orentas et al., 1999). Consistent with these findings, we found a slight reduction (32.9 %) in the number of dorsal olig2⁺ cells without detectable changes in total length of GANT61-treated larvae compared to control-treated zebrafish (**Figure 35A, C**). To further validate the method, we manually imaged and analysed GANT61-treated larvae with a two-photon microscope and found a similar reduction (31.2 %) in GANT61-treated fish compared with control-treated larvae (**Figure 35 B**).

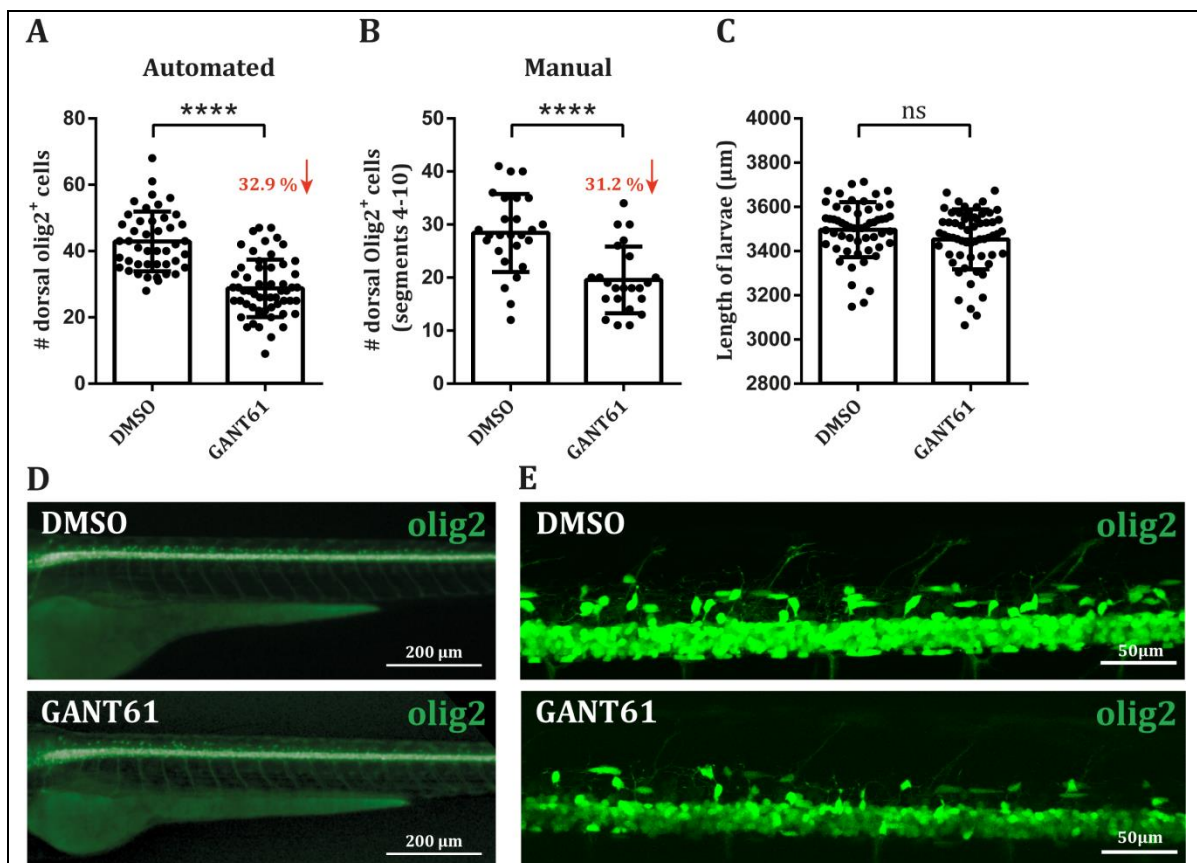
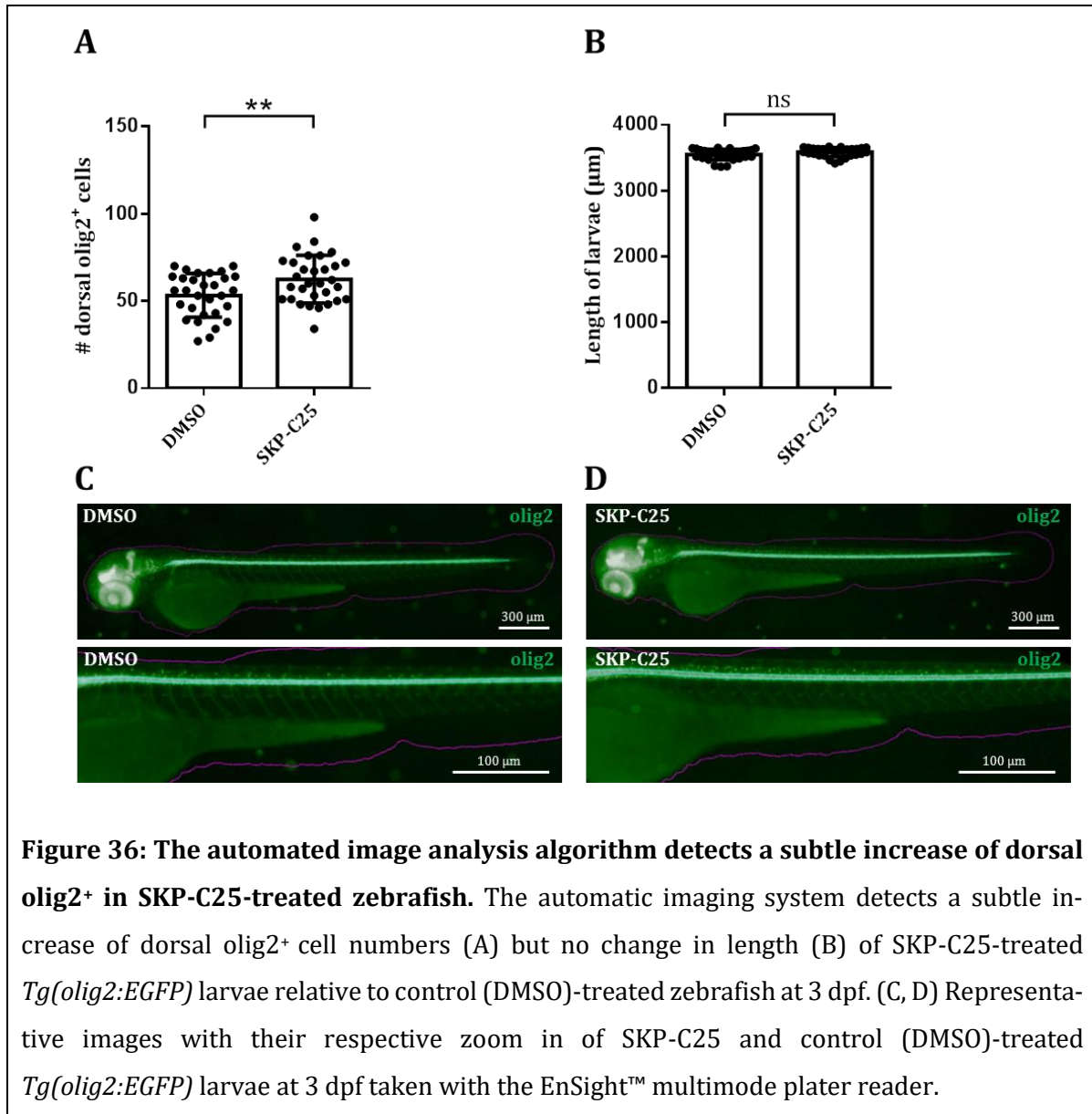


Figure 35: The automated image analysis algorithm accurately detects a subtle reduction of dorsal olig2⁺ cell number in GANT61-treated zebrafish. The automatic imaging system detects a subtle reduction (32.9 %) of dorsal olig2⁺ cells (A) but no change in the length (C) of GANT61-treated *Tg(olig2:EGFP)* larvae relative to control (DMSO)-treated zebrafish at

3 dpf. A similar reduction (31,2 %) in the number of dorsal olig2⁺ cells within the spinal cord segments 4-10 of TSA-treated *Tg(olig2:EGFP)* larvae relative to control-treated zebrafish could be observed by two-photon imaging and manual analysis with Fiji (B). (D) Representative lateral images (anterior to the left and dorsal up) of GANT61 and control (DMSO)-treated *Tg(olig2:EGFP)* larvae at 3 dpf taken with the EnSight™ multimode plate reader. (E) Representative lateral images (anterior to the left and dorsal up) of spinal cord segments 4-10 of GANT61 and control (DMSO)-treated *Tg(olig2:EGFP)* larvae at 3 dpf taken with a two-photon microscope.

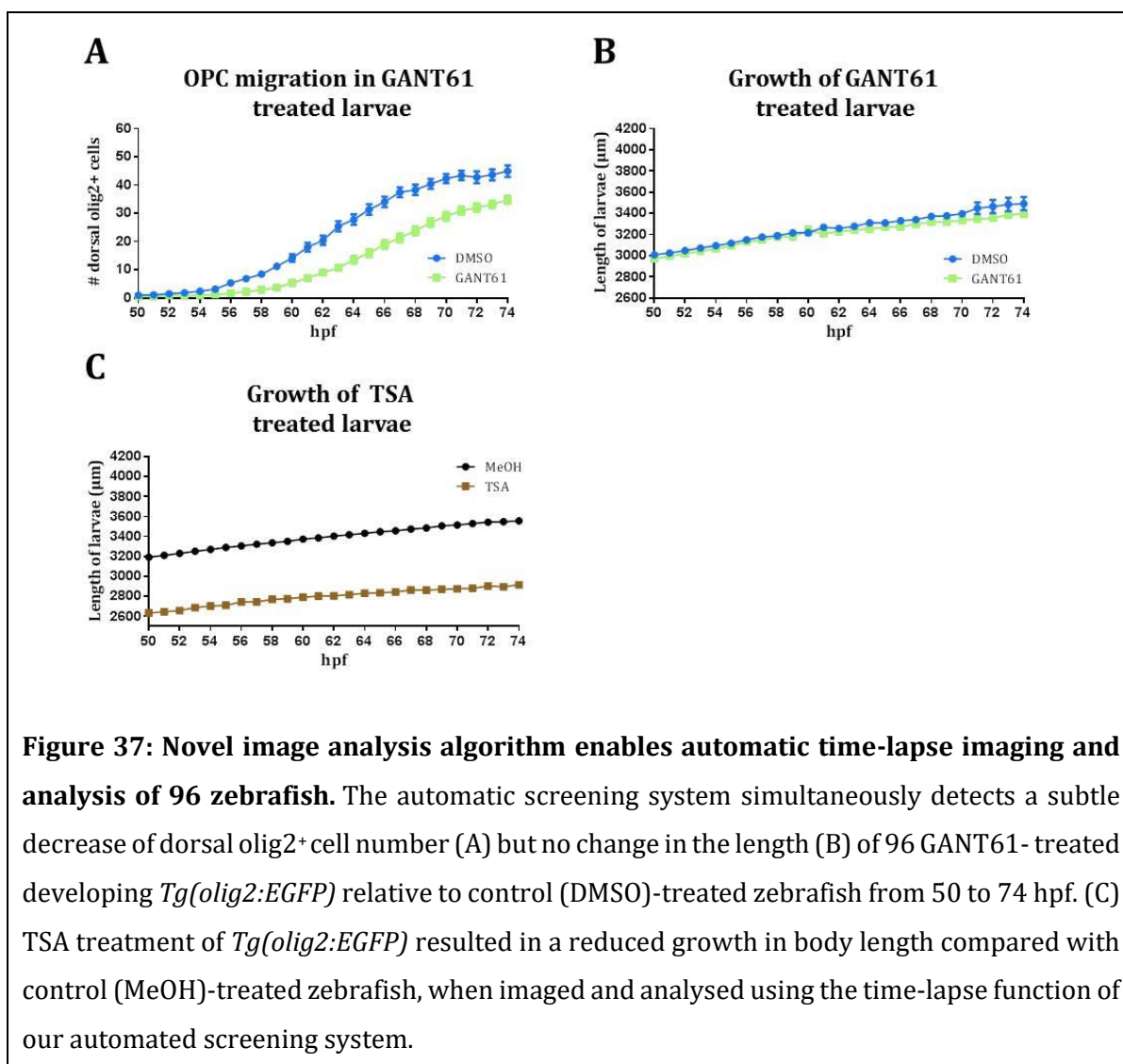
We next treated *Tg(olig2:EGFP)* larvae with SKP-C25 to investigate whether our system is also capable of detecting a subtle increase in the number of dorsal olig2⁺ Ol lineage cells. It has been previously shown that inhibition of the Skp2 SCF ubiquitin ligase complex by SKP-C25 results in an increased dorsal olig2⁺ cell number in zebrafish (Early et al., 2018). Consistent with the previous findings we observed a slight but significant increase in the number of dorsal olig2⁺ cells in SCP-C25-treated fish relative to control-treated zebrafish with our automated system (**Figure 36A**). We could not detect any developmental defects in the length of SCKP-C25-treated zebrafish (**Figure 36B**). This data demonstrate that our automated screening system reliably detects slight changes in the number of dorsal olig2⁺ cells and in the length of zebrafish. Therefore, the EnSight™ multimode plate reader with our novel analysis algorithm can not only be used to screen for drugs affecting Ol recruitment but also to assess possible toxic side effects by detecting the length and examining the respective zebrafish images.



4.3.7 Novel image analysis algorithm enables automatic time-lapse imaging and analysis of 96 zebrafish

To test the capability of our automated imaging protocol for time-lapse applications, we simultaneously imaged dorsally migrating Ol lineage cells and body growth of 96 developing *Tg(olig2:EGFP)* larvae from 50 to 74 hpf at a frame rate of one image per hour. Indeed, the EnSight™ reader was able to simultaneously image dorsal olig2⁺ cell migration and body growth in real-time during early larva development in 96 fish. When we plotted the data obtained by our analysis algorithm, we confirmed the decreased number of dorsally migrating olig2⁺ cells in GANT61-treated larvae without a decrease in total length of the larvae (**Figure 37A, B**). The time-lapse function of the EnSight™ multimode plate reader combined with the automated image analysis algorithm was also capable of automatically detecting changes in

the growth of TSA-treated *Tg(olig2:EGFP)* larvae compared to control-treated zebrafish (**Figure 37C**).



5 Discussion

Aim of this study was to establish an *in vivo* platform to screen for inhibitors of human GPR17 as potential therapeutic compounds promoting remyelination in patients with MS. We chose zebrafish as animal model because of its high genetical and experimental versatility. Therefore, to achieve our aim, the research strategy was driven by the following main objectives: detailed investigation of the role of Gpr17 in zebrafish, development of humanized zebrafish models by generating transgenic lines that harbor wild-type human or chimeric h/zf-GPR17, and establishment of an automated screening system to facilitate the search for inhibitors of human GPR17 in zebrafish.

5.1 Expression and function of Gpr17 in zebrafish is similar to mice

Prior to investigating whether hGPR17 and h+zfGpr17 could be used as tools to humanize Gpr17 in zebrafish, we deciphered that the expression and function of endogenous zebrafish Gpr17 is similar to that observed in mice.

5.1.1 *Gpr17* is expressed in OPCs, pre-Ols but not in mature Ols in zebrafish

By applying the RNAscope® technology, we found robust expression of *gpr17* mRNA from 56 hpf to 4 dpf in olig2⁺ Ol lineage cells in *Tg(olig2:EGFP)* zebrafish larvae. Notably, *Gpr17* mRNA expression was observed in all dorsal olig2⁺ cells at 56 hpf. Since OPCs start to get specified at approximately 30 hpf and begin to migrate dorsally at approximately 50 hpf in zebrafish spinal cord segments 4-10 (Kirby et al., 2006; Preston and Macklin, 2015), we conclude that *gpr17* mRNA starts to be expressed in OPCs in zebrafish. At 3 and 4 dpf, we observed Ol lineage cells lacking *gpr17* mRNA expression, which might correspond to fully mature Ols that start to be formed around this time of development. Because olig2 is expressed in all subpopulations during Ol maturation, it is difficult to distinguish between OPCs and mature Ols after 3 dpf. Consistently, we detected no *gpr17* mRNA expression in mature Ols that are GFP-labeled in *Tg(claudinK:EGFP)* and *Tg(mbp:EGFP)* zebrafish lines, suggesting that *gpr17* is downregulated in mature Ols. Conversely, nkx2.2a⁺ cells exhibit detectable expression of *gpr17* mRNA in the *Tg(nkx2.2a:mEGFP)* zebrafish line at 2.5 dpf. Nkx2.2a is a transcription factor that starts to be expressed in pre-Ols (Kucenas et al., 2008), therefore we conclude that *gpr17* mRNA is also expressed in pre-Ols. In summary, our findings indicate that in zebrafish *gpr17* is expressed in OPCs and pre-Ols, and then downregulated in mature Ols. This pattern of expression is not unique because Gpr56, another GPCR that has been shown to be a negative regulator of Ol development in zebrafish, is also expressed in OPCs and downregulated in mature Ols

(Ackerman et al., 2015). Furthermore, we did not detect any *gpr17* mRNA expression within *ngn1*⁺ cells, such as Rohon-Beard sensory neurons, hindbrain interneurons, clusters of neuronal precursors or dorsal root ganglia neurons, in *Tg(ngn1:EGFP)* larvae at 3 and 4 dpf. Hence, we assume no substantial Gpr17 protein expression in the predominant types of zebrafish neurons, although we cannot rule out low *gpr17* mRNA expression in other neuronal subtypes in zebrafish. Furthermore, *gpr17* expression in the PNS could not be detected. Taken together, the expression pattern of zebrafish *gpr17* is similar to mice: GPR17 is expressed in OPCs and pre-OLs, and it is downregulated in mature OLs for terminal differentiation into mature myelinating OLs (Chen et al., 2009). A difference in the expression of Gpr17 is that in mice GPR17 is expressed in the transition phase between OPCs and pre-OLs (Boda et al., 2011) whereas our data show that in fish *gpr17* is already detected in early OPCs. However, it should be noted that the expression data obtained in mice were generated by IHC stainings visualizing GPR17 protein (Boda et al., 2011), whereas the data that we obtained in zebrafish were generated by visualizing *gpr17* mRNA. Unfortunately, our custom-made Gpr17 antibody did not work in IHC stainings and needs to be further investigated to clarify Gpr17 receptor expression in zebrafish. Therefore, Gpr17 protein expression in zebrafish might be slightly delayed due to the temporary shift in mRNA translation of Gpr17.

5.1.2 Absence of Gpr17 decreases OPC migration and therefore the number of dorsal OPCs and mature OLs

In principle there are three major experimental approaches to decipher the role of a gene *in vivo*: gene overexpression, knockdown or knockout experiments. In this thesis we performed *gpr17* knockdown and *gpr17* knockout experiments, since the overexpression of *gpr17* mRNA did not alter OL development and myelination in zebrafish (Schmitt, 2019).

When we knocked down Gpr17, we found fewer dorsal mature OLs but unchanged numbers of ventral mature OLs in *Tg(claudinK:EGFP)* and *Tg(mpb:EGFP)* zebrafish larvae between 3 and 5 dpf. These observations could be explained by either a dorsal dysregulation of the maturation/differentiation process from OPCs to OLs or a decreased OPC development and migration that would finally affect the total number of dorsal OLs. *Gpr17* knockdown in *Tg(olig2:EGFP)* larvae also displayed less dorsal olig2⁺ OL lineage cells from 3 till 5 dpf. Furthermore, less olig2⁺ cells were also detected during earlier embryonic development from 50 till 74 hpf, when first oligodendroglial cells present in the dorsal spinal cord are migrating OPCs that subsequently differentiate into pre-OLs (Preston and Macklin, 2015). If the differentiation process from OPCs had been affected after *gpr17* knockdown, we would have expected an unchanged number of dorsal olig2⁺ cells but less mature OLs. Hence, the decreased number of dorsal mature OLs is

Discussion

not a result of affected OPC differentiation but rather a result of direct or indirect reduction of dorsal OPC migration after *gpr17* knockdown. Because MOs are known to induce p53-dependent apoptosis and several other off-target effects (Robu et al., 2007) that could affect OPC migration, we analysed and subsequently ruled out increased apoptosis, decreased proliferation or affected general larval development as indirect cause for the reduced number of dorsal OPCs and Ols. This is consistent with previous observations in our group demonstrating *gpr17* MO specificity in *gpr17* rescue experiments (Schmitt, 2019). Furthermore, it is known that in the absence of axons the formation of Ols is also decreased (Almeida et al., 2018a). However, we did not detect any changes in the neuronal network of *gpr17* morphants compared to CoMO injected larvae, thus indicating that neuronal network changes are not the cause for the reduced number of Ol lineage cells.

Since a poor correlation between MO induced and mutant phenotypes has been described, assuming off-target effects after MO knockdown (Kok et al., 2015), we have also generated a *gpr17* knockout zebrafish (*Mut5*) to confirm the *gpr17* MO effect and to obtain further evidence for the functional role of Gpr17 in zebrafish. In *Mut5*, CRISPR/Cas-9 genome editing caused a 43 base pair deletion in the coding region of *gpr17* resulting in a frameshift that produces an early stop codon. According to the HMMTOP transmembrane topology prediction server (Tusnády and Simon, 2001), the resulting truncated protein (15.2 kDa) lacks the regions between the transmembrane domains 4 to 7 as well as the intracellular loop 2 and the entire C-terminal cytoplasmic tail compared with the native 7-TM structure of GPCRs. Since the missing domains are essential for G protein coupling and activation for further downstream signaling (Inoue et al., 2019; Katritch et al., 2013), we assume this truncated Gpr17 receptor to be non-functional.

Consistent with our *gpr17* knockdown data, we found a reduced number of dorsal claudinK⁺ and mbp⁺ mature Ols but an unchanged number of ventral mature Ols during development in *Mut5*^{-/-} mutants compared to control larvae. As a consequence, we also discovered fewer myelinated axons in the dorsal spinal cord and an unaltered number of ventral myelinated axons. This phenotype also resulted from an impaired migration of olig2⁺ OPCs in *gpr17* mutant larvae. Likewise, we ruled out CRISPR/Cas-9 off-target effects, such as increased apoptosis, decreased proliferation or affected general and neuronal larval development, as a cause for the reduced number of dorsal OPCs and Ols. Furthermore, we demonstrated knockout specificity by *gpr17* mRNA rescue experiments. It has to be noted that, unlike the *gpr17* morphants, we found a slightly reduced growth of *Mut5*^{-/-} mutants compared to control fish. However, whereas we evaluated the same reporter fish line after *gpr17* MO and CoMO injections, we compared *Mut5*^{-/-} mutants with *gpr17*^{+/+} control fish from different genetic backgrounds.

Because we did not detect any alteration in the general and morphological development of larvae, we assumed that the minor reduction observed during growth of *Mut5^{-/-}* is a consequence of the different genetic background of the investigated larvae. In summary, our data from *gpr17* morphants and knockout mutants collectively demonstrate that impairment of *gpr17* inhibits OPC migration into the dorsal spinal cord of zebrafish.

Inconsistent with the *gpr17* morphants, the *gpr17* knockout larvae compensate the mutant phenotype since already at 3 dpf the numbers of olig2⁺ Ol lineage cells approach the control fish phenotype. Such discrepancy between morphants and mutants has been previously described in zebrafish and reveals a possible transcriptional up- or downregulation of other genes that may compensate the mutant phenotype (Rossi et al., 2015). After MO knockdown there might still be enough target protein left preventing regulatory transcriptional feedback mechanisms.

5.1.3 Gpr17 is a negative regulator of Ol differentiation in zebrafish

OPC specification, migration and differentiation occur rapidly in zebrafish. Already at 3 dpf, first mature Ols are present in the dorsal spinal cord, meaning that a single OPC migrates only during approximately 24 hours from the ventral spinal cord (Preston and Macklin, 2015). Although migration and differentiation are two independently regulated molecular processes, when OPCs start to differentiate they form associations with axons for further ensheathment and myelination, and migration stops (Kirby et al., 2006). Therefore, a possible reason for the disturbed OPC migration observed in *gpr17* morphants and knockout larvae is because OPCs prematurely differentiate and consequently lose their ability to migrate.

Indeed, in *Tg(nkx2.2a:mEGFP)* larvae, both after *gpr17* knockdown and in the complete absence of Gpr17 in *Mut5^{-/-}* mutants we measured an increased expression of *nkx2.2a*, which labels maturing pre-OLs, in their ventral spinal cords. This observation is consistent with previous results in our group that showed an increase in *nkx2.2a* mRNA expression in the ventral spinal cord of *gpr17* morphants compared with CoMO injected larvae by WISH analyses (Schmitt, 2019). Altogether, these findings support the notion that in the absence of Gpr17, OPCs prematurely differentiate into pre-OLs in the ventral spinal cord. This is in line with the observation that Ol maturation is accelerated in mice in the absence of GPR17 (Chen et al., 2009).

Interestingly, in contrast to zebrafish, *gpr17* knockout mice do not show alterations in OPC migration and total numbers of Ols. A conceivable reason to explain this discrepancy is the finding that in mice GPR17 starts to be expressed only in the terminal phase or transition

Discussion

phase from OPCs to pre-Ols (Boda et al., 2011) and not earlier as we have observed in zebrafish. Therefore, absence of GPR17 would affect OPC migration at a later time point in mice, when most OPCs have already migrated to their target locations. Furthermore, it has been shown that in mice a subset of OPCs directly derive from the dorsal part of the spinal cord and consequently do not have to migrate dorsally before myelinating their target axons (Fogarty et al., 2005). The location of these dorsally derived OPCs would not be affected in the absence of GPR17 and would start to differentiate earlier. Moreover, gliogenesis in mice starts later compared with zebrafish. First mature myelinating Ols can be found already at 3 dpf in zebrafish (Preston and Macklin, 2015) whereas in mice mature myelinating Ols begin to be detected at P10 (Baumann and Pham-Dinh, 2001; Preston and Macklin, 2015), so migrating OPCs have more time to reach their final destination.

Notably, similar discrepancies have been observed between zebrafish and mice after depletion of other Ol differentiation inhibitors, such as Lingo1b. In mice, electron microscope studies have shown increased numbers of myelinating Ols in Lingo-1 knockout animals compared with their wild type littermates (Mi et al., 2005) whereas transgenic mice overexpressing Lingo-1 displayed a delayed onset of myelination (Lee et al., 2007). However, in zebrafish (Yin and Hu, 2014) fewer migrating OPCs and mature Ols were found in the dorsal spinal cord of *Lingo1b* morphants compared with CoMO injected larvae. Interestingly, thicker and more myelinated mauthner axons in ventral spinal cord of zebrafish were detected by electron microscopy. They therefore conclude that OPCs differentiate earlier in the ventral spinal cord, prematurely losing their ability to migrate dorsally.

Clearly, electron microscopy images of the ventral spinal cord of *gpr17* knockout- compared to wildtype larvae would be appropriate to further confirm the functional role of Gpr17 as an Ol differentiation inhibitor in zebrafish. We expect more myelinated axons in the ventral spinal cord of *Mut5*^{-/-} larvae at an earlier developmental stage relative to control larvae.

Our findings define Gpr17 as the third receptor to join the group of myelination regulating GPCRs in zebrafish, further manifesting zebrafish as an animal model to investigate key regulators of Ol development and myelination. Whereas Gpr126 is expressed in Schwann cells initiating the terminal differentiation for myelination in the PNS (Monk et al., 2009), Gpr56 has been found in astrocytes, neurons and early Ol lineage cells positively regulating Ol proliferation and negatively regulating OPC differentiation in the CNS (Ackerman et al., 2015).

Altogether, our data demonstrate that Gpr17 is a negative regulator of Ol differentiation in zebrafish, similar to the functional role of GPR17 that has been observed in mammals (Chen

et al., 2009). Therefore, zebrafish with its experimental and genetic power provides a suitable model organism to screen for inhibitors of human GPR17 by introducing hGPR17 or h+zfGpr17 in *gpr17* knockout fish.

5.2 Human and chimeric receptors can be used as tools to humanize zebrafish

Complex biological processes are difficult to recapitulate *in vitro* and therefore require *in vivo* analysis. Although a lot of important research has been performed using animal models, such as mice, the transferability of these results to the human organism should still be considered critical. Therefore, the field of translational biomedical research has aimed for *in vivo* models to perform studies of human cells, diseases and organs, and has already provided humanized mice and human-mouse chimeras (Shultz et al., 2007; Walsh et al., 2017).

In particular, with regard to demyelinating diseases, drugs emerging from preclinical studies in animal MS models have a poor record of success in human clinical trials (Baker and Amor, 2015). Reasons for that are manifold, such as toxicity, side effects, lack of efficacy or structural differences between the animal and human target. Especially, the ligand binding domain of GPCRs needs to be conserved to identify compounds that are transferable between different species, such as mice and humans. Therefore, using humanized animal models expressing either human receptors or chimeric receptors consisting of the human ligand binding domain and the signaling domains of the respective animal might provide a more successful approach to find drugs transferable to humans.

While many studies report on various homologous chimeric receptors to study downstream signaling or ligand binding (Yin et al., 2004), we apply for the first time in zebrafish an orthologous chimeric GPR17 receptor containing the human ligand binding domain and the zebrafish signaling domain. To investigate the functionality but also the functional difference of hGPR17 and h+zfGpr17, we initially performed transient overexpression experiments by injecting the respective mRNA into single-stage eggs of *Tg(claudinK:EGFP)* larvae. Consistent with the overexpression of native zebrafish Gpr17 (Schmitt, 2019), the transient overexpression of hGPR17 and h+zfGpr17 in zebrafish did not alter the number of mature claudinK⁺ Ols. To rule out the possibility that hGPR17 and h+zfGpr17 were not expressed or not functional in zebrafish, we performed *gpr17* morphants and *gpr17* mutant rescue experiments. We demonstrated that mRNA injection of hGPR17 and h+zfGpr17 partially rescued the *gpr17* morphant- and completely rescued the *gpr17 Mut5^{-/-}* phenotype, thus demonstrating that hGPR17 h+zfGpr17 were functionally expressed in zebrafish. These experiments also showed no

Discussion

functional differences between hGPR17 and h+zfGpr17. This demonstrates a proof of principle concept for the generation of chimeric receptors that could be used for the humanization of zebrafish GPCRs in case of human receptors that are not functional in zebrafish.

Notably, these findings differ from those in mice, where GPR17 overexpression resulted in a decreased Ol maturation and hypomyelination (Chen et al., 2009). However, it is worth noting that the overexpression of GPR17 in mice was under the control of a specific promoter that led to a strong artificial expression of GPR17 in immature Ols, when endogenous GPR17 expression is significantly down-regulated. Conversely, the overexpression of zfGPR17, hGPR17 or h+zfGpr17 in zebrafish was not regulated by a specific promoter and therefore expression of Gpr17 could be assumed at earlier larvae developmental stages and unphysiological in all type of cells. Possible reasons for the different effects after GPR17 overexpression in mice and zebrafish are described elsewhere (Schmitt, 2019).

Expression of hGPR17 as well as h+zfGpr17 in zebrafish could be used to screen for inhibitors of human GPR17 as potential therapy to promote remyelination in MS patients. For that purpose, we propose to bath the *hGPR17* or *h+zfGpr17* injected *Mut5^{-/-}* larvae with potential inhibitors of human GPR17, which should prevent the rescue effect of both receptors in the *gpr17* knockout animals. For a simple readout, we propose to bath receptor mRNA injected *Mut5^{-/-} Tg(olig2:EGFP)* larvae with potential inhibitors of hGPR17 and compare the number of dorsal olig2⁺ Ol lineage cells with uninjected *Mut5^{-/-} Tg(olig2:EGFP)* fish at 56 hpf. Although zebrafish embryos are known to be generally permeable to small molecules (Mathias et al., 2012), a limitation that must be considered is that these substances have to penetrate the chorion as well as several cell membranes to reach their target. In case the physicochemical properties of compounds prevent penetration, these substances could be injected together with the respective receptor mRNA.

Altogether, our findings demonstrate that human and chimeric GPR17 can humanize zebrafish, which could be used as tools to perform chemical screens *in vivo* thus providing a novel experimental approach in the field of translational biomedical research.

5.3 A rapid automated screening system

Despite the large number of offspring, the limiting factor in performing high-throughput screens with zebrafish is still the imaging and analysis capacity of conventional and established imaging techniques, such as two-photon/confocal or standard fluorescent microscopy. Beforehand, larvae need to be manually fixed and positioned in low melting agarose. The time-consuming manual fixation and positioning of larvae in low melting agarose together with the manual analysis of the obtained images make screening of huge compound libraries laborious. Moreover, the slow imaging speed of conventional microscopes limits the number of fish that can be imaged within an appropriate and comparable time frame. Therefore, there is still an urgent need for the development of affordable automated high-throughput imaging systems using quantifiable fluorescent reporter lines to take full advantage of zebrafish for drug discovery.

We have established a novel automated screening system that determines the number of dorsal olig2⁺ Ol lineage cells in *Tg(olig2:EGFP)* larvae and thereby greatly facilitates the screening of zebrafish larvae. We decided to use the Perkin Elmer's EnSight™ multimode plate reader, which has been designed to acquire images with high speed of each well of a 96 well plate. Together with Perkin Elmer, we developed an automated image analysis algorithm that is implemented in Perkins Elmer's Kaleido™ software to detect the zebrafish circumference, the ventral spinal cord and dorsal olig2⁺ cells in *Tg(olig2:EGFP)*. Thus, the image analysis algorithm provides not only the number of dorsal olig2⁺ Ol lineage cells but also the morphometric parameters of zebrafish. The transcription factor olig2 is expressed in all subtypes of Ol development and therefore the reporter line *Tg(olig2:EGFP)* provides an appropriate tool to investigate the single stages of Ol differentiation depending on the considered developmental timepoint (Shin et al., 2003). To further improve our screening system, we also developed a positioning protocol to force each larva to be placed in its lateral position within a well of a 96 well plate, which is required for a proper image acquisition of dorsal Ol lineage cells in zebrafish. Using the positioning protocol, we could improve the percentage of properly positioned fish to 95 % compared to 50 % without using the protocol.

We initially validated our screening platform by bathing *Tg(olig2:EGFP)* larvae with TSA and GANT61, both substances known to reduce Ol numbers (Almeida et al., 2018b; Takada and Appel, 2010) and demonstrating that the automated image analysis algorithm detects a similar percentage of compound induced reduction both in the number of dorsal olig2⁺ cells as well as in the length of zebrafish compared to data observed with a two-photon microscope and manual image analysis. Since the goal of most screenings aiming at myelination is to

Discussion

identify substances that increase the number of Ol lineage cells (Buckley et al., 2010; Early et al., 2018), we also demonstrated that our system is capable of detecting slight increases in dorsal cell numbers in SKP-C25-treated (Early et al., 2018) *Tg(olig2:EGFP)* larvae. Moreover, because zebrafish has additionally emerged as a tool for toxicity assessment (MacRae and Peterson, 2015; Padilla et al., 2012), the morphometric parameters of zebrafish provided by our algorithm can also be used for toxicity screens of compounds analyzing length of zebrafish.

Before screening compound libraries, it has to be determined which statistical tests and what sample size would be required to reach statistical validity. Since the number and standard deviation of dorsally migrated olig2⁺ cells detected by the automated analysis algorithm revealed to be Gaussian distributed with consistent variances, we concluded that parametric statistical tests for analysis are appropriate. Moreover, from these data, we calculated a sample size of 8 larvae per compound to detect a 37 % change in cell number with 95 % power and a significance level of 0.05 (Kane SP. Sample Size Calculator. ClinCalc: <https://clincalc.com/stats/samplesize.aspx>. Updated July 24, 2019. Accessed August 8, 2019.). To ensure statistical validity despite possible imaging errors, we propose to increase the number of larvae to 12 per compound, which would also be sufficient to detect smaller changes in the number of olig2⁺ cells but with less power.

Although recent studies using zebrafish have described a multi-level screening platform (Buckley et al., 2010) and an automated high-resolution *in vivo* screening (Early et al., 2018) to identify novel pro-myelinating compounds and novel regulators of Ol development, there still remains a need for affordable and easy to handle automated high-throughput *in vivo* screening platforms. In 2018, Early et al. presented an automated high-resolution *in vivo* screen using *Tg(mbp:EGFP)* by combining the automated VAST positioning system with confocal microscopy (Early et al., 2018). However, the combination of VAST and confocal microscopy is very expensive and the obtained images are not quantified on line but need to be manually transferred to ImageJ. Our system allows for much faster data acquisition using a plate reader and automated on line analysis. Within 17 minutes 96 zebrafish larvae are positioned in the multi-well plate and analysed within 6 minutes. For example, 288 animals from three plates can be processed in less than 90 minutes whereas manual analyses with stereomicroscopy by an expert to assess cell number in the dorsal spinal cord would take significantly longer (approximately 30 hr) (Early et al., 2018).

We also demonstrated that our automated imaging protocol has the capacity for time-lapse applications. Time-lapse imaging is a powerful tool to study the dynamics of (re-)myelination in great detail (Hu et al., 2017; Kirby et al., 2006). Fully capturing the dynamics of the

underlying processes is particularly important for the complete characterization of compounds intended to promote (re-)myelination. However, with conventional time-lapse imaging only a single compound-treated fish can be recorded at a time, while the untreated control has to be investigated at a different time. Such time differences make direct comparison of the observations difficult, especially between rapidly developing and highly variable living organisms like zebrafish larvae. We confirmed that our imaging protocol is capable of simultaneous time-lapse imaging of dorsally migrating Ol lineage cells and body growth of 96 individual developing *Tg(olig2:EGFP)* zebrafish larvae. Indeed, by using the automated time-lapse function, we could image and confirm the delayed time course of dorsally migrating olig2⁺ cells in GANT61-treated larvae and the affected growth of TSA-treated compared with control-treated larvae in parallel, consequently demonstrating the resolving power of our system for this sort of analyses.

It has to be noted that the algorithm in our system has been optimized for the reporter line *Tg(olig2:EGFP)*. The transcription factor olig2 is expressed in all subtype of Ol lineage cells and therefore the automated system can only be used for investigating general effects on Ol development. For more precise information about specific subpopulations during Ol development, reporter lines for mature Ols, such as *Tg(mbp:EGFP)* or *Tg(claudinK:EGFP)*, need to be investigated. We assume our automated image analysis algorithm to be flexible and that by adapting the analysis input parameters also other reporter lines with cytosolic GFP expression can be detected and automatically analysed.

We envisage that our automated imaging platform in combination with the humanized *Mut5-/- Tg(olig2:EGFP)* zebrafish model will provide a reasonable system that will greatly facilitate the search for inhibitors of human GPR17 in zebrafish. Furthermore, it also offers a broad field of application for all scientists not only for compound screens of broad interest but also for investigating effects on Ol development and myelination *in vivo* in zebrafish.

5.4 Gliotherapeutics as a promising strategy to promote remyelination in MS patients

With more than 50 %, glial cells represent the majority of the cells in the human nervous system (von Bartheld et al., 2016) and exhibit fundamental roles in nervous system formation, function but also dysfunction. Surprisingly, there are no available drugs targeting glial cells for the treatment of diseases (Lloyd and Miron, 2019) such as MS. Remyelination fails in patients with MS, despite the large numbers of OPCs in demyelinated lesions, which should be capable of restoring the damaged myelin sheath. That indicates insufficient Ol differentiation due to either the absence of pro-myelinating signals or the presence of myelination inhibitors in the MS lesion (Fancy et al., 2011). That hypothesis is supported by the fact that enhanced OPCs proliferation under non pathological conditions does not necessarily result in increased myelination *in vivo* (Buckley et al., 2008) suggesting a missing trigger for further OPC differentiation. Therefore, one promising strategy among others to promote remyelination is to identify compounds that stimulate Ol differentiation (Franklin and Ffrench-Constant, 2008b; Huang et al., 2011a).

With this aim, phenotype-driven screens with compound libraries are commonly used approaches to identify novel compounds that promote Ol differentiation and remyelination (Pruss, 2010). Eight phenotype-driven compound screens have already been performed *in vitro* (reviewed in Cole et al., 2017) and from 159 hits only five compounds, such as Clemastin and Benztropine, could be confirmed *in vivo* (Deshmukh et al., 2013; Mei et al., 2014). Likewise, several promising candidate pathways that promote regeneration of myelin when manipulated have been identified, among others, retinoid x receptor gamma (R α R γ), Wnt pathway and the promising Nogo-A and Lingo-1 (Fancy et al., 2009; Huang et al., 2011b; Mi et al., 2005; Samanta et al., 2015). Notably, among all of them, only one compound has finally achieved to be trialled in humans, demonstrating that hits from preclinical studies in animal MS models have a poor record of success in human clinical trials (Baker and Amor, 2015). Thus, the Nogo/Lingo-1 receptor complex has been shown to be a negative regulator of Ol differentiation and that antibody antagonists of Lingo-1 promote remyelination in a MOG induced murine EAE model (Chong et al., 2012; Mi et al., 2007). The Lingo-1 antibody has already been tested in phase II clinical trials for the treatment of MS. Moreover, an antibody against NOGO-A is currently in a second phase I trial (Ineichen et al., 2017). Altogether, this highlights the need for fast and easy to handle phenotype-driven screening platforms in humanized *in vivo* models to discover new compounds interacting with potential targets.

Similar to Nogo A and Lingo-1, the orphan GPR17 has been shown to be a negative regulator of Ol differentiation (Chen et al., 2009). GPR17 is highly abundant within active white matter plaques of MS patients and, therefore, might act as a myelination inhibitor preventing remyelination in MS plaques. In agreement with this hypothesis, absence of GPR17 favors remyelination in a murine autoimmune model of MS (Ou et al., 2016), thus proposing antagonists of GPR17 as a promising gliotherapy to promote remyelination in patients with MS. Our automated screening platform, combining a fast and easy to handle phenotype-driven *in vivo* screen with a GPR17-humanized zebrafish, will support the identification of such compounds inhibiting GPR17.

Moreover, other GPCRs, which are cell type-specifically expressed in the Ol lineage, have been identified regulating Ol development and myelination. For example, Gpr37 has been also shown to be a negative regulator of Ol development and myelination, so Gpr37 antagonists might provide a therapy to induce remyelination in patients with MS (Yang et al., 2016). We envisage that our screening approach for GPR17, taking advantage of the animal model zebrafish, can also be adapted for other GPCRs, such as GPR37. If this is the case, zebrafish promises to become the model of choice for phenotype-driven compound screens aiming for human Ol development.

5.5 Summary

In the search for therapies to promote remyelination in patients with MS, the orphan GPCR GPR17, an Ol differentiation inhibitor in mice, has attracted particular attention, because it is upregulated in MS plaques and its absence promotes remyelination in a murine autoimmune model of MS (Chen et al., 2009; Ou et al., 2016). Thus, inhibition of GPR17 potentially represents a novel therapeutic approach to promote remyelination. Since, rodent animal models are not applicable for high throughput screenings of compound libraries, zebrafish has emerged as a powerful tool to perform large scale chemical screens affecting myelination and Ol biology (Preston and Macklin, 2015; Zon and Peterson, 2005). Therefore, this thesis aimed to investigate whether the role of Gpr17 is conserved in zebrafish in order to develop a “humanized” zebrafish, expressing either human or a chimeric GPR17, for the screening of GPR17 inhibitors.

Similar to mice, we found that *gpr17* mRNA is expressed in OPCs and pre-Ols and downregulated in mature Ols in the developing zebrafish. We could not observe any *gpr17* mRNA expression in neurons nor in the PNS. *Gpr17* knockdown and knockout revealed to have a similar phenotype in zebrafish: in the absence of Gpr17, OPCs prematurely differentiate in the ventral spinal cord, losing their ability to migrate to their dorsal destination and, consequently, less OPCs, pre-Ols, mature Ols and myelinated axons could be found in the dorsal spinal cord. Therefore, we conclude that Gpr17 is an Ol differentiation inhibitor in zebrafish. Collectively, we found an expression pattern and functional role of Gpr17 in zebrafish that is similar to data reported in mice making zebrafish a perfect tool to screen for inhibitors of GPR17. Further experiments, such as electron microscope images of the ventral spinal cord investigating the early myelination in the absence of Gpr17, are needed to fully comprehend the role of Gpr17 in zebrafish. With *gpr17* knockout rescue experiments we demonstrated that human and chimeric GPR17 are functional in zebrafish providing a proof of principle tool for humanizing zebrafish in order to screen for inhibitors of human GPR17 in zebrafish.

Together with Perkin Elmer company we developed an automated screening system using the EnSight™ multimode plate reader and the Ol lineage reporter line *Tg(olig2:EGFP)*. We established a protocol to laterally position the larvae in a 96- well plate, thereby increasing the number of proper positioned fish to 95 %. Furthermore, we demonstrated sensitivity and precision of our automated imaging and analysis system by comparing data obtained with convenient microscopy and manual analysis with results of our novel automated screening system. In comparison to other automated imaging systems aiming at Ol development in zebrafish, our automated screening platform provides an automated on line image analysis, parameters for data verification and a time-lapse application.

In summary, the present study reveals that the functional role of Gpr17 in zebrafish is similar to mice and that zebrafish can be humanized with human or chimeric GPR17 receptors in order to perform compound screens for inhibitors of human GPR17 as a potential therapy for patients with MS. We additionally developed an automated screening system to facilitate and speed up the search of inhibitors of human GPR17 with humanized zebrafish.

6 Conclusion and outlook

Aim of this study was to investigate the role of Gpr17 in zebrafish to establish an *in vivo* platform which allows identification of inhibitors of human GPR17 by using a “humanized” zebrafish line.

Collectively, this work deciphered the expression pattern and the functional role of Gpr17 in zebrafish to be similar to mice, and provided a proof of principle concept to “humanize” zebrafish with a human and a chimeric GPR17 receptor as a tool to search for inhibitors of human GPR17 *in vivo*. Furthermore, we developed and validated an automated screening system that automatically detects changes in the number of dorsal olig2⁺ Ol lineage cells, which will facilitate the search for antagonists of human GPR17. Additionally, our screening system provides features to simultaneously assess the toxicity of the investigated compounds.

With our automated screening system, comparing the number of dorsal olig2⁺ in *hGPR17* or *h+zfGpr17* injected *Mut5*^{-/-} *Tg(olig2:EGFP)* with control injected fish will provide a fast and easily analyzable readout for the search of inhibitors of human GPR17. Antagonist of human GPR17 should prevent the rescue effect of *hGPR17* or *h+zfGpr17* injection into *Mut5*^{-/-} *Tg(olig2:EGFP)*. Successful compounds should then be characterized in more detail *in vitro*.

Development of a transgenic zebrafish reporter line that stably expresses either human or chimeric GPR17 would further simplify and accelerate our screening platform. The respective receptor mRNAs would no longer need to be injected beforehand since the stably expressing fish line could be directly bathed with the compounds to be investigated.

We assume our approach of introducing human or chimeric GPCRs in the respective knockout background of zebrafish as a tool to identify modulators of human receptors in zebrafish to be applicable for a broad range of other GPCRs. Compounds could be screened immediately for their *in vivo* efficacy and toxicity without previously undergoing extensive *in vitro* screens known for rather low prospects of success.

We envisage our automated image analysis algorithm to be flexible and that by adapting the analysis input parameters other reporter lines with cytosolic GFP expression can be analysed. Moreover, we expect that the algorithm in combination with the EnSight™ plate reader can also be modified to detect and analyse other organs in different transgenic reporter lines such as heart, brain or kidney. Therefore, the automated screening system could not only be used to investigate effects on Ol development but also other organs in zebrafish.

7 References

- Ackerman, S.D., Garcia, C., Piao, X., Gutmann, D.H., and Monk, K.R. (2015). The adhesion GPCR Gpr56 regulates oligodendrocyte development via interactions with G α 12/13 and RhoA. *Nat. Commun.* *6*, 6122.
- Almeida, R.G., Czopka, T., Ffrench-Constant, C., and Lyons, D.A. (2011). Individual axons regulate the myelinating potential of single oligodendrocytes in vivo. *Development* *138*, 4443–4450.
- Almeida, R.G., Pan, S., Cole, K.L.H., Williamson, J.M., Early, J.J., Czopka, T., Klingseisen, A., Chan, J.R., and Lyons, D.A. (2018a). Myelination of Neuronal Cell Bodies when Myelin Supply Exceeds Axonal Demand. *Curr. Biol.* *28*, 1296-1305.e5.
- Almeida, R.G., Pan, S., Cole, K.L.H., Williamson, J.M., Early, J.J., Czopka, T., Klingseisen, A., Chan, J.R., and Lyons, D.A. (2018b). Myelination of Neuronal Cell Bodies when Myelin Supply Exceeds Axonal Demand. *Curr. Biol.* *28*, 1296-1305.e5.
- Anderson, D.J. (2001). Stem cells and pattern formation in the nervous system: the possible versus the actual. *Neuron* *30*, 19–35.
- Bai, Q., Sun, M., Stolz, D.B., and Burton, E.A. (2011). Major isoform of zebrafish P0 is a 23.5 kDa myelin glycoprotein expressed in selected white matter tracts of the central nervous system. *J. Comp. Neurol.* *519*, 1580–1596.
- Baker, D., and Amor, S. (2015). Mouse models of multiple sclerosis: lost in translation? *Curr. Pharm. Des.* *21*, 2440–2452.
- Barres, B.A., Lazar, M.A., and Raff, M.C. (1994). A novel role for thyroid hormone, glucocorticoids and retinoic acid in timing oligodendrocyte development. *Development* *120*, 1097–1108.
- von Bartheld, C.S., Bahney, J., and Herculano-Houzel, S. (2016). The search for true numbers of neurons and glial cells in the human brain: A review of 150 years of cell counting. *J. Comp. Neurol.* *524*, 3865–3895.
- Baumann, N., and Pham-Dinh, D. (2001). Biology of oligodendrocyte and myelin in the mammalian central nervous system. *Physiol. Rev.* *81*, 871–927.
- Becker, C.G., and Becker, T. (2008). Adult zebrafish as a model for successful central nervous system regeneration. *Restor. Neurol. Neurosci.* *26*, 71–80.
- Bened-Jensen, T., and Rosenkilde, M.M. (2010). Distinct expression and ligand-binding profiles of two constitutively active GPR17 splice variants. *Br. J. Pharmacol.* *159*, 1092–1105.
- Bercury, K.K., and Macklin, W.B. (2015). Dynamics and mechanisms of CNS myelination. *Dev. Cell* *32*, 447–458.
- Bertrand, N., Castro, D.S., and Guillemot, F. (2002). Proneural genes and the specification of neural cell types. *Nat. Rev. Neurosci.* *3*, 517–530.
- Bill, B.R., Petzold, A.M., Clark, K.J., Schimmenti, L.A., and Ekker, S.C. (2009). A primer for morpholino use in zebrafish. *Zebrafish* *6*, 69–77.
- Blackburn, P.R., Campbell, J.M., Clark, K.J., and Ekker, S.C. (2013). The CRISPR system--keeping

References

- zebrafish gene targeting fresh. *Zebrafish* *10*, 116–118.
- Blader, P., Plessy, C., and Strähle, U. (2003). Multiple regulatory elements with spatially and temporally distinct activities control neurogenin1 expression in primary neurons of the zebrafish embryo. *Mech. Dev.* *120*, 211–218.
- Bläsius, R., Weber, R.G., Lichter, P., and Ogilvie, A. (1998). A novel orphan G protein-coupled receptor primarily expressed in the brain is localized on human chromosomal band 2q21. *J. Neurochem.* *70*, 1357–1365.
- Boda, E., Viganò, F., Rosa, P., Fumagalli, M., Labat-Gest, V., Tempia, F., Abbracchio, M.P., Dimou, L., and Buffo, A. (2011). The GPR17 receptor in NG2 expressing cells: focus on in vivo cell maturation and participation in acute trauma and chronic damage. *Glia* *59*, 1958–1973.
- Bribián, A., Barallobre, M.J., Soussi-Yanicostas, N., and de Castro, F. (2006). Anosmin-1 modulates the FGF-2-dependent migration of oligodendrocyte precursors in the developing optic nerve. *Mol. Cell. Neurosci.* *33*, 2–14.
- Brösamle, C., and Halpern, M.E. (2002). Characterization of myelination in the developing zebrafish. *Glia* *39*, 47–57.
- Buckley, C.E., Goldsmith, P., and Franklin, R.J.M. (2008). Zebrafish myelination: a transparent model for remyelination? *Dis. Model. Mech.* *1*, 221–228.
- Buckley, C.E., Marguerie, A., Roach, A.G., Goldsmith, P., Fleming, A., Alderton, W.K., and Franklin, R.J.M. (2010). Drug reprofiling using zebrafish identifies novel compounds with potential pro-myelination effects. *Neuropharmacology* *59*, 149–159.
- Bussmann, J., and Schulte-Merker, S. (2011). Rapid BAC selection for tol2-mediated transgenesis in zebrafish. *Development* *138*, 4327–4332.
- Cai, Z., Fan, L.-W., Lin, S., Pang, Y., and Rhodes, P.G. (2011). Intranasal administration of insulin-like growth factor-1 protects against lipopolysaccharide-induced injury in the developing rat brain. *Neuroscience* *194*, 195–207.
- Calver, A.R., Hall, A.C., Yu, W.P., Walsh, F.S., Heath, J.K., Betsholtz, C., and Richardson, W.D. (1998). Oligodendrocyte population dynamics and the role of PDGF in vivo. *Neuron* *20*, 869–882.
- Campbell, J.M., Hartjes, K.A., Nelson, T.J., Xu, X., and Ekker, S.C. (2013). New and TALEnted genome engineering toolbox. *Circ. Res.* *113*, 571–587.
- Carson, M.J., Behringer, R.R., Brinster, R.L., and McMorris, F.A. (1993). Insulin-like growth factor I increases brain growth and central nervous system myelination in transgenic mice. *Neuron* *10*, 729–740.
- Casarosa, S., Fode, C., and Guillemot, F. (1999). Mash1 regulates neurogenesis in the ventral telencephalon. *Development* *126*, 525–534.
- Ceruti, S., Villa, G., Genovese, T., Mazzon, E., Longhi, R., Rosa, P., Bramanti, P., Cuzzocrea, S., and Abbracchio, M.P. (2009). The P2Y-like receptor GPR17 as a sensor of damage and a new potential target in spinal cord injury. *Brain* *132*, 2206–2218.
- Chen, Y., Wu, H., Wang, S., Koito, H., Li, J., Ye, F., Hoang, J., Escobar, S.S., Gow, A., Arnett, H.A., et al. (2009). The oligodendrocyte-specific G protein-coupled receptor GPR17 is a cell-intrinsic timer of myelination. *Nat. Neurosci.* *12*, 1398–1406.
- Chitnis, A., and Kintner, C. (1996). Sensitivity of proneural genes to lateral inhibition affects

- the pattern of primary neurons in *Xenopus* embryos. *Development* *122*, 2295–2301.
- Chong, S.Y.C., Rosenberg, S.S., Fancy, S.P.J., Zhao, C., Shen, Y.-A.A., Hahn, A.T., McGee, A.W., Xu, X., Zheng, B., Zhang, L.I., et al. (2012). Neurite outgrowth inhibitor Nogo-A establishes spatial segregation and extent of oligodendrocyte myelination. *Proc. Natl. Acad. Sci. U. S. A.* *109*, 1299–1304.
- Chung, A.-Y., Kim, P.-S., Kim, S., Kim, E., Kim, D., Jeong, I., Kim, H.-K., Ryu, J.-H., Kim, C.-H., Choi, J., et al. (2013). Generation of demyelination models by targeted ablation of oligodendrocytes in the zebrafish CNS. *Mol. Cells* *36*, 82–87.
- Ciana, P., Fumagalli, M., Trincavelli, M.L., Verderio, C., Rosa, P., Lecca, D., Ferrario, S., Parravicini, C., Capra, V., Gelosa, P., et al. (2006). The orphan receptor GPR17 identified as a new dual uracil nucleotides/cysteinyl-leukotrienes receptor. *EMBO J.* *25*, 4615–4627.
- Claus Stolt, C., Rehberg, S., Ader, M., Lommès, P., Riethmacher, D., Schachner, M., Bartsch, U., and Wegner, M. (2002). Terminal differentiation of myelin-forming oligodendrocytes depends on the transcription factor Sox10. *Genes Dev.* *16*, 165–170.
- Cole, K.L.H., Early, J.J., and Lyons, D.A. (2017). Drug discovery for remyelination and treatment of MS. *Glia* *65*, 1565–1589.
- Czopka, T. (2016). Insights into mechanisms of central nervous system myelination using zebrafish. *Glia* *64*, 333–349.
- Czopka, T., French-Constant, C., and Lyons, D.A. (2013). Individual oligodendrocytes have only a few hours in which to generate new myelin sheaths in vivo. *Dev. Cell* *25*, 599–609.
- Davison, J.M., Akitake, C.M., Goll, M.G., Rhee, J.M., Gosse, N., Baier, H., Halpern, M.E., Leach, S.D., and Parsons, M.J. (2007). Transactivation from Gal4-VP16 transgenic insertions for tissue-specific cell labeling and ablation in zebrafish. *Dev. Biol.* *304*, 811–824.
- Deshmukh, V.A., Tardif, V., Lyssiotis, C.A., Green, C.C., Kerman, B., Kim, H.J., Padmanabhan, K., Swoboda, J.G., Ahmad, I., Kondo, T., et al. (2013). A regenerative approach to the treatment of multiple sclerosis. *Nature* *502*, 327–332.
- Dizon, M.L. V., Maa, T., and Kessler, J.A. (2011). The bone morphogenetic protein antagonist noggin protects white matter after perinatal hypoxia-ischemia. *Neurobiol. Dis.* *42*, 318–326.
- Driever, W., Stemple, D., Schier, A., and Solnica-Krezel, L. (1994). Zebrafish: genetic tools for studying vertebrate development. *Trends Genet.* *10*, 152–159.
- Driever, W., Solnica-Krezel, L., Schier, A.F., Neuhauss, S.C., Malicki, J., Stemple, D.L., Stainier, D.Y., Zwartkruis, F., Abdelilah, S., Rangini, Z., et al. (1996). A genetic screen for mutations affecting embryogenesis in zebrafish. *Development* *123*, 37–46.
- Du, C., Duan, Y., Wei, W., Cai, Y., Chai, H., Lv, J., Du, X., Zhu, J., and Xie, X. (2016). Kappa opioid receptor activation alleviates experimental autoimmune encephalomyelitis and promotes oligodendrocyte-mediated remyelination. *Nat. Commun.* *7*, 11120.
- Dugas, J.C., Cuellar, T.L., Scholze, A., Ason, B., Ibrahim, A., Emery, B., Zamanian, J.L., Foo, L.C., McManus, M.T., and Barres, B.A. (2010). Dicer1 and miR-219 Are required for normal oligodendrocyte differentiation and myelination. *Neuron* *65*, 597–611.
- Early, J.J., Cole, K.L.H., Williamson, J.M., Swire, M., Kamadurai, H., Muskavitch, M., and Lyons, D.A. (2018). An automated high-resolution in vivo screen in zebrafish to identify chemical regulators of myelination. *Elife* *7*, 1–31.

References

- Emery, B. (2010). Regulation of oligodendrocyte differentiation and myelination. *Science* *330*, 779–782.
- Fancy, S.P.J., Zhao, C., and Franklin, R.J.M. (2004). Increased expression of Nkx2.2 and Olig2 identifies reactive oligodendrocyte progenitor cells responding to demyelination in the adult CNS. *Mol. Cell. Neurosci.* *27*, 247–254.
- Fancy, S.P.J., Baranzini, S.E., Zhao, C., Yuk, D.-I., Irvine, K.-A., Kaing, S., Sanai, N., Franklin, R.J.M., and Rowitch, D.H. (2009). Dysregulation of the Wnt pathway inhibits timely myelination and remyelination in the mammalian CNS. *Genes Dev.* *23*, 1571–1585.
- Fancy, S.P.J., Chan, J.R., Baranzini, S.E., Franklin, R.J.M., and Rowitch, D.H. (2011). Myelin regeneration: a recapitulation of development? *Annu. Rev. Neurosci.* *34*, 21–43.
- Fogarty, M., Richardson, W.D., and Kessaris, N. (2005). A subset of oligodendrocytes generated from radial glia in the dorsal spinal cord. *Development* *132*, 1951–1959.
- Franklin, R.J.M. (2015). Regenerative Medicines for Remyelination: From Aspiration to Reality. *Cell Stem Cell* *16*, 576–577.
- Franklin, R.J.M., and Ffrench-Constant, C. (2008a). Remyelination in the CNS: from biology to therapy. *Nat. Rev. Neurosci.* *9*, 839–855.
- Franklin, R.J.M., and Ffrench-Constant, C. (2008b). Remyelination in the CNS: From biology to therapy. *Nat. Rev. Neurosci.* *9*, 839–855.
- Fredriksson, R., Lagerström, M.C., Lundin, L.-G., and Schiöth, H.B. (2003). The G-protein-coupled receptors in the human genome form five main families. Phylogenetic analysis, paralogon groups, and fingerprints. *Mol. Pharmacol.* *63*, 1256–1272.
- Gammill, L.S., and Bronner-Fraser, M. (2003). Neural crest specification: Migrating into genomics. *Nat. Rev. Neurosci.* *4*, 795–805.
- Gautier, H.O.B., Evans, K.A., Volbracht, K., James, R., Sitnikov, S., Lundgaard, I., James, F., Lao-Peregrin, C., Reynolds, R., Franklin, R.J.M., et al. (2015). Neuronal activity regulates remyelination via glutamate signalling to oligodendrocyte progenitors. *Nat. Commun.* *6*, 8518.
- Gensert, J.M., and Goldman, J.E. (1997). Endogenous progenitors remyelinate demyelinated axons in the adult CNS. *Neuron* *19*, 197–203.
- Giera, S., Deng, Y., Luo, R., Ackerman, S.D., Mogha, A., Monk, K.R., Ying, Y., Jeong, S.-J., Makinodan, M., Bialas, A.R., et al. (2015). The adhesion G protein-coupled receptor GPR56 is a cell-autonomous regulator of oligodendrocyte development. *Nat. Commun.* *6*, 6121.
- Goldshmit, Y., Sztal, T.E., Jusuf, P.R., Hall, T.E., Nguyen-Chi, M., and Currie, P.D. (2012). Fgf-dependent glial cell bridges facilitate spinal cord regeneration in zebrafish. *J. Neurosci.* *32*, 7477–7492.
- Gray, C., Loynes, C.A., Whyte, M.K.B., Crossman, D.C., Renshaw, S.A., and Chico, T.J.A. (2011). Simultaneous intravital imaging of macrophage and neutrophil behaviour during inflammation using a novel transgenic zebrafish. *Thromb. Haemost.* *105*, 811–819.
- Greer, J.M., and McCombe, P.A. (2011). Role of gender in multiple sclerosis: clinical effects and potential molecular mechanisms. *J. Neuroimmunol.* *234*, 7–18.
- Gross-Thebing, T., Paksa, A., and Raz, E. (2014). Simultaneous high-resolution detection of multiple transcripts combined with localization of proteins in whole-mount embryos. *BMC Biol.* *12*, 55.

- Groves, A.K., Barnett, S.C., Franklin, R.J.M., Crang, A.J., Mayer, M., Blakemore, W.F., and Noble, M. (1993). Repair of demyelinated lesions by transplantation of purified O-2A progenitor cells. *Nature* 362, 453–455.
- Hall, B.K. (2008). The neural crest and neural crest cells: Discovery and significance for theories of embryonic organization. *J. Biosci.* 33, 781–793.
- Hauser, A.S., Attwood, M.M., Rask-Andersen, M., Schiöth, H.B., and Gloriam, D.E. (2017). Trends in GPCR drug discovery: new agents, targets and indications. *Nat. Rev. Drug Discov.* 16, 829–842.
- Hayakawa, K., Pham, L.-D.D., Som, A.T., Lee, B.J., Guo, S., Lo, E.H., and Arai, K. (2011). Vascular endothelial growth factor regulates the migration of oligodendrocyte precursor cells. *J. Neurosci.* 31, 10666–10670.
- Hayakawa, K., Seo, J.H., Pham, L.-D.D., Miyamoto, N., Som, A.T., Guo, S., Kim, K.-W., Lo, E.H., and Arai, K. (2012). Cerebral endothelial derived vascular endothelial growth factor promotes the migration but not the proliferation of oligodendrocyte precursor cells in vitro. *Neurosci. Lett.* 513, 42–46.
- Heise, C.E., O’Dowd, B.F., Figueroa, D.J., Sawyer, N., Nguyen, T., Im, D.S., Stocco, R., Bellefeuille, J.N., Abramovitz, M., Cheng, R., et al. (2000). Characterization of the human cysteinyl leukotriene 2 receptor. *J. Biol. Chem.* 275, 30531–30536.
- Hennen, S., Wang, H., Peters, L., Merten, N., Simon, K., Spinrath, A., Blättermann, S., Akkari, R., Schrage, R., Schröder, R., et al. (2013). Decoding signaling and function of the orphan G protein-coupled receptor GPR17 with a small-molecule agonist. *Sci. Signal.* 6, ra93.
- Hooijmans, C.R., Hlavica, M., Schuler, F.A.F., Good, N., Good, A., Baumgartner, L., Galeno, G., Schneider, M.P., Jung, T., de Vries, R., et al. (2019). Remyelination promoting therapies in multiple sclerosis animal models: a systematic review and meta-analysis. *Sci. Rep.* 9, 822.
- Howe, K., Clark, M., Torroja, C., Torrance, J., Berthelot, C., Muffato, M., Collins, J.E., Humphray, S., McLaren, K., Matthews, L., et al. (2013). The zebrafish reference genome sequence and its relationship to the human genome. *Nature* 496, 498–503.
- Hu, B., Chen, M., Huang, R., Huang, Y., Xu, Y., Yin, W., Li, L., and Hu, B. (2017). In vivo imaging of mauthner axon regeneration, remyelination and synapses re-establishment after laser axotomy in zebrafish larvae. *Exp. Neurol.*
- Huang, J.K., Fancy, S.P.J., Zhao, C., Rowitch, D.H., Ffrench-Constant, C., and Franklin, R.J.M. (2011a). Myelin regeneration in multiple sclerosis: targeting endogenous stem cells. *Neurotherapeutics* 8, 650–658.
- Huang, J.K., Jarjour, A.A., Nait Oumesmar, B., Kerninon, C., Williams, A., Krezel, W., Kagechika, H., Bauer, J., Zhao, C., Baron-Van Evercooren, A., et al. (2011b). Retinoid X receptor gamma signaling accelerates CNS remyelination. *Nat. Neurosci.* 14, 45–53.
- Huebner, E.A., and Strittmatter, S.M. (2009). Axon regeneration in the peripheral and central nervous systems. *Results Probl. Cell Differ.* 48, 339–351.
- Hughes, E.G., Kang, S.H., Fukaya, M., and Bergles, D.E. (2013). Oligodendrocyte progenitors balance growth with self-repulsion to achieve homeostasis in the adult brain. *Nat. Neurosci.* 16, 668–676.
- Ibarrola, N., Mayer-Pröschel, M., Rodriguez-Peña, A., and Noble, M. (1996). Evidence for the existence of at least two timing mechanisms that contribute to oligodendrocyte generation in

References

vitro. *Dev. Biol.* *180*, 1–21.

Ineichen, B. V., Plattner, P. S., Good, N., Martin, R., Linnebank, M., and Schwab, M. E. (2017). Nogo-A Antibodies for Progressive Multiple Sclerosis. *CNS Drugs* *31*, 187–198.

Inoue, A., Raimondi, F., Kadji, F. M. N., Singh, G., Kishi, T., Uwamizu, A., Ono, Y., Shinjo, Y., Ishida, S., Arang, N., et al. (2019). Illuminating G-Protein-Coupling Selectivity of GPCRs. *Cell* *177*, 1933–1947.e25.

James Briscoe¹, * and Bennett G. Novitsch (2008). Regulatory pathways linking progenitor patterning, cell fates and neurogenesis in the ventral neural tube. *Phil. Trans. R. Soc. B* *20*, 57–70.

Johe, K. K., Hazel, T. G., Muller, T., Dugich-Djordjevic, M. M., and McKay, R. D. (1996). Single factors direct the differentiation of stem cells from the fetal and adult central nervous system. *Genes Dev.* *10*, 3129–3140.

Jung, S.-H., Kim, S., Chung, A.-Y., Kim, H.-T., So, J.-H., Ryu, J., Park, H.-C., and Kim, C.-H. (2010). Visualization of myelination in GFP-transgenic zebrafish. *Dev. Dyn.* *239*, 592–597.

Karttunen, M. J., Czopka, T., Goedhart, M., Early, J. J., and Lyons, D. A. (2017). Regeneration of myelin sheaths of normal length and thickness in the zebrafish CNS correlates with growth of axons in caliber. *PLoS One* *12*, e0178058.

Katritch, V., Cherezov, V., and Stevens, R. C. (2013). Structure-function of the G protein-coupled receptor superfamily. *Annu. Rev. Pharmacol. Toxicol.* *53*, 531–556.

Kazakova, N., Li, H., Mora, A., Jessen, K. R., Mirsky, R., Richardson, W. D., and Smith, H. K. (2006). A screen for mutations in zebrafish that affect myelin gene expression in Schwann cells and oligodendrocytes. *Dev. Biol.* *297*, 1–13.

Kimmel, C. B., Ballard, W. W., Kimmel, S. R., Ullmann, B., and Schilling, T. F. (1995). Stages of embryonic development of the zebrafish. *Dev. Dyn.* *203*, 253–310.

Kirby, B. B., Takada, N., Latimer, A. J., Shin, J., Carney, T. J., Kelsh, R. N., and Appel, B. (2006). In vivo time-lapse imaging shows dynamic oligodendrocyte progenitor behavior during zebrafish development. *Nat. Neurosci.* *9*, 1506–1511.

Kobelt, G., Thompson, A., Berg, J., Gannedahl, M., Eriksson, J., MSCOI Study Group, and European Multiple Sclerosis Platform (2017). New insights into the burden and costs of multiple sclerosis in Europe. *Mult. Scler.* *23*, 1123–1136.

Kok, F. O., Shin, M., Ni, C.-W., Gupta, A., Grosse, A. S., van Impel, A., Kirchmaier, B. C., Peterson-Maduro, J., Kourkoulis, G., Male, I., et al. (2015). Reverse genetic screening reveals poor correlation between morpholino-induced and mutant phenotypes in zebrafish. *Dev. Cell* *32*, 97–108.

Kokel, D., and Peterson, R. T. (2011). Using the zebrafish photomotor response for psychotropic drug screening. *Methods Cell Biol.* *105*, 517–524.

Kondo, T., and Raff, M. (2000). Basic helix-loop-helix proteins and the timing of oligodendrocyte differentiation. *Development* *127*, 2989–2998.

Kucenas, S., Snell, H., and Appel, B. (2008). *nkx2.2a* promotes specification and differentiation of a myelinating subset of oligodendrocyte lineage cells in zebrafish. *Neuron Glia Biol.* *4*, 71–81.

Kwan, K. M., Fujimoto, E., Grabher, C., Mangum, B. D., Hardy, M. E., Campbell, D. S., Parant, J. M.,

- Yost, H.J., Kanki, J.P., and Chien, C.-B. (2007). The Tol2kit: a multisite gateway-based construction kit for Tol2 transposon transgenesis constructs. *Dev. Dyn.* *236*, 3088–3099.
- Ladher, R., and Schoenwolf, G.C. (2005). ch. 1 Making a neural tube: Neural induction and neurulation. *Dev. Neurobiol.* 1–20.
- Langenau, D.M., Ferrando, A.A., Traver, D., Kutok, J.L., Hezel, J.-P.D., Kanki, J.P., Zon, L.I., Look, A.T., and Trede, N.S. (2004). In vivo tracking of T cell development, ablation, and engraftment in transgenic zebrafish. *Proc. Natl. Acad. Sci. U. S. A.* *101*, 7369–7374.
- Lassmann, H. (2013). Pathology and disease mechanisms in different stages of multiple sclerosis. *J. Neurol. Sci.* *333*, 1–4.
- Lecca, D., Trincavelli, M.L., Gelosa, P., Sironi, L., Ciana, P., Fumagalli, M., Villa, G., Verderio, C., Grumelli, C., Guerrini, U., et al. (2008). The recently identified P2Y-like receptor GPR17 is a sensor of brain damage and a new target for brain repair. *PLoS One* *3*, e3579.
- Lee, H.K., Chaboub, L.S., Zhu, W., Zollinger, D., Rasband, M.N., Fancy, S.P.J., and Deneen, B. (2015). Daam2-PIP5K is a regulatory pathway for Wnt signaling and therapeutic target for remyelination in the CNS. *Neuron* *85*, 1227–1243.
- Lee, X., Yang, Z., Shao, Z., Rosenberg, S.S., Levesque, M., Pepinsky, R.B., Qiu, M., Miller, R.H., Chan, J.R., and Mi, S. (2007). NGF regulates the expression of axonal LINGO-1 to inhibit oligodendrocyte differentiation and myelination. *J. Neurosci.* *27*, 220–225.
- Li, H., Lu, Y., Smith, H.K., and Richardson, W.D. (2007). Olig1 and Sox10 interact synergistically to drive myelin basic protein transcription in oligodendrocytes. *J. Neurosci.* *27*, 14375–14382.
- Lloyd, A.F., and Miron, V.E. (2019). The pro-remyelination properties of microglia in the central nervous system. *Nat. Rev. Neurol.* *15*, 447–458.
- Lu, Q.R., Sun, T., Zhu, Z., Ma, N., Garcia, M., Stiles, C.D., and Rowitch, D.H. (2002). Common developmental requirement for Olig function indicates a motor neuron/oligodendrocyte connection. *Cell* *109*, 75–86.
- Ludwin, S.K., and Maitland, M. (1984). Long-term remyelination fails to reconstitute normal thickness of central myelin sheaths. *J. Neurol. Sci.* *64*, 193–198.
- Ma, Q., Chen, Z., del Barco Barrantes, I., de la Pompa, J.L., and Anderson, D.J. (1998). neurogenin1 is essential for the determination of neuronal precursors for proximal cranial sensory ganglia. *Neuron* *20*, 469–482.
- MacRae, C.A., and Peterson, R.T. (2015). Zebrafish as tools for drug discovery. *Nat. Rev. Drug Discov.* *14*, 721–731.
- Maisel, M., Herr, A., Milosevic, J., Hermann, A., Habisch, H.-J., Schwarz, S., Kirsch, M., Antoniadis, G., Brenner, R., Hallmeyer-Elgner, S., et al. (2007). Transcription profiling of adult and fetal human neuroprogenitors identifies divergent paths to maintain the neuroprogenitor cell state. *Stem Cells* *25*, 1231–1240.
- März, M., Schmidt, R., Rastegar, S., and Strähle, U. (2011). Regenerative response following stab injury in the adult zebrafish telencephalon. *Dev. Dyn.* *240*, 2221–2231.
- Mathias, J.R., Saxena, M.T., and Mumm, J.S. (2012). Advances in zebrafish chemical screening technologies. *Future Med. Chem.* *4*, 1811–1822.
- McCurley, A.T., and Callard, G. V (2010). Time Course Analysis of Gene Expression Patterns in Zebrafish Eye During Optic Nerve Regeneration. *J. Exp. Neurosci.* *2010*, 17–33.

References

- McMorris, F.A., and Dubois-Dalcq, M. (1988). Insulin-like growth factor I promotes cell proliferation and oligodendroglial commitment in rat glial progenitor cells developing in vitro. *J. Neurosci. Res.* *21*, 199–209.
- Mei, F., Fancy, S.P.J., Shen, Y.-A.A., Niu, J., Zhao, C., Presley, B., Miao, E., Lee, S., Mayoral, S.R., Redmond, S.A., et al. (2014). Micropillar arrays as a high-throughput screening platform for therapeutics in multiple sclerosis. *Nat. Med.* *20*, 954–960.
- Mei, F., Mayoral, S.R., Nobuta, H., Wang, F., Despons, C., Lorrain, D.S., Xiao, L., Green, A.J., Rowitch, D., Whistler, J., et al. (2016). Identification of the Kappa-Opioid Receptor as a Therapeutic Target for Oligodendrocyte Remyelination. *J. Neurosci.* *36*, 7925–7935.
- Mi, S., Miller, R.H., Lee, X., Scott, M.L., Shulag-Morskaya, S., Shao, Z., Chang, J., Thill, G., Levesque, M., Zhang, M., et al. (2005). LINGO-1 negatively regulates myelination by oligodendrocytes. *Nat. Neurosci.* *8*, 745–751.
- Mi, S., Hu, B., Hahm, K., Luo, Y., Kam Hui, E.S., Yuan, Q., Wong, W.M., Wang, L., Su, H., Chu, T.-H., et al. (2007). LINGO-1 antagonist promotes spinal cord remyelination and axonal integrity in MOG-induced experimental autoimmune encephalomyelitis. *Nat. Med.* *13*, 1228–1233.
- Milner, R., Anderson, H.J., Rippon, R.F., McKay, J.S., Franklin, R.J.M., Marchionni, M.A., Reynolds, R., and Ffrench-Constant, C. (1997). Contrasting effects of mitogenic growth factors on oligodendrocyte precursor cell migration. *Glia* *19*, 85–90.
- Mogha, A., D’Rozario, M., and Monk, K.R. (2016). G Protein-Coupled Receptors in Myelinating Glia. *Trends Pharmacol. Sci.* *37*, 977–987.
- Monk, K.R., and Talbot, W.S. (2009). Genetic dissection of myelinated axons in zebrafish. *Curr. Opin. Neurobiol.* *19*, 486–490.
- Monk, K.R., Naylor, S.G., Glenn, T.D., Mercurio, S., Perlin, J.R., Dominguez, C., Moens, C.B., and Talbot, W.S. (2009). A G protein-coupled receptor is essential for Schwann cells to initiate myelination. *Science* *325*, 1402–1405.
- Morest, D.K., and Silver, J. (2003). Precursors of neurons, neuroglia, and ependymal cells in the CNS: What are they? Where are they from? How do they get where they are going? *Glia* *43*, 6–18.
- Morris, J.K., Willard, B.B., Yin, X., Jeserich, G., Kinter, M., and Trapp, B.D. (2004). The 36K protein of zebrafish CNS myelin is a short-chain dehydrogenase. *Glia* *45*, 378–391.
- Münzel, E.J., Schaefer, K., Obirei, B., Kremmer, E., Burton, E.A., Kuscha, V., Becker, C.G., Brösamle, C., Williams, A., and Becker, T. (2012). Claudin k is specifically expressed in cells that form myelin during development of the nervous system and regeneration of the optic nerve in adult zebrafish. *Glia* *60*, 253–270.
- Münzel, E.J., Becker, C.G., Becker, T., and Williams, A. (2014). Zebrafish regenerate full thickness optic nerve myelin after demyelination, but this fails with increasing age. *Acta Neuropathol. Commun.* *2*, 77.
- Murcia-Belmonte, V., Medina-Rodríguez, E.M., Bribián, A., de Castro, F., and Esteban, P.F. (2014). ERK1/2 signaling is essential for the chemoattraction exerted by human FGF2 and human anosmin-1 on newborn rat and mouse OPCs via FGFR1. *Glia* *62*, 374–386.
- Murphy, M., Reid, K., Dutton, R., Brooker, G., and Bartlett, P.F. (1997). Neural stem cells. *J. Investig. Dermatology. Symp. Proc.* *2*, 8–13.
- Murtie, J.C., Zhou, Y.-X., Le, T.Q., Vana, A.C., and Armstrong, R.C. (2005). PDGF and FGF2

- pathways regulate distinct oligodendrocyte lineage responses in experimental demyelination with spontaneous remyelination. *Neurobiol. Dis.* *19*, 171–182.
- Najm, F.J., Madhavan, M., Zaremba, A., Shick, E., Karl, R.T., Factor, D.C., Miller, T.E., Nevin, Z.S., Kantor, C., Sargent, A., et al. (2015). Drug-based modulation of endogenous stem cells promotes functional remyelination in vivo. *Nature* *522*, 216–220.
- Nakashima, K., Takizawa, T., Ochiai, W., Yanagisawa, M., Hisatsune, T., Nakafuku, M., Miyazono, K., Kishimoto, T., Kageyama, R., and Taga, T. (2001). BMP2-mediated alteration in the developmental pathway of fetal mouse brain cells from neurogenesis to astrocytogenesis. *Proc. Natl. Acad. Sci. U. S. A.* *98*, 5868–5873.
- Nawaz, S., Schweitzer, J., Jahn, O., and Werner, H.B. (2013). Molecular evolution of myelin basic protein, an abundant structural myelin component. *Glia* *61*, 1364–1377.
- Nawaz, S., Sánchez, P., Schmitt, S., Snaidero, N., Mitkovski, M., Velte, C., Brückner, B.R., Alexopoulos, I., Czopka, T., Jung, S.Y., et al. (2015). Actin Filament Turnover Drives Leading Edge Growth during Myelin Sheath Formation in the Central Nervous System. *Dev. Cell* *34*, 139–151.
- Norton, J.D., Deed, R.W., Craggs, G., and Sablitzky, F. (1998). Id helix-loop-helix proteins in cell growth and differentiation. *Trends Cell Biol.* *8*, 58–65.
- Orentas, D.M., Hayes, J.E., Dyer, K.L., and Miller, R.H. (1999). Sonic hedgehog signaling is required during the appearance of spinal cord oligodendrocyte precursors. *Development* *126*, 2419–2429.
- Ou, Z., Sun, Y., Lin, L., You, N., Liu, X., Li, H., Ma, Y., Cao, L., Han, Y., Liu, M., et al. (2016). Olig2-Targeted G-Protein-Coupled Receptor Gpr17 Regulates Oligodendrocyte Survival in Response to Lysolecithin-Induced Demyelination. *J. Neurosci.* *36*, 10560–10573.
- Padilla, S., Corum, D., Padnos, B., Hunter, D.L., Beam, A., Houck, K.A., Sipes, N., Kleinstreuer, N., Knudsen, T., Dix, D.J., et al. (2012). Zebrafish developmental screening of the ToxCast™ Phase I chemical library. *Reprod. Toxicol.* *33*, 174–187.
- Park, H.-C., Mehta, A., Richardson, J.S., and Appel, B. (2002). *olig2* is required for zebrafish primary motor neuron and oligodendrocyte development. *Dev. Biol.* *248*, 356–368.
- Park, H.-C., Shin, J., Roberts, R.K., and Appel, B. (2007). An *olig2* reporter gene marks oligodendrocyte precursors in the postembryonic spinal cord of zebrafish. *Dev. Dyn.* *236*, 3402–3407.
- Patel, J.R., McCandless, E.E., Dorsey, D., and Klein, R.S. (2010). CXCR4 promotes differentiation of oligodendrocyte progenitors and remyelination. *Proc. Natl. Acad. Sci. U. S. A.* *107*, 11062–11067.
- Perron, M., and Harris, W.A. (2000). Determination of vertebrate retinal progenitor cell fate by the Notch pathway and basic helix-loop-helix transcription factors. *Cell. Mol. Life Sci.* *57*, 215–223.
- Pfeiffer, S.E., Warrington, A.E., and Bansal, R. (1993). The oligodendrocyte and its many cellular processes. *Trends Cell Biol.* *3*, 191–197.
- Pichler, F.B., Laurenson, S., Williams, L.C., Dodd, A., Copp, B.R., and Love, D.R. (2003). Chemical discovery and global gene expression analysis in zebrafish. *Nat. Biotechnol.* *21*, 879–883.
- Prayoonwiwat, N., and Rodriguez, M. (1993). The potential for oligodendrocyte proliferation during demyelinating disease. *J. Neuropathol. Exp. Neurol.* *52*, 55–63.

References

- Preston, M.A., and Macklin, W.B. (2015). Zebrafish as a model to investigate CNS myelination. *Glia* 63, 177–193.
- Prineas, J.W., and Connell, F. (1979). Remyelination in multiple sclerosis. *Ann. Neurol.* 5, 22–31.
- Pruss, R.M. (2010). Phenotypic screening strategies for neurodegenerative diseases: a pathway to discover novel drug candidates and potential disease targets or mechanisms. *CNS Neurol. Disord. Drug Targets* 9, 693–700.
- Qi, A.-D., Harden, T.K., and Nicholas, R.A. (2013). Is GPR17 a P2Y/leukotriene receptor? examination of uracil nucleotides, nucleotide sugars, and cysteinyl leukotrienes as agonists of GPR17. *J. Pharmacol. Exp. Ther.* 347, 38–46.
- Qian, X., Shen, Q., Goderie, S.K., He, W., Capela, A., Davis, A.A., and Temple, S. (2000). Timing of CNS cell generation: a programmed sequence of neuron and glial cell production from isolated murine cortical stem cells. *Neuron* 28, 69–80.
- Quintana, F.J., Iglesias, A.H., Farez, M.F., Caccamo, M., Burns, E.J., Kassam, N., Oukka, M., and Weiner, H.L. (2010). Adaptive autoimmunity and Foxp3-based immunoregulation in zebrafish. *PLoS One* 5, e9478.
- Raphael, A.R., and Talbot, W.S. (2011). New insights into signaling during myelination in zebrafish. *Curr. Top. Dev. Biol.* 97, 1–19.
- Raport, C.J., Schweickart, V.L., Chantry, D., Eddy, R.L., Shows, T.B., Godiska, R., and Gray, P.W. (1996). New members of the chemokine receptor gene family. *J. Leukoc. Biol.* 59, 18–23.
- Rask-Andersen, M., Almén, M.S., and Schiöth, H.B. (2011). Trends in the exploitation of novel drug targets. *Nat. Rev. Drug Discov.* 10, 579–590.
- Reid, M. V, Murray, K.A., Marsh, E.D., Golden, J.A., Simmons, R.A., and Grinspan, J.B. (2012). Delayed myelination in an intrauterine growth retardation model is mediated by oxidative stress upregulating bone morphogenetic protein 4. *J. Neuropathol. Exp. Neurol.* 71, 640–653.
- Reinoß, P. (2014). Functional analysis of the transmembrane receptor Gpr17 for CNS myelination in zebrafish.
- Rennekamp, A.J., and Peterson, R.T. (2015). 15 Years of Zebrafish Chemical Screening. *Curr. Opin. Chem. Biol.* 24, 58–70.
- Rhodes, K.E., Raivich, G., and Fawcett, J.W. (2006). The injury response of oligodendrocyte precursor cells is induced by platelets, macrophages and inflammation-associated cytokines. *Neuroscience* 140, 87–100.
- Richardson, W.D., Pringle, N., Mosley, M.J., Westermarck, B., and Dubois-Dalcq, M. (1988). A role for platelet-derived growth factor in normal gliogenesis in the central nervous system. *Cell* 53, 309–319.
- Robu, M.E., Larson, J.D., Nasevicius, A., Beiraghi, S., Brenner, C., Farber, S.A., and Ekker, S.C. (2007). p53 activation by knockdown technologies. *PLoS Genet.* 3, e78.
- Rossi, A., Kontarakis, Z., Gerri, C., Nolte, H., Hölper, S., Krüger, M., and Stainier, D.Y.R. (2015). Genetic compensation induced by deleterious mutations but not gene knockdowns. *Nature* 524, 230–233.
- Samanta, J., Grund, E.M., Silva, H.M., Lafaille, J.J., Fishell, G., and Salzer, J.L. (2015). Inhibition of Gli1 mobilizes endogenous neural stem cells for remyelination. *Nature* 526, 448–452.

- Scafidi, J., Hammond, T.R., Scafidi, S., Ritter, J., Jablonska, B., Roncal, M., Szigeti-Buck, K., Coman, D., Huang, Y., McCarter, R.J., et al. (2014). Intranasal epidermal growth factor treatment rescues neonatal brain injury. *Nature* *506*, 230–234.
- Schaefer, K., and Brösamle, C. (2009). Zwilling-A and -B, two related myelin proteins of teleosts, which originate from a single bicistronic transcript. *Mol. Biol. Evol.* *26*, 495–499.
- Schebesta, M., and Serluca, F.C. (2009). *olig1* Expression identifies developing oligodendrocytes in zebrafish and requires hedgehog and notch signaling. *Dev. Dyn.* *238*, 887–898.
- Schmitt, NK (2018). Zebrafisch as a model organism to study the in vivo role of G-protein coupled receptor 17 in myelination
- Schoenwolf, G.C., and Smith, J.L. (1990). Mechanisms of neurulation : traditional viewpoint and recent advances. *270*, 243–270.
- Schweitzer, J., Becker, T., Schachner, M., Nave, K.-A., and Werner, H. (2006). Evolution of myelin proteolipid proteins: gene duplication in teleosts and expression pattern divergence. *Mol. Cell. Neurosci.* *31*, 161–177.
- Shi, W., Fang, Z., Li, L., and Luo, L. (2015). Using zebrafish as the model organism to understand organ regeneration. *Sci. China. Life Sci.* *58*, 343–351.
- Shin, D., Lin, S.-T., Fu, Y.-H., and Ptáček, L.J. (2013). Very large G protein-coupled receptor 1 regulates myelin-associated glycoprotein via *Gas/Gaq*-mediated protein kinases A/C. *Proc. Natl. Acad. Sci. U. S. A.* *110*, 19101–19106.
- Shin, J., Park, H.-C., Topczewska, J.M., Mawdsley, D.J., and Appel, B. (2003). Neural cell fate analysis in zebrafish using *olig2* BAC transgenics. *Methods Cell Sci.* *25*, 7–14.
- Shingo, T., Sorokan, S.T., Shimazaki, T., and Weiss, S. (2001). Erythropoietin regulates the in vitro and in vivo production of neuronal progenitors by mammalian forebrain neural stem cells. *J. Neurosci.* *21*, 9733–9743.
- Shiow, L.R., Favrais, G., Schirmer, L., Schang, A.-L., Cipriani, S., Andres, C., Wright, J.N., Nobuta, H., Fleiss, B., Gressens, P., et al. (2017). Reactive astrocyte COX2-PGE2 production inhibits oligodendrocyte maturation in neonatal white matter injury. *Glia* *65*, 2024–2037.
- Shou, J., Rim, P.C., and Calof, A.L. (1999). BMPs inhibit neurogenesis by a mechanism involving degradation of a transcription factor. *Nat. Neurosci.* *2*, 339–345.
- Shultz, L.D., Ishikawa, F., and Greiner, D.L. (2007). Humanized mice in translational biomedical research. *Nat. Rev. Immunol.* *7*, 118–130.
- Sim, F.J., Zhao, C., Penderis, J., and Franklin, R.J.M. (2002). The age-related decrease in CNS remyelination efficiency is attributable to an impairment of both oligodendrocyte progenitor recruitment and differentiation. *J. Neurosci.* *22*, 2451–2459.
- Simon, K., Hennen, S., Merten, N., Blättermann, S., Gillard, M., Kostenis, E., and Gomeza, J. (2016). The orphan G protein-coupled receptor GPR17 negatively regulates oligodendrocyte differentiation via *Gai/o* and its downstream effector molecules. *J. Biol. Chem.* *291*, 705–718.
- Simon, K., Merten, N., Schröder, R., Hennen, S., Preis, P., Schmitt, N., Peters, L., Schrage, R., Vermeiren, C., Gillard, M., et al. (2017). The Orphan Receptor GPR17 Is Unresponsive to Uracil Nucleotides and Cysteinyl Leukotrienes s. 518–532.
- Simpson, P.B., and Armstrong, R.C. (1999). Intracellular signals and cytoskeletal elements

References

- involved in oligodendrocyte progenitor migration. *Glia* 26, 22–35.
- Suster, M.L., Abe, G., Schouw, A., and Kawakami, K. (2011). Transposon-mediated BAC transgenesis in zebrafish. *Nat. Protoc.* 6, 1998–2021.
- Takada, N., and Appel, B. (2010). Identification of genes expressed by zebrafish oligodendrocytes using a differential microarray screen. *Dev. Dyn.* 239, 2041–2047.
- Temple, S. (2001). The development of neural stem cells. *Nature* 414, 112–117.
- Thummel, R., Burket, C.T., Brewer, J.L., Sarras, M.P., Li, L., Perry, M., McDermott, J.P., Sauer, B., Hyde, D.R., and Godwin, A.R. (2005). Cre-mediated site-specific recombination in zebrafish embryos. *Dev. Dyn.* 233, 1366–1377.
- Tintore, M., Vidal-Jordana, A., and Sastre-Garriga, J. (2019). Treatment of multiple sclerosis - success from bench to bedside. *Nat. Rev. Neurol.* 15, 53–58.
- Tusnády, G.E., and Simon, I. (2001). The HMMTOP transmembrane topology prediction server. *Bioinformatics* 17, 849–850.
- Ulloa, F., and Martí, E. (2010). Wnt won the war: Antagonistic role of Wnt over Shh controls dorso-ventral patterning of the vertebrate neural tube. *Dev. Dyn.* 239, 69–76.
- Urnov, F.D., Rebar, E.J., Holmes, M.C., Zhang, H.S., and Gregory, P.D. (2010). Genome editing with engineered zinc finger nucleases. *Nat. Rev. Genet.* 11, 636–646.
- Waehneltd, T. V, and Jeserich, G. (1984). Biochemical characterization of the central nervous system myelin proteins of the rainbow trout, *Salmo gairdneri*. *Brain Res.* 309, 127–134.
- Walsh, N.C., Kenney, L.L., Jangalwe, S., Aryee, K.-E., Greiner, D.L., Brehm, M.A., and Shultz, L.D. (2017). Humanized Mouse Models of Clinical Disease. *Annu. Rev. Pathol.* 12, 187–215.
- Wang, S., Sdrulla, A.D., DiSibio, G., Bush, G., Nofziger, D., Hicks, C., Weinmaster, G., and Barres, B.A. (1998). Notch receptor activation inhibits oligodendrocyte differentiation. *Neuron* 21, 63–75.
- Watanabe, M., Toyama, Y., and Nishiyama, A. (2002). Differentiation of proliferated NG2-positive glial progenitor cells in a remyelinating lesion. *J. Neurosci. Res.* 69, 826–836.
- Wilson, L., and Maden, M. (2005). The mechanisms of dorsoventral patterning in the vertebrate neural tube. *Dev. Biol.* 282, 1–13.
- Wilson, H.C., Scolding, N.J., and Raine, C.S. (2006). Co-expression of PDGF alpha receptor and NG2 by oligodendrocyte precursors in human CNS and multiple sclerosis lesions. *J. Neuroimmunol.* 176, 162–173.
- Yan, H., and Rivkees, S.A. (2002). Hepatocyte growth factor stimulates the proliferation and migration of oligodendrocyte precursor cells. *J. Neurosci. Res.* 69, 597–606.
- Yang, H.-J., Vainshtein, A., Maik-Rachline, G., and Peles, E. (2016). G protein-coupled receptor 37 is a negative regulator of oligodendrocyte differentiation and myelination. *Nat. Commun.* 7, 10884.
- Ye, P., Kollias, G., and D’Ercole, A.J. (2007). Insulin-like growth factor-I ameliorates demyelination induced by tumor necrosis factor-alpha in transgenic mice. *J. Neurosci. Res.* 85, 712–722.
- Yin, W., and Hu, B. (2014). Knockdown of *Lingo1b* protein promotes myelination and

- oligodendrocyte differentiation in zebrafish. *Exp. Neurol.* 251, 72–83.
- Yin, D., Gavi, S., Wang, H., and Malbon, C.C. (2004). Probing receptor structure/function with chimeric G-protein-coupled receptors. *Mol. Pharmacol.* 65, 1323–1332.
- Yuen, T.J., Johnson, K.R., Miron, V.E., Zhao, C., Quandt, J., Harrisingh, M.C., Swire, M., Williams, A., McFarland, H.F., Franklin, R.J.M., et al. (2013). Identification of endothelin 2 as an inflammatory factor that promotes central nervous system remyelination. *Brain* 136, 1035–1047.
- Zalc, B. (2016). The acquisition of myelin: An evolutionary perspective. *Brain Res.* 1641, 4–10.
- Zhan, H., and Gong, Z. (2010). Delayed and restricted expression of UAS-regulated GFP gene in early transgenic zebrafish embryos by using the GAL4/UAS system. *Mar. Biotechnol. (NY)*. 12, 1–7.
- Zhao, B., Zhao, C.Z., Zhang, X.Y., Huang, X.Q., Shi, W.Z., Fang, S.H., Lu, Y.B., Zhang, W.P., Xia, Q., and Wei, E.Q. (2012). The new P2Y-like receptor G protein-coupled receptor 17 mediates acute neuronal injury and late microgliosis after focal cerebral ischemia in rats. *Neuroscience* 202, 42–57.
- Zhao, X., He, X., Han, X., Yu, Y., Ye, F., Chen, Y., Hoang, T., Xu, X., Mi, Q.-S., Xin, M., et al. (2010). MicroRNA-mediated control of oligodendrocyte differentiation. *Neuron* 65, 612–626.
- Zhou, Q., Choi, G., and Anderson, D.J. (2001). The bHLH transcription factor Olig2 promotes oligodendrocyte differentiation in collaboration with Nkx2.2. *Neuron* 31, 791–807.
- Zon, L.I., and Peterson, R.T. (2005). In vivo drug discovery in the zebrafish. *Nat. Rev. Drug Discov.* 4, 35–44.

Publications

Annala, S., Feng, X., Shridhar, N., Eryilmaz, F., Patt, J., Yang, J., Pfeil, E.M., Cervantes-Villagrana, R.D., Inoue, A., **Häberlein, F.**, et al. (2019). Direct targeting of Gαq and Gα11 oncoproteins in cancer cells. *Sci. Signal.* 12, eaau5948.

Greunke, C., Hage-Hülsmann, A., Sorkalla, T., Keksel, N., **Häberlein, F.**, and Häberlein, H. (2015). A systematic study on the influence of the main ingredients of an ivy leaves dry extract on the β2-adrenergic responsiveness of human airway smooth muscle cells. *Pulm. Pharmacol. Ther.* 31, 92–98.

Krebs, K.M., Pfeil, E.M., Simon, K., Grundmann, M., **Häberlein, F.**, Bautista-Aguilera, O.M., Gütschow, M., Weaver, C.D., Fleischmann, B.K., and Kostenis, E. (2018). Label-Free Whole Cell Biosensing for High-Throughput Discovery of Activators and Inhibitors Targeting G Protein-Activated Inwardly Rectifying Potassium Channels. *ACS Omega* 3, 14814–14823.

Nagarajan B., Harder A., Japp A., **Häberlein F.**, Mingardo E., Kleinert H., Yilmaz Ö., Zoons A., Rau B., Christ A., Kubitscheck U., Eiberger B., Sandhoff R., Eckhardt M., Hartmann D., Odermatt B. (accepted 09/2019). CNS myelin protein 36K regulates oligodendrocyte differentiation through Notch. *Glia*.

Schulte-Michels, J., Wolf, A., Aatz, S., Engelhard, K., Sieben, A., Martinez-Osuna, M., **Häberlein, F.**, and Häberlein, H. (2016). α-Hederin inhibits G protein-coupled receptor kinase 2-mediated phosphorylation of β2-adrenergic receptors. *Phytomedicine* 23, 52–57.

Poster Presentations

Häberlein, F., Schmitt, NK., Mingardo, E., Gomeza, J., Odermatt, B., Kostenis, E. Chimeric human/zebrafish GPR17 receptors as tools to study myelination *in vitro* and *in vivo*. GRK1873 International symposium (Bonn, DE, August, 29.-30.)

Acknowledgements

Zuerst möchte ich mich bei meiner Doktormutter Frau Prof. Dr. Evi Kostenis für die Betreuung meines Projektes, ihre Hilfsbereitschaft aber vor Allem für ihr großes Vertrauen bedanken. Des Weiteren möchte ich mich für die super Zusammenarbeit bei meinem Zweitgutachter Prof. Dr. Benjamin Odermatt bedanken, dessen Tür stets offen war. Ein besonderes Dankeschön geht an Dr. Jesús Gomeza für seine wissenschaftliche Unterstützung und für die zahlreichen motivierenden Gespräche, die uns manchmal die Köpfe zum Rauchen gebracht haben.

Ich möchte mich auch bei Prof. Kubitschek und Prof. Bendas für die Übernahme des fachfremden und fachnahen Mitglieds meiner Prüfungskommission bedanken. Ich bedanke mich auch bei der Graduiertenschule GRK1873, die mir geholfen hat, mich wissenschaftlich weiterzuentwickeln und mir die Möglichkeit geboten hat, mich wissenschaftlich zu vernetzen.

Vielen Dank an die Mitarbeiter der AG Kostenis und AG Odermatt, die mich nicht nur arbeitstechnisch unterstützt haben, sondern unter denen ich auch gute Freunde gefunden habe. Ein besonderer Dank geht hier an Öznur Yilmaz und Tobias Lindenberg für die uneingeschränkte Hilfe im Labor und im Fischraum, an Nicole Merten für die vielen konstruktiven Gespräche und Ideen, an Enrico Mingardo für seine Unterstützung an der Theke und im Labor und an die Island-Urlauber Caroline Kolvenbach, Bhuvaneshwari Nagarajan, Nina-Katharina Schmitt und Stephan Terporten. Auch bedanke ich mich bei Dr. Sebastian Franken für die vielen hilfreichen Gespräche. Ganz besonders bedanke ich mich bei Nina-Katharina Schmitt und Bhuvaneshwari Nagarajan für die super Einarbeitung, für ihre Hilfe und Unterstützung im beruflichen als auch privaten Leben. Herzlich möchte ich mich auch bei Dr. Maik Hintze bedanken, der mir immer mit Rat zur Seite stand.

Zu guter Letzt möchte ich mich herzlich bei meinen Freunden und meiner Familie bedanken, insbesondere bei meinen Jungs aus der Heimat (Emil, Scheche, Andre, Willi, Eugen, Dennis, Artur, Fero, Wladi), den Jungs aus Bonn (Max, Marius, Marvin, Gill, Felix, Christian, Sebi), dass sie meine Promotionszeit mit unvergesslich viel Spass und Erinnerungen gefüllt haben. Ein ganz besonderes Dankeschön geht an meine Eltern, Niklas und meine Freundin Vera, die mich immer uneingeschränkt sowohl in privaten als auch in beruflichen Angelegenheiten unterstützt und ausgehalten haben. **Vielen Dank!**